INVESTIGATION OF INTERACTION BETWEEN PRESSURE RELIEF VALVE AND TURBINES DURING A TRANSIENT FLOW IN A HYDROPOWER PLANT

A THESIS SUBMITTED TO
THE GRADUATE SCHOOL OF NATURAL AND APPLIED SCIENCES
OF
MIDDLE EAST TECHNICAL UNIVERSITY

BY

MEHMET ALİ ÇETİNTAŞ

IN PARTIAL FULFILLMENT OF THE REQUIREMENTS
FOR
THE DEGREE OF MASTER OF SCIENCE
IN
CIVIL ENGINEERING

FEBRUARY 2022

Approval of the thesis:

INVESTIGATION OF INTERACTION BETWEEN PRESSURE RELIEF VALVE AND TURBINES DURING A TRANSIENT FLOW IN A HYDROPOWER PLANT

submitted by **MEHMET ALİ ÇETİNTAŞ** in partial fulfillment of the requirements for the degree of **Master of Science in Civil Engineering, Middle East Technical University** by,

Prof. Dr. Halil Kalıpçılar
Dean, Graduate School of **Natural and Applied Sciences** _____

Prof. Dr. Erdem Canbay
Head of the Department, **Civil Engineering** _____

Prof. Dr. Zafer Bozkuş
Supervisor, **Civil Engineering, METU** _____

Assoc.Prof. Dr. Kutay Çelebioğlu
Co-Supervisor, **ETU Hydro, TOBB ETU** _____

ExaminingCommitteeMembers:

Prof. Dr. A. Burcu Altan Sakarya
Civil Engineering, METU _____

Prof. Dr. Zafer Bozkuş
Civil Engineering, METU _____

Assoc. Prof. Dr. Elif Oğuz
Civil Engineering, METU _____

Assoc. Prof. Dr. Melih Çalamak
Civil Engineering, METU _____

Assoc. Prof. Dr. Ali Ersin Dinçer
Civil Engineering, Abdullah Gül University _____

Date: 11.02.2022

I hereby declare that all information in this document has been obtained and presented in accordance with academic rules and ethical conduct. I also declare that, as required by these rules and conduct, I have fully cited and referenced all material and results that are not original to this work.

Name, Last name : Mehmet Ali Çetintaş

Signature :

ABSTRACT

INVESTIGATION OF INTERACTION BETWEEN PRESSURE RELIEF VALVE AND TURBINES DURING A TRANSIENT FLOW IN A HYDROPOWER PLANT

Çetintaş, Mehmet Ali
M.S., Department of Civil Engineering
Supervisor: Prof. Dr. Zafer Bozkuş
Co-Supervisor: Assoc.Prof.Dr. Kutay Çelebioğlu

February 2022, 125 pages

The main goal of the present study is to investigate the effect of pressure relief valve (PRV) on the hydraulic transients generated by multiple turbine operations. To achieve this goal, a numerical model of KEPEZ-I Hydropower plant is constructed in the Bentley HAMMER software, which employs the Method of Characteristics (MoC) for computations. The MoC has been proven worldwide as a versatile and accurate tool for solving non-linear, hyperbolic, partial differential equations in space-time domain for hydraulic transients. The available field data for some specific turbine operations were used to calibrate the numerical model first. The simultaneously measured data from the field such as turbine closure and PRV opening adjustments, and pressure measurements were very useful in establishing and validating the numerical model in the software for the further analyses. Once the confidence was gained for the accuracy of the model a number of numerical simulations were performed for various turbine operations to understand the response of the plant to the transients. Since a pressure relief valve (PRV) is mounted in the hydropower plant already, the study mainly focuses on the effect of PRV on the transients generated by those turbine operations. Different scenarios such as instant load rejection, load acceptance, load variation are applied to the system with

and without PRV. The operating conditions of the hydropower plant are analyzed, and the operation limits are determined to prevent any damage to the system by using the computer software. Potentially, most critical operational cases for the penstocks are selected, and the effects of the PRV are observed on the transient flow. It is found that PRV reduces approximately 50% of sudden pressure increase near the turbines. The power plant is protected against the adverse effects of water hammer transients as long as it is operated within the guidelines specified in the thesis.

Keywords: Waterhammer, PRV, Hydraulic Transients, HAMMER

ÖZ

ZAMANA BAĞLI DEĞİŞEN AKIMDA BİR HİDROELEKTRİK SANTRALDE BASINÇ DÜŞÜRÜCÜ VANA İLE TÜRBİNLER ARASINDAKİ ETKİLEŞİMİN ARAŞTIRILMASI

Çetintaş, Mehmet Ali
Yüksek Lisans, İnşaat Mühendisliği Bölümü
Tez Yöneticisi: Prof. Dr. Zafer Bozkuş
Ortak Tez Yöneticisi: Doç. Dr. Kutay Çelebioğlu

Şubat 2022, 125 sayfa

Bu çalışmanın temel amacı, basınç düşürücü vanasının (BDV) çoklu türbin operasyonları tarafından üretilen zamana bağlı değişen (ZBD) akımlar üzerindeki etkisini araştırmaktır. Bu amaca ulaşmak için, hesaplamalarında Karakteristikler Metodu (KM) kullanan Bentley HAMMER yazılımında KEPEZ-I Hidroelektrik santralinin sayısal bir modeli oluşturulmuştur. KM, ZBD akımlar için uzay-zaman alanında doğrusal olmayan, hiperbolik, kısmi diferansiyel denklemleri çözme konusunda çok yönlü ve doğru bir araç olarak dünya çapında kanıtlanmıştır. Bazı özel türbin operasyonları için mevcut saha verileri, önce sayısal modeli kalibre etmek için kullanıldı. Türbin kapatma ve BDV açma ayarlarıve basınç ölçümleri gibi sahadan eş zamanlı olarak ölçülen veriler, daha sonraki analizler için yazılımdaki sayısal modelin oluşturulmasında ve doğrulanmasında çok faydalı oldu. Modelin doğruluğuna yönelik güven kazanıldıktan sonra, santralin ZBD akımlara tepkisini anlamak için çeşitli türbin işletme koşullarında bir dizi sayısal simülasyon yapıldı. Hidroelektrik santralde halihazırda bir basınç düşürücü vanası (BDV) monte edildiğinden, çalışma esas olarak BDV'nin bu türbin operasyonları tarafından üretilen akımlar üzerindeki etkisine odaklanmaktadır. Analizlerde BDV'li ve BDV'siz sisteme anlık yük reddi, yük kabulü, yük değişimi gibi farklı senaryolar

uygulanmaktadır. Hidroelektrik santralinin işletme koşulları analiz edilmekte ve bilgisayar yazılımı kullanılarak sisteme herhangi bir zarar gelmemesi için işletme limitleri belirlenmektedir. Potansiyel olarak, cebri borular için en kritik operasyonel durumlar seçildi ve BDV'nin ZBD akım üzerindeki etkileri gözlemlendi. BDV'nin türbinlerin yakınında oluşan ani basınç artışını yaklaşık %50 oranında azalttığı belirlenmiştir. Santral, tezde belirtilen esaslar dahilinde çalıştırıldığı sürece su darbesinin olumsuz etkilerine karşı korunmaktadır.

Anahtar Kelimeler: Su Darbesi, BDV, Zamana Bağlı Değişen Akım, HAMMER

To My Parents Hilmi & Neriman

To My Brother Osman Oğuz

ACKNOWLEDGEMENTS

The finalization of the thesis could not have been completed without professional guidance, supports, advice, criticism of my thesis advisor Prof. Dr. Zafer Bozkuş, and co-advisor Assoc. Prof. Dr. Kutay Çelebioğlu. I wish to express my deepest admiration for their wisdom and gratitude for their support in my difficult times. I would like to thank them for their infinite patience in the study's progress. It was a pleasure to work with them and learn valuable lessons from their suggestions.

I want to thank Assoc. Prof. Dr. Ali Ersin Dinçer, who is also a jury member, for his suggestions and comments about the computer program and critical points of the thesis study.

I would like to express my special thanks to the remaining jury members, Prof. Dr. A. Burcu Altan Sakarya, Assoc. Prof. Dr. Melih Çalamak, and Assoc. Prof. Dr. Elif Oğuz for their valuable comments on the thesis draft and for their precious time.

I want to thank TOBB ETU Hydro, FENSU Engineering Construction Energy LTD. CO., and Fevzi Büyüksolak for their support in collecting data for the study.

I would like to extend my regards to Bora Cengiz, who is my manager at MITAS Industry Inc., for his patience and support in the thesis progress.

My dearest family supports me in every part of my life. I would like to thank my mother, Neriman, for her deepest love, care, and support. My brother, Osman Oğuz, deserves special thanks. He is always with me on any subject. I really appreciate his patience, support, and help in my life. I also thank Refika Çetintaş for her advice about the thesis process and her support in my life.

TABLE OF CONTENTS

ABSTRACT v

ÖZ vii

ACKNOWLEDGEMENTS x

TABLE OF CONTENTS xi

LIST OF TABLES xiii

LIST OF FIGURES xiv

CHAPTERS

1 INTRODUCTION 1

1.1 Introduction 1

1.2 Scope of the Study 3

1.3 Organization of the Thesis 5

2 LITERATURE REVIEW 7

2.1 Historical Background 7

2.2 Hydropower Plants 11

2.3 Hydraulic Turbines 15

2.4 Pressure Relief Valves 21

3 TRANSIENT FLOW 25

3.1 Definition of Transient Flow 25

3.2 Water Hammer 26

3.3 Derivation of The Acoustic Wave Speed Equation 30

3.4 Governing Equations of Transient Flow 34

3.5 Solution of Transient Flow Equations by Method of Characteristics 36

4 COMPUTER SOFTWARE 43
4.1 Necessity of Computer Program 43
4.2 Interface and Toolbars of the Bentley HAMMER 44
5 CASE STUDY AND DISCUSSION OF RESULTS 53
5.1 Information about KEPEZ-I Hydropower Plant 53
5.2 Model Development and Validation Methodology 58
5.2.1 Case 1: HAMMER Model with only GPV 65
5.2.2 Case 2: HAMMER Model with GPV and PRV 70
5.2.3 Case 3: HAMMER model with Turbine and PRV 76
5.3 Transient Analysis for KEPEZ – I Hydropower Plant 83
5.3.1 Scenario 1: Instant Load Rejection 84
5.3.2 Scenario 2: Load Rejection 90
5.3.3 Scenario 3: Load Acceptance 99
5.3.4 Scenario 4: Load Variation 107
5.4 Discussion of the Results 115
6 CONCLUSIONS 119
REFERENCES 123

LIST OF TABLES

TABLES

Table 2.1 Rotational speed of turbine according to number of poles and frequency of electric grid (ESHA, 2004) 19
Table 5.1 Pipe parameters 56
Table 5.2 Basic Characteristics of Turbines in HPP 57
Table 5.3 Elevations of Main Nodes in Model 58
Table 5.4 Pipe characteristics 59
Table 5.5 Measured Data Comparison for 8.5 MW and 9.35 MW Tests 64
Table 5.6 Discharge values corresponding to Turbine Power 108

LIST OF FIGURES

FIGURES

Figure 2.1 Illustration of a Run-of-river HPP (Dursun, 2013) 12
Figure 2.2 Pelton Turbine Nozzles and Blades (Dursun, 2013) 16
Figure 2.3 Solid Model of Francis type turbine in KEPEZ - I HPP (Sepetci, 2017) 17
Figure 2.4 Cross-sectional View of Solid Model of Turbine in KEPEZ - I HPP (Sepetci, 2017) 17
Figure 2.5 Model of PRV in KEPEZ - I HPP 22
Figure 2.6 Photograph of PRV in KEPEZ - I HPP 23
Figure 3.1 Water hammer effect in time between $0 < t \leq L/a$ (Chaudhry, 1987) 28
Figure 3.2 Water hammer effect in time between $L/a < t \leq 2L/a$ (Chaudhry, 1987) 28
Figure 3.3 Water hammer effect in time between $2L/a < t \leq 3L/a$ (Chaudhry, 1987) 29
Figure 3.4 Water hammer effect in time between $3L/a < t \leq 4L/a$ (Chaudhry, 1987) 29
Figure 3.5 Control volume and momentum equation components (Calamak, 2010; Wylie et al., 1993) 30
Figure 3.6 Parameters of continuity equation (Dursun, 2013; Streeter & Wylie, 1967) 32
Figure 3.7 Free-body diagram of semi-cylinder of a pipe 34
Figure 3.8 Control volume that indicates parameters for momentum equation 35
Figure 3.9 Characteristics Lines in x-t solution domain 38
Figure 4.1 Default Interface of HAMMER 45
Figure 4.2 Calculation options window for (a) initial conditions and (b) transient analysis 46
Figure 4.3 Transient Results Viewer 47
Figure 4.4 Pressure and Flow versus Time graph 48

Figure 4.5 An example of Transient Calculation Summary 49
Figure 4.6 Flextable of pipes..... 50
Figure 4.7 Profile that illustrates the water flow path and hydraulic grade line along the penstock 51
Figure 4.8 Properties menu for a pipe and a pipe 52
Figure 5.1 Plan view and Cross-Section of Intake Structure 55
Figure 5.2 Surge Tank of Kepez – I HPP 56
Figure 5.3 HAMMER Model..... 58
Figure 5.4 Operation Principle of Wicket Gate (Krivchenko, 1994)..... 60
Figure 5.5 Pressure Variation and Operating Rules of 9.35 MW and 8.5 MW Tests in the Field 63
Figure 5.6 HAMMER Model for Case 1 65
Figure 5.7 Comparison of Operating Rules for GPV in Case 1 and Wicket Gate, PRV in Field for 8.5 MW Test..... 66
Figure 5.8 Comparison of Pressure Variation between Field data (8.5 MW Test) and Case 1 with Flow Variation..... 67
Figure 5.9 Comparison of Operating Rules for GPV in Case 1 and Wicket Gate, PRV in Field for 9.35 MW Test..... 68
Figure 5.10 Pressure and Discharge Variation for Field data and Case 1 and Flow variation for Case 1 in 9.35 MW Test..... 69
Figure 5.11 HAMMER Model for Case 2 70
Figure 5.12 Comparison of Operating Rules for GPV in Case 2 and Wicket Gate in Field for 8.5 MW Test 71
Figure 5.13 Comparison of Operating Rules for PRV in Case 2 and measured data for 8.5 MW Test..... 71
Figure 5.14 Pressure and Discharge Variation for Field data and Case 2 in 8.5 MW Test..... 72
Figure 5.15 Comparison of GPV Operating Rule in Case 1 and Wicket gate Operating Rule in Measured Data for 9.35 MW Test..... 73

Figure 5.16 Comparison of PRV Operating Rules in Case 2 and measured data for 9.35 MW Test 74
Figure 5.17 Pressure and Discharge Variation for Field data and Case 2 in 9.35 MW Test 75
Figure 5.18 Comparison of Wicket Gate Operating Rules in Case 3 and measured data for 8.5 MW Test 77
Figure 5.19 Comparison of PRV Operating Rules in Case 3 and measured data for 8.5 MW Test 77
Figure 5.20 Pressure and Discharge Variation for Field data and Case 3 for 8.5 MW Test 79
Figure 5.21 Comparison of Wicket Gate Operating Rules in Case 3 and measured data for 9.35 MW Test 80
Figure 5.22 Comparison of PRV Operating Rules in Case 3 and measured data for 9.35 MW Test 81
Figure 5.23 Pressure and Discharge Variation for Field data and Case 3 for 9.35 MW Test 82
Figure 5.24 Pressure and Discharge Variation for Scenario 1 with and without PRV in 8.5 MW Test 85
Figure 5.25 HGLs along the Penstock for 8.5 MW Test in Scenario 1 with and without PRV 87
Figure 5.26 Pressure and Discharge Variation for Scenario 1 with and without PRV in 9.35 MW Test 88
Figure 5.27 HGLs along the Penstock for 9.35 MW Test in Scenario 1 with and without PRV 89
Figure 5.28 Pressure and Discharge Variations for different wicket gate closure times in Load Rejection Scenario for 8.35 MW 92
Figure 5.29 PRV and Wicket Gate Operating Rules for Load Rejection 8.5 MW Test 15 seconds closure 93
Figure 5.30 Pressure and Discharge Variation for Scenario 2 with and without PRV in 8.5 MW Test 94

Figure 5.31 HGLs along the Penstock for 8.5 MW Test in Scenario 2 with and without PRV 95
Figure 5.32 Pressure and Discharge Variations for different wicket gate closure times in Load Rejection Scenario for 9.35 MW 96
Figure 5.33 Pressure and Discharge Variation for Scenario 2 with and without PRV in 9.35 MW Test 97
Figure 5.34 HGLs along the Penstock for 9.35 MW Test in Scenario 2 with and without PRV 98
Figure 5.35 Pressure and Discharge Variations for different wicket gate opening times in Scenario 3, 8.5 MW Test 100
Figure 5.36 Wicket Gate Opening in 5 seconds for Scenario 3 (8.5 MW) 101
Figure 5.37 Pressure and Discharge Variation of 5 seconds Wicket Gate Opening Case for Scenario 3 (8.5 MW) 102
Figure 5.38 HGLs along the Penstock for 5 seconds Wicket Gate Opening Case in Scenario 3 (8.35 MW) 103
Figure 5.39 Pressure and Discharge Variations for different wicket gate opening times in Scenario 3 (9.35 MW) 104
Figure 5.40 Wicket Gate Opening in 5 seconds for Scenario 3 (9.35 MW) 105
Figure 5.41 Pressure and Discharge Variation of 5 seconds Wicket Gate Opening Case for Scenario 3 (9.35 MW) 106
Figure 5.42 HGLs along the Penstock for 5 seconds Wicket Gate Opening Case in Scenario 3 (9.35 MW) 107
Figure 5.43 Pressure and Discharge Variations for Different Load Reduction Cases without PRV 109
Figure 5.44 Wicket Gate Operating Rule for Load Reduction from 9.35 MW to 4.5 MW Turbine Power in 6 seconds 110
Figure 5.45 Pressure and Discharge Variation of Load Reduction from 9.35 MW to 4.5 MW in 6 seconds 111
Figure 5.46 HGL's along the Penstock for Load Reduction from 9.35 MW to 4.5 MW in 6 seconds 112

Figure 5.47 Wicket Gate Operating Rule for Scenario 4 113
Figure 5.48 Pressure and Discharge Variation for Scenario 4 114
Figure 5.49 HGLs along the Penstock for Load Variation Scenario.....115

LIST OF SYMBOLS AND ABBREVIATIONS

A	The cross-sectional area of the pipe (m^2)
a	Acoustic pressure wave speed throughout the fluid in pipe (m/s)
CS	Control surface
CV	Control Volume
D	Pipe inside diameter (m)
E	Young's Modulus (Modulus of Elasticity) (N/m^2)
e	Thickness of pipes (m)
f	Darcy friction factor
g	Gravitational acceleration
H	Piezometric head in the pipe (m)
HPP	Hydropower Plant
HGL	Hydraulic Grade Line
PRV	Pressure Relief Valve
GPV	General Purpose Valve
H_0	Initial piezometric head during steady-state flow (m)
K	Bulk modulus of elasticity of fluid (N/m^2)
L	Length of the pipe (m)
MoC	Method of Characteristics
P	Pressure (N/m^2)
rpm	Revolution per minute
Q	Discharge in the pipe (m^3/s)
t	Time (s)
V	Velocity (m/s)
V_0	Initial velocity (m/s)
V_f	Final velocity (m/s)
γ	Unit weight of fluid (N/m^3)
ΔA	Change in cross-sectional area of the pipe (m^2)
ΔH	Change in piezometric head of the fluid in the pipe (m)
ΔS	Stretching of the pipe in length (m)
ΔV	Change in velocity of fluid in the pipe (m/s)
$\Delta \rho$	Change in density of the fluid (kg/m^3)
μ	Poisson's ratio
ρ	Density of fluid (kg/m^3)
σ_f	Allowable tensile stress (N/m^2)
τ_w	Shear stress (N/m^2)

CHAPTER 1

INTRODUCTION

1.1 Introduction

Hydropower is electricity produced from generators driven by turbines that convert the potential energy of flowing water into mechanical energy. One either needs a large fall of water or fast flowing water to produce a feasible amount of energy. Since hydropower is a renewable energy source, it does not consume the raw materials of nature. As a result, many countries focused on improving strategies for using renewable energy sources such as hydropower, wind, geothermal, and solar. Engineering studies were carried out to increase the number of hydropower plants without harming the environment.

Energy Market Regulatory Authority (EMRA) of Turkey (2020) stated that economic activity slowed down, and energy demand decreased in 2020 due to the countermeasures against COVID-19 pandemic in Turkey. However, some steps were taken to restore the economic growth, and their influence were observed in the electric demand at the end of the year. Although the adverse effects of COVID-19 reduced energy demand of many countries, Turkey's energy demand increased 0.8% in 2020. The share of renewable energy increased from 45.4% to 48% between 2019 and 2020. Since the regulations are focused on different renewable energy sources, the share of hydropower plants in electricity production decreased from 30.20% to 26.55% in 2020.

According to the DSI report published in (2020), the number of hydropower plants has increased from 644 to 714 in Turkey since 2018. These hydropower plants have 31,391 MW of installed capacity with 108.005 billion kWh average production annually.

Hydropower plants have many advantages over other alternatives for energy production or electric generation. However, it is crucial to design and operate the hydropower plants properly to use efficiently, which means continuously and reliably producing energy from the water. Some operating conditions may cause destructive results in the water conveying system while operating the hydropower plant to generate electricity. Generally, destructive phenomena occur in transient cases where flow parameters change with respect to time. Because steady-state flow, has constant flow parameters such as discharge and pressure in time, problematic situations are barely observed in the system. Therefore, all the potential operation cases should be considered in the design stage to avoid the hazardous effect of transient flow that causes sudden pressure changes in the penstock system.

The main reason for the transient flow formation is the operational changes that cause sudden variations in the velocity of the flowing water, which in turn create rapid changes in pressures at the hydropower plant while in operation. Routine load acceptance, load variations, power failures, rapid valve closure, operational problems are examples of some of the sources of the changes in the system. These events lead to either high pressure increases or decreases depending on its nature. Then, these pressure changes (increase or decrease) start traveling in the pipeline with a hammering sound. That is why this phenomenon is called water hammer. High and low pressures are reasons for the cavitation, column separation, etc., in the system. Some components of the hydropower plant may be affected and damaged by this incident. Penstock may burst suddenly or collapse because of high or low pressures, respectively. There may even be human deaths in the field, as seen in the water hammer related accidents before in the hydropower plants. For instance, Sayano-Shushenskaya HPP took severe damages because of adverse effects of water hammer event on the 17th of August 2009. The location of the power plant is on the Yenisei River in Russia. Seleznev et al. (2014) stated that Turbine No. 2 was the first turbine affected due to the influence of continuous high-frequency vibrations. As a result, Turbine 2 closed suddenly, and water hammer occurred at the turbine inlet.

This phenomenon caused a pressure surge in the penstock. Turbine 2, with its equipment, was lifted off its seat, and powerhouse flooded. Other turbines took damage, and the generator exploded. In the reports prepared after investigations, authorities stated that 75 people died in the accident.

PRV is one of the protective measures that prevents the system from adverse effects of transient flow due to sudden changes in flow velocity. They are opened with the help of a spring or weight according to a set pressure point or they can be controlled by the governor with servomotors and behaves as a throttle control valve in the system. In KEPEZ – I HPP, PRV is controlled by governor and opened with wicket gate closure operation in order to discharge the pressurized water from the system before excessive pressures are formed.

In this study, the KEPEZ-I Hydropower plant, which was rehabilitated in 2018 with MILHES project, is analyzed with the help of simulations by using computer software named HAMMER. Operational cases are investigated, and since the system has a surge tank and PRV, the effects of these protective measures are discussed by comparing the field data and simulation results.

1.2 Scope of the Study

Hydropower plants are spreading worldwide to gain energy from renewable energy sources. Since the population is ascending and cities are scaling up day by day, energy need is increasing dramatically. In order to encounter this energy demand, scientists and engineers must find more alternatives and more suitable plants without damaging nature or human beings. However, it is challenging to design and improve a hydropower plant because of hydraulic transients. Analyses should be performed, and precautions should be taken in the design stage before construction.

In this study, KEPEZ-I Hydropower plant is analyzed after MILHES project is finished and tests are applied to the system. MILHES project is a rehabilitation

project that aims to recalculate transient flow behavior by using up-to-date design approaches and mounting suitable turbines designed by Turkish engineers by considering the results of the fluid mechanics in the plant. The primary purpose of changing the turbines is to increase the total power of the plant and the efficiency of the turbines.

The study aims to investigate fluid transients in KEPEZ-I Hydropower Plant whose turbines are changed with rehabilitation project and analyze the effect of the PRV on the pressure changes resulting from water hammer. The place of the plant is in Antalya, Turkey. Model is constructed-in computer software from the reservoir to the tailwater canal to simulate the transients using the same parameters used in real life. The hydropower plant has three turbine systems, the installed capacity of each turbine is 8.8 MW, and the total capacity of the facility is 26.4 MW. The penstocks convey water from headpond to the powerhouse. In the system, the PRV and surge tank is used as protective measures to prevent a dramatic increase or decrease of pressure from the water hammer. Minor losses and head losses decrease the energy of the fluid in the penstocks and junctions as water flows towards the turbines. The losses are calculated with the model and validated from the values which are taken from the report of the FENSU Engineering Construction Energy Company. The company observed the details of the system in the field, measured the dimensions of necessary elements, and calculated hydraulic losses. It is understood that since the water of the Mediterranean region includes caustic lime, the inside diameter of penstocks is smaller than the diameters which are given in the construction plans. Lime also affects the friction coefficient of the penstocks. Therefore, all these parameters are taken into consideration.

In the present study, the effects of the PRV are analyzed for different scenarios after computer software model is validated from field data which are collected from the tests for instant load rejection case. The software program uses unsteady pipe flow equations, namely, continuity and momentum. After simulation results obtained from the numerical model are validated with the help of measured field data,

different scenarios will be undertaken, and results will be analyzed to find the most critical case. The advantages, disadvantages, and effects of the PRV and surge tank will be discussed by comparing the cases and considering the measured field data.

1.3 Organization of the Thesis

The first chapter covers the introduction, scope, and organization of the study,

Chapter 2 provides a brief history of the transient flow, and literature review of the water hammer with mainly valves and turbines. Previous studies on KEPEZ-I Hydropower Plant are given in the literature review part. Chapter 2 also includes brief information about hydropower plants, hydraulic turbines, and pressure relief valves for the sake of completeness.

In Chapter 3, the transient flow concept is discussed, and the common causes for the water hammer events are explained with the help of equations and derivations. Numerical solutions of the transient flow (i.e., MoC) in closed conduits are presented. The water hammer theory is detailed, and effects on pressure and other parameters can be observed.

In Chapter 4, the computer software used in this study is introduced, and the solution method and interface of the Bentley HAMMER is presented.

The main subjects of Chapter 5 are details of the KEPEZ-I Hydropower plant and the introduction of the performed numerical simulation cases. Results of the scenarios, validation of the model with the field data, and effect of the protective measures are discussed.

In Chapter 6, the results of the study are summarized, and conclusions are expressed. According to the results of the scenarios with protective measures, the contribution of the study is emphasized, and a number of suggestions is made for further academic research.

CHAPTER 2

LITERATURE REVIEW

2.1 Historical Background

It is possible to go as far as Allievi (1902) or Joukowsky (1898) in the last quarter of the 19th century in order to summarize the early studies on fluid transients. It is also worth mentioning some researchers who contributed to the field in modern times, such as Streeter and Wylie (1993), Chaudhry(1987), Thorley (2004), and many others.

However, here the focus will be given on the various studies involving valve closure scenarios, HPPs, and protection measures, mainly the effect of PRVs on the transients generated by turbine operations.

P.H. Azoury et al. (1986) presented an approach that uses method of characteristics with the help of a computer program to investigate the influences of valve closing behaviors on transients for a basic pipe system. They formed linear and non-linear valve closures to indicate the different effects on the pipe and cavitation that were observed in the system. They analyzed the effects for short and long pipe systems and included the frictional losses in their calculations. The study's primary purpose was to provide a fundamental method about valve closure and its parameters for further studies so that researchers could specialize the valve closure per their systems and understand the effects of valve closure schedule on water hammer.

Hu Peicheng et al. (1989) studied the effect of impulse relief valve and safety membranes in the Libzgengqu Water Power Station in China. They tested the sytem for load rejection cases and compared the results with surge tank. Since the safety

membranes and relief valve could balance the pressure changes, the study concluded that there is no need for surge tanks for economic reasons.

Bozkuş (2008) simulated valve closure scenarios in a FORTRAN program that use method of characteristics to find optimum valve closure times in controlling water hammer. Because there are different pipe characteristics in Çamlıdere-Ivedik Water treatment Plant Pipeline system, he developed a computer program that uses interpolation feature of the method of characteristics. He concluded that valve closure scenarios directly affect the water hammer pressure intensity. Therefore, after the simulations, he suggested optimum valve closure times to be on the safe side while operating the plant.

Zhang J. et al. (2008) studied installing a pressure regulating valvein turbine spiral case of a hydropower plant in China, to replace a surge tank. They performed different simulations by changing valve diameter, operating rules in combination with the turbine wicket gate. They concluded that using PRV instead of a surge tank reduces water hammer pressure, turbine speed, and economic investment more effectively.

Zhang K. et al. (2008) constructed a simple model to analyze the simulation results for design strategies of PRV. Four different design parameters are investigated in the study: location, diameter, set point, opening, and closure time periods. They compared all the simulation results for upstream and downstream control separately. They concluded that in order to achieve optimum PRV design strategy, interdependent design parameters should be considered, and dynamic hydraulic simulations should be performed in the design stage.

Vakil and Firoozabadi (2009) developed a computational model of Karun 4 hydropower plant with a Francis turbine to simulate valve closures effects on water hammer just upstream the turbine unit. After they modeled the Francis turbine and hydropower plant, valve-closure law was validated to investigate the impact of different valve closure scenarios on transient flow. They analyzed the pressure,

turbine speed, and discharge per different valve closure laws and suggested better alternatives according to validated results.

Riasi et al. (2011) investigated transient flow using surge tank and relief valve in hydropower stations by a numerical method using MoC. In the study, the unsteady friction model is used for the simulations in order to improve the accuracy of the results of transient analysis. Then, the influence of surge tank and pressure relief valve on peak pressures in turbine inlet and turbine speed is analyzed with the simulations. They concluded that new generation of pressure relief valves can be installed instead of surge tanks to protect the system.

Calamak and Bozkus (2012) studied flywheels that reduce the turbine's rotational speed rise while pressure waves are formed by water hammer. The study also includes pressure relief valves that reduce the water hammer pressures, and safety membranes that absorb the pressure changes. Simulations are done with and without protective measures to compare their effect on the water hammer pressures by a computer program that uses method of characteristics. They concluded that these protective measures can be used instead of surge tanks and air chambers to reduce costs.

Dursun (2013) and Dursun et al.(2015) analyzed the effect of the pressure relief valve on the water hammer pressures and turbine speed for Yeşilvadi Hydropower Plant. They compared the SCADA data of the field tests, taken from the company of the project, with the results of the computer program. After validating the model of the computer program, they simulated an unprotected system to indicate the difference between the pressures and turbine speeds for system with and without PRV. They concluded that PRV decreases pressure oscillations and turbine speeds while water hammer occurs. However, if the closing and opening times of the PRV are not carried out correctly, second pressure waves are formed in the system.

Dinçer and Bozkuş (2016) investigated water hammer effects on pumped-storage hydropower plants supported by wind energy. They used a computer program,

HAMMER, which solves continuity and momentum equations with the help of method of characteristics. Water hammer is analyzed for different cases, and protective measures are suggested according to simulation results. They concluded that negative pressures are more dangerous than positive pressures in the pipeline system. Therefore, they offered to use a surge tank or lower the pipeline elevation in a negative pressure area.

Sepetçi et al. (2016) studied the preliminary design of the rehabilitation project of KEPEZ - I Hydropower Plant. The scope of the project was increasing the power and efficiency of the system by mounting new turbines, generators, and SCADA system. They modeled the existing system with a computer program and validated the results using the measured data. Then, they obtained the hydraulic parameters with the model to design a system with new pieces of equipment against water hammer effects.

Rezaei et al. (2017) studied protective devices that reduce the adverse effects of water hammer caused by sudden pump trips. They investigated the unprotected system simulations before proposing protective measures. Then, flywheel, air chamber, and in-line check valves are added to the system, and results are compared in terms of protection and economy. They performed simulations by combining the application of protective measures and compared their effects with single application of protective measures. It is concluded that the combined application of protective measures is more efficient and cheap if sufficient studies are held in order to determine the best combination.

Çelebioğlu (2019) studied the effect of the calcination on the roughness coefficient of the pipeline in the KEPEZ – I Hydropower plant. He formed a one-dimensional model of the system to validate friction coefficient values with site measurements. Also, a sample is taken from the pipes for the laboratory tests. Multimethodology is proposed to analyze roughness coefficient differences for the pipes. Finally, he concluded that calcination has affected the pipe roughness coefficient and increased

to 0.3 mm. He stated that this value could be taken as the roughness coefficient of the highly calcinated pipes.

2.2 Hydropower Plants

In order to obtain electricity from kinetic energy of flowing water, hydropower plants are constructed, and water is transferred through pipeline systems from upper elevations to lower elevations. When the pressurized water reaches the turbine, it creates enough force to start rotating the turbine connected to the generator. Therefore, if the flow rate increases, produced energy increases proportionally.

Since water can be stored with natural phenomena such as rain and snow, the hydrologic cycle proceeds until the environmental balance is damaged. This cycle provides water to hydropower plants without any limitation. Although it is a sustainable and renewable energy source, hydropower plants may cause unconvertible damages to the environment. Therefore, the designing stage of the system before the construction is a necessary process. Feasibility studies, suitable topography selection, hydrology analysis, designing of the pipeline system and turbine, researching environmental effects determine the performance and efficiency of the system. Additionally, in the design stage, transient analyses are simulated, and necessary precautions are considered to decrease or prevent any probability of sudden pressure variations and thus, water hammer. Computer programs enable engineers to foresee future events that can occur in the hydropower plants' operation stage with the help of accurate simulations.

Hydropower plants can be categorized into four main types: run-of-river HPP, diversion canal HPP, HPP with storage plant, and pump storage HPP. KEPEZ -I HPP is constructed on Duden river with a diversion weir. Water is received from the diversion weir with an intake structure to convey the water to the forebay. An energy tunnel transmits the water up to a surge tank. Then, the connection between the surge

tank and powerhouse is done by steel penstock. Figure 2.1 indicates a sketch of similar hydropower plant.

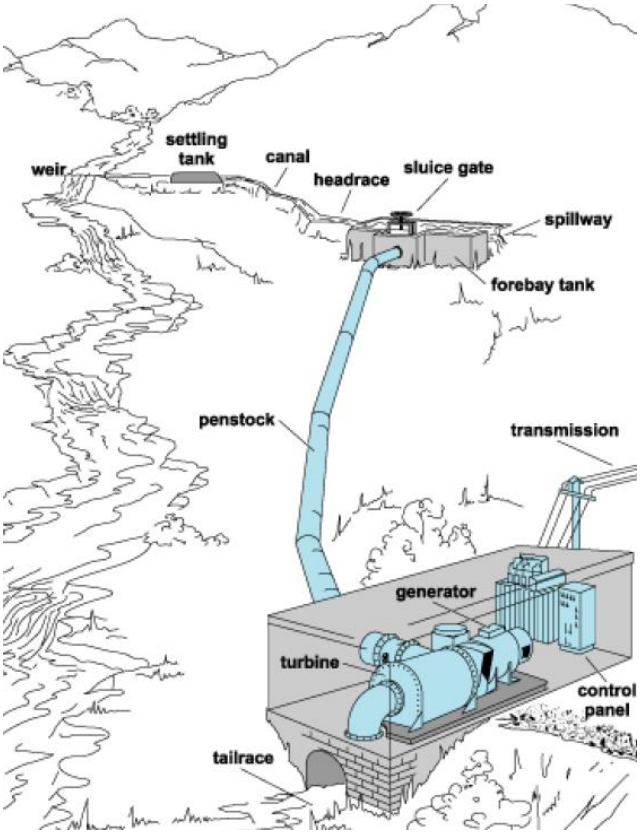

Figure 2.1 Illustration of a Run-of-river HPP (Dursun, 2013)

As seen in Figure 2.1, the turbine is connected to the generator to produce electricity. The generator converts the mechanical energy to electrical energy and transmits it to the electrical grid. Turbine rotational speed and generator are affected by any change in grid frequency. Governor seeks to keep the turbine at synchronous speed by regulating the wicket gate opening. These regulations cause instability in the flow and transient events in penstocks. Hence, water hammer generates pressure waves in the system, and sudden pressure changes are observed.

The safety of the hydropower plant can be satisfied by calculating transient event effects in the design stage. Water hammer may cause pipe bursting or collapse, damage to turbine components, vapor pocket formation, cavitation, water column

separation, etc. Therefore, hydraulic parameters of the system should be calculated clearly, and pressure limitations should be determined in order to operate the system properly.

In the designing stage, components of the system and related parameters should be determined and calculated initially. Then, an investigation of transient conditions is observed for different operations. After evaluations are completed, if the parameters are not within reasonable limits, suggested protective measures should be added to the system or system parameters, and components should be re-calculated. In these calculations, allowable limits for the members of the HPP is determined. Turbine speed and the allowable stress in penstocks are the main parameters in determining wicket gate closure patterns for reduction of electrical load in the grid. If the wicket gate is closed rapidly, allowable stress of the pipe exceeds and pipe bursts, and if the wicket gate is closed slowly, the turbine reaches runaway speed, and turbine blades take irreversible damages. Negative pressures are also considered in turbine start-up cases. If the wicket gate is opened rapidly, the piezometric head in the penstocks drops below the pipe elevation, and pressure decreases to negative gage values. Hence, the pipe collapses because of suction effects. Turbine runaway speed is provided by manufacturer and allowable stress of penstock is calculated from circumferential or Hoop stress in order to check the limits of the system which is explained in Chapter 3. In KEPEZ – I HPP, runaway speed of the turbine is 1430 rpm which is provided by TOBB ETU Hydro and the allowable stress of the steel penstock is calculated as 1.9 MPa with a safety factor of 2.

Water hammer may occur in HPPs if flowrate in the system is changed by some external source, such as opening or closing of valves, turbines or malfunction of some devices, etc. However, the leading and critical causes of the water hammer are load rejection, load acceptance, and load variation in a hydropower plant. The severity of hydraulic transient in a hydropower plant is directly about the electric grid connected to the generator.

In load rejection case, a failure in electricity transmission causes a sudden decrease in energy demand, so electrical torque is removed from system with respect to time. Since there is no resistance force that prevents the turbine rotation, turbine speed increases until runaway speed if the wicket gate is not closed in a reasonable time (Calamak, 2010). On the other hand, electrical load may directly drop to zero, or the grid may be disconnected from the generator with an emergency shutdown. This phenomenon is called instant load rejection.

Load acceptance occurs when the generator is connected to the electrical grid and turbine operation begins. The minimum gate opening that enables the turbine to reach the synchronous speed without any power output is called speed no load gate position (SNL) (Bentley, 2010). At the beginning of the operation, wicket gate is opened at SNL position, and after turbine reaches the synchronous speed, generator is connected to the grid. Wicket gate should be opened quickly to meet the energy load of the grid. This quick action results in water hammer, and sudden changes in pressure occur in the penstocks. The load acceptance case is not severe in terms of high pressures, but the formation of negative pressures may cause column separation and cavitation.

In load variation case, electricity demand changes with time because human events affect the need for electricity per day, month, season. Since the electrical energy cannot be stored, the generator of the system is operated according to demand at that time. In order to maintain constant frequency for grid and system, governor adjusts the wicket gate opening and flow amount that will enter to turbine. Opening and closing of wicket gate cause fluctuations in the flow, and pressure variations start in the system. When the pressure changes are compared with other cases, load variation is not severe per load rejection and load acceptance (Chaudhry, 1987).

If the designing stage is not completed correctly, water hammer may cause excessive pressures, overspeed of turbine and pump, column separation in the pipeline system. Therefore, hydropower plants may take significant damage, and environmental

problems, loss of lives, collapsing of structure occur after construction of the plant. As a result, proper protective measure selection is essential in this stage. Although increasing pipe diameter, changing the material type, and rearranging the profile are not economical solutions, there are many different devices and structures that help decrease transient effects. Surge tanks, air chambers, valves, flywheels, and safety membranes enable the system to supply or remove water and dissipate energy. The appropriate protective measure can be selected after optimization, effectiveness, dependability, and economic feasibility studies are completed for the facility with analyzing and comparing the results of calculations. KEPEZ -I HPP is protected by a simple surge tank with a 5 m orifice diameter and PRV from water hammer effects that are caused by operations of the system.

2.3 Hydraulic Turbines

In a hydropower plant, water is conveyed with the help of penstocks from a reservoir to a turbine. The potential energy of the water is translated to the mechanical rotational energy by turbine. Water hits the runner blades, and the turbine shaft transmits the energy to the generator.

There are two main types of turbines: impulse and reaction turbines. In impulse turbines, the nozzles convert the water pressure into the high-speed jet to apply force on the runner. After nozzles release the pressurized water jets, they hit the bowl-shaped runners, turning the shaft that connects turbine and generator. As a result, hydraulic velocity energy transforms into rotational mechanical energy and electrical energy. Pelton turbines are an example of them. Figure 2.2 shows the Pelton type turbine nozzles and blades.

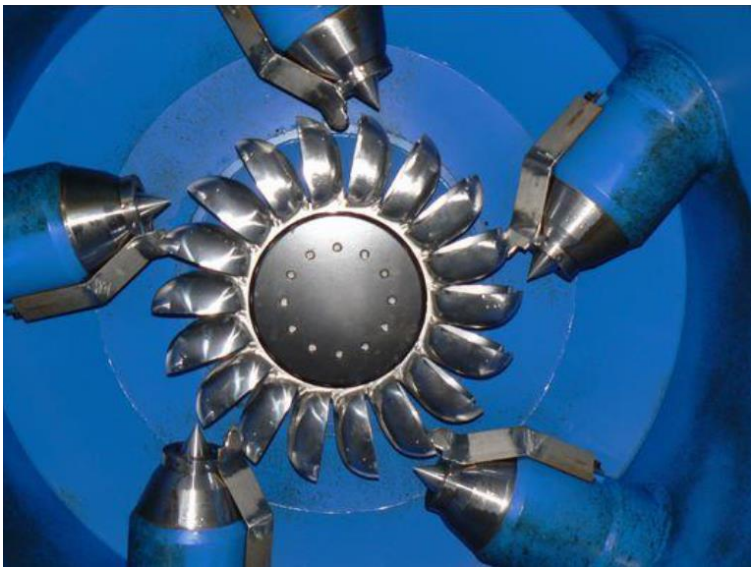

Figure 2.2 Pelton Turbine Nozzles and Blades (Dursun, 2013)

On the other hand, if the water pressure is directly conveyed to the runners with the help of a spiral case, this type is named reaction turbines such as Francis, Kaplan turbines. Reaction turbines fill with water and receive all the pressure and velocity of the flow. In KEPEZ – I HPP there are three Francis type turbine units with 8.8 MW installed capacity. One of the turbine units was rehabilitated with the new one that is designed according to up-to-date design approaches in MILHES Project. The efficiency and capacity of the turbine increased due to this renovation. The solid model of the turbine unit is indicated in Figure 2.3, and the cross-sectional view is shown in Figure 2.4.

As seen in Figure 2.3, water is conveyed to the spiral case of the turbine with a penstock. Spiral case transmits the water to the wicket gate and runners with minimum friction loss. Wicket gate opening determines the discharge of the water flow that turns the runner blades in order to produce mechanical energy. Two servomotors change the wicket gate opening with forward or backward movement according to the regulated speed in the proportional valve by governor. PRV is mounted to the spiral case of the turbine with a by-pass pipe which is about 4 m away

from the beginning of the spiral case. The diameter of the by-pass pipe is 0.6 m, and thickness is 30 mm.

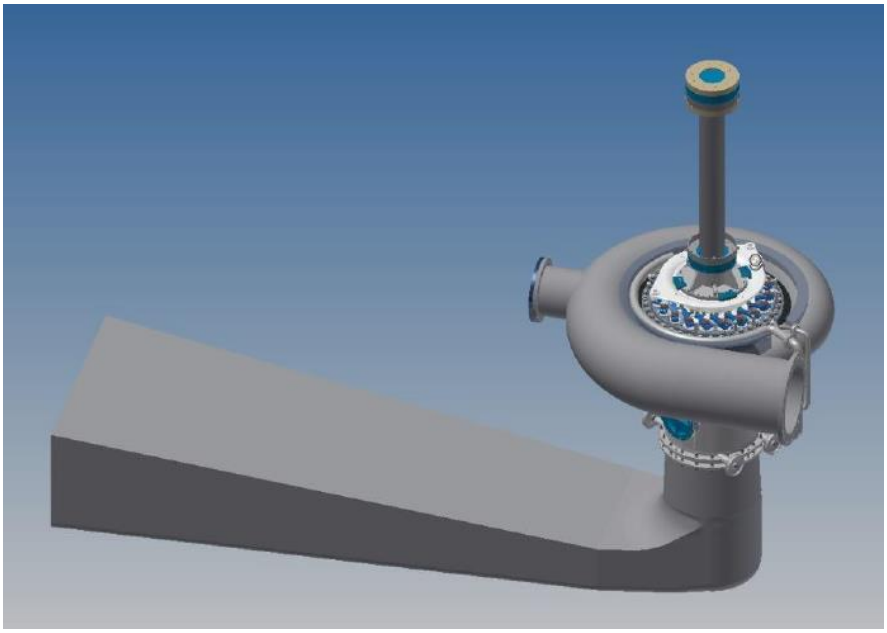

Figure 2.3 Solid Model of Francis type turbine in KEPEZ - I HPP (Sepetci, 2017)

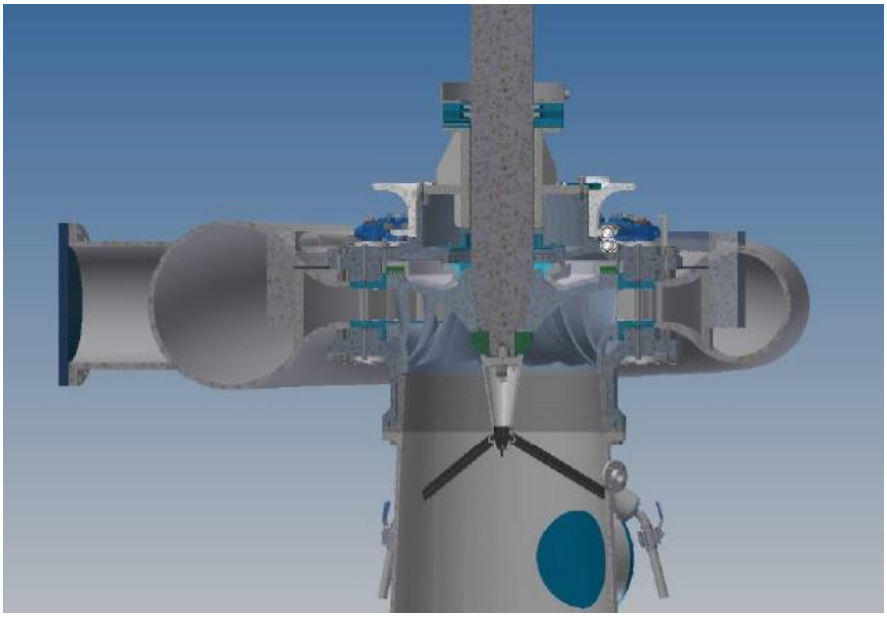

Figure 2.4 Cross-sectional View of Solid Model of Turbine in KEPEZ - I HPP (Sepetci, 2017)

Runner blades and draft tube can be observed from Figure 2.4. After the energy of the water is extracted, the turbine releases the water to the tailwater channel with the help of the draft tube.

Fundamental definitions of the turbine are necessary to understand the working concept.

Turbine head, H_T, is equal to the net head of the system. In other words, the elevation difference between the reservoir and tailwater gives the gross head of the system, and turbine head can be found by extracting hydraulic losses from the gross head.

Turbine power or capacity, P, is equal to amount of energy that is lost by fluid per second while it flows through the turbine. If the efficiency of the turbine is added to the formula, it gives the power that is produced by the system by extracting the energy of the flowing water. Discharge of the fluid is Q (m^3/s), H (m) indicates the net head and η indicates the turbine efficiency. P can be expressed in Watts if ρ is taken as 1000 kg/m^3 and g is taken as 9.81 m/s^2. Equation 2.1 defines the turbine power.

$$P = \rho g Q H \eta \tag{2.1}$$

Turbine efficiency, η, is the ratio of produced mechanical energy to the received energy from the kinetic energy of the water. Friction and minor losses affect the difference between energy input and output in the turbine. Also, there may be water leakage in the turbine mounting points. As a result, the efficiency of a turbine changes per its manufacturing method, installation method, etc. Manufacturers provide efficiency curves for every turbine.

Rotational speed, n, or synchronous speed, is the angular speed of the runners that rotate the generator shaft. It can be defined as the rotation quantity per unit time. Because the electrical torque or load that is provided from the grid should synchronize with the turbine-generator system torque value, the rotational speed is

determined per the electrical frequency of the distribution grid. After the turbine and distribution grid frequencies are equal to each other, electric generation starts when the turbine torque exceeds electrical torque. Rotational speeds and frequency relation is analyzed from Table 3.1.

Table 2.1 Rotational speed of turbine according to number of poles and frequency of electric grid (ESHA, 2004)

Number of poles	Frequency		Number of poles	Frequency	
	50 Hz	60Hz		50 Hz	60 Hz
2	3000	3600	16	375	450
4	1500	1800	18	333	400
6	1000	1200	20	300	360
8	750	900	22	272	327
10	600	720	24	250	300
12	500	600	26	231	377
14	428	540	28	214	257

Runaway speed, n_f, is the maximum speed that the turbine may reach before taking damage mechanically. When the power supply to the turbine motor suddenly cuts off because the electrical load on the turbine is eliminated, the turbine torque increases with rotational speed. If there is no control gate, the entrained water amount rises in the turbine, and the rotational speed reaches its maximum level, called runaway speed. The main problem of the runaway speed is that the turbine elements are damaged because of the high speed. Also, if the wicket gates are closed rapidly to cover the turbine elements, the transient flow occurs, and water pressure increases as the water are compressed with the gate. Then, the penstock may collapse because of the high pressures. It is essential to keep the equilibrium between the water pressure and speed of the turbine elements. One of the main results of doing transient analysis is this situation.

Specific speed, n_s, represents the speed curve of a turbine in transient conditions. It is a constant value for turbines that have similar operating conditions. Turbine curve can be expressed as linear in steady-state analysis, but four-quadrant representations should be applied for the turbine characteristics in the transient analysis. Specific speed enables engineers to select four-quadrant curves to express the turbine. Because it is difficult to collect data of turbine characteristics during transient state conditions, steady-state model tests are used to plot four-quadrant characteristic curves. The turbine is always running at positive discharge and positive rotational speed. Hence, the graphical representation of the turbine can be expressed in the first quadrant with the parameters wicket gate opening, discharge, and head. Specific speed can be defined with the below equation.

$$n_{QE} = \frac{n\sqrt{Q}}{E^{\frac{3}{4}}} \tag{2.2}$$

where;

Q : Flow rate (m^3/s)

E : Specific hydraulic energy of machine (J/kg)

n : Turbine rotational speed (t/s)

Also, it can be expressed as;

$$n_s = \frac{n * \sqrt{P}}{H^{\frac{5}{4}}} \tag{2.3}$$

where;

P : Installed capacity of the turbine (kW)

n : Turbine rotational speed (rpm)

H : Piezometric head of the turbine (m)

The discharge and power output of the turbine are regulated by the wicket gate. Governor controls the wicket gate opening and closure to protect the turbine from runaway after sudden pressure changes because of transients. Then, the spiral case transmits water to the turbine uniformly. The stability of the flow is guaranteed by the wicket gate and spiral case. If the stability of the water flow cannot be satisfied, the frequency of the grid and generator are not equal, and energy generation stops.

2.4 Pressure Relief Valves

PRV is installed upstream of the turbine, and the PRV's efficiency increases if the PRV's location is close to the turbine. It controls the transients by reducing the rate of the net change in velocity of the flow and by discharging the water from the system. When the pressure amount in the pipeline reaches the set point limit, the valve opens to allow outflow of the water. After the pressure drops below the specified limit, the valve is closed completely. PRV can be controlled by a spring or weight. On the other hand, throttling valve type pressure regulating valves or pressure relief valves are controlled by a governor with the help of servomotors. Input data is entered to the governor system for opening and closing times according to wicket gate pattern. (Chaudhry, 1987).

Zhang K. et al. (2008) stated that the main difference between a regulating valve is the controller. Generally, regulating valves are controlled by a proportional integral derivative type controller in order to satisfy accurate and continuous maintenance of the set pressure limit in the system. On the other hand, a predefined pattern is entered into the controller of the relief valve, and it follows the path after triggered.

PRVs also can be used to supply water into the system to prevent negative pressures with a by-pass pipe. The minimum set pressure limit is defined to the PRV or controller system, and PRV is opened to decrease the adverse effects of pressure

drop in the penstocks by admitting water to system. Cavitation or column separation can be compensated with PRV. However, PRVs are not as efficient as surge tanks for negative pressures.

In KEPEZ – I HPP, PRV is mounted into the spiral case of the turbine unit with a by-pass pipe. The valve is connected to a servomotor which is controlled by the governor. Figure 2.5 indicates the PRV model of KEPEZ – I HPP. After PRV is triggered, the piston starts its movement, and the valve accepts the water from the by-pass pipe with an upward motion and opens the flow path.

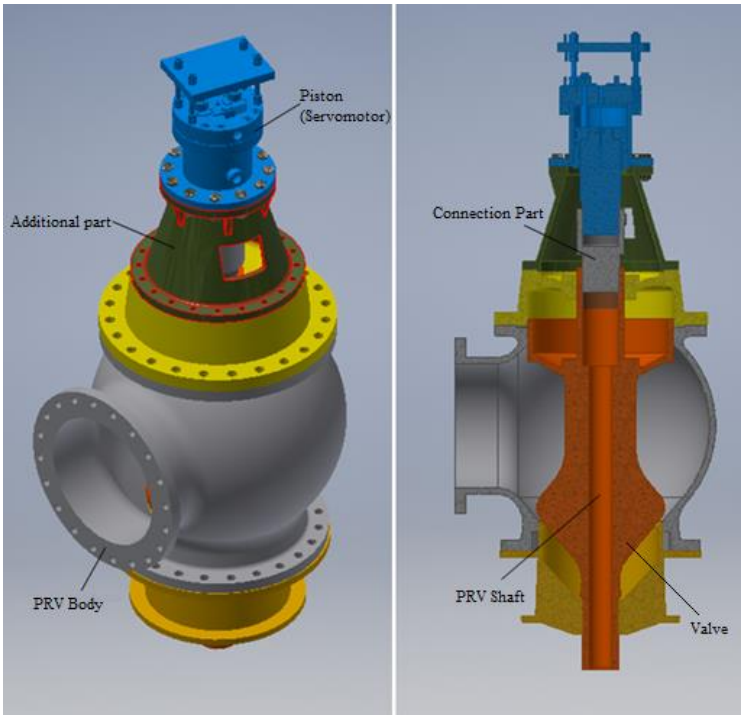

Figure 2.5 Model of PRV in KEPEZ - I HPP

A governor system regulates the PRV and wicket gate opening or closing rules with pressurized hydraulic oil system. Proportional valves determine the speed of the servomotors by defining the oil pressure amount that will flow to the pistons. There are two servomotors that control the wicket gate's guide vanes and one servomotor that regulate the PRV. Also, there are two different proportional valves that determine the rate of the servomotor movements separately for wicket gate and PRV.

Proportional valve controls the piston movement with a location sensor that is mounted on the piston. According to provided information, valve regulates the oil flow to maintain the rate of the operating rule. A user defines operating rules to the proportional valves in the governor system, and pistons are regulated per oil pressure. Therefore, PRV and wicket gate operating rules can be arranged with a combined algorithm that enables them to work together in order to reduce the adverse effect of water hammer. PRV does not need a set pressure limit to be triggered.

PRV leads local protection in the systems. It relieves the pressure or discharge in a portion of the pipeline system. Therefore, PRV should be mounted to the critical point exposed to excessive pressures or the occurrence point of the water hammer pressures. In KEPEZ – I HPP, PRV is directly mounted into the turbine's spiral case, which is the critical point for the system. Figure 2.6 indicates the photograph of the PRV in HPP. The piston and the pipes that convey the pressurized oil are shown in the above part of the PRV. The by-pass pipe that connects the spiral case and PRV and relief pipe that discharge the water to tail water channel are in the below part of the PRV.

Figure 2.6 Photograph of PRV in KEPEZ - I HPP

CHAPTER 3

TRANSIENT FLOW

The essential concepts and principles of transient flow are reviewed in this chapter. Firstly, transient flow definition is given, and derivation of the water hammer equations is expressed with the help of wave speed, continuity, and momentum equations. After that, a mathematical technique called the method of characteristics that converts two non-linear, hyperbolic partial differential equations into four ordinary differential equations is described.

3.1 Definition of Transient Flow

Steady flow can be described as a condition that pressure, discharge, and velocity do not change over time at any point in the system. On the other hand, unsteady flow occurs when the mentioned flow parameters are changed with respect to time at a specific location. It can be said that a steady state is a particular instance of unsteady flow. Therefore, equations of the unsteady flow must satisfy steady flow cases. The term “transient flow” is used to describe an intermediate-stage flow that is observed when the flow conditions alternate between two steady states.

Transient flow can be divided into two types: quasi-steady flow and true transient flow. The progressive variation of discharges and pressure with time is the key characteristic of the quasi-steady flow. As a result, the flow appears constant throughout short time intervals. However, fluid inertia, the elasticity of the liquid and the pipe are the main elements that influence the true transient flow. There are two types of true transient flow. If the pipe and flow elasticity does not affect the flow, it can be called rigid-column flow, and if these parameters affect the flow, it is called water hammer.

3.2 Water Hammer

A hydraulic transient, or pressure surge, happens when the steady-state velocity in a pipe system quickly changes. Water hammer is a type of unsteady flow because of these changes in direction and magnitude of the velocity. This phenomenon causes a sudden variation of pressure and forms waves in the water. The sound of the collision of waves to an object and the movement of water is like a hammering sound. Therefore, it is called water hammer. Dramatic increase or decrease of the water provides more stress to the elements of the system. There are many causes of water hammer which is mentioned as below;

- Pump operations may cause a rapid change in flow. The hydraulic grade line on the pump side may decrease under the pipeline elevation or increase dramatically with the collapse of the void spaces. Pressure reaches vapor pressure value and causes column separation and cavitation with a decrease in hydraulic grade line, or high pressures can be occurred because of a sudden increase in the hydraulic grade line.
- Valve operations may cause high or low pressures in the penstock system. While closing or opening the valve, pressure changes will occur if the critical time determined from the wave speed and penstock length is not satisfied.
- Hydraulic turbine operations result in changes in the velocity and pressure of the water. When the turbine is closed with power failure, the governor starts to close wicket gate. If the wicket gate can not be closed in the required time, turbine can take damages, and if the wicket gate is closed more rapidly than the critical time, pressure will increase dramatically. In addition, in load acceptance case, discharge variation causes changes in parameters.
- Additionally, since energy equation parameters will change, water level alterations in reservoirs lead to pressure increase or decrease. Earthquakes, winds or landslides, power failures, emergency closures may affect the system's velocity, and water hammer may occur.

- If protective measures such as pressure relief valve, surge tank, air chambers are located, selected or operated wrongly, they may cause transient flow in the hydropower plants.

There has been extensive research on the causes and investigation of water hammer. Modeling of the water hammer is another main research subject for scientists. It is started with Joukowsky (1898), who carried out many experiments for transient flow. He came up with Equation 3.1 at the end of his experiments.

$$\Delta P = \pm \rho a \Delta V \tag{3.1}$$

where,

ΔP : Pressure increase in N/m^2

ρ : Fluid density in kg/m^3

a : Acoustic pressure wave speed through the fluid in the pipe in m/s

ΔV : The change in the velocity of the flow in m/s

In rapid closure cases, the above equation can be used to determine the pressure change. Rapid closure is described as a closure that takes less time than the wave reflection period. The time it takes for a wave to travel the length of a pipe and return to its source is known as wave reflection period. The wave reflection time for a pipe length "L" is 2L/a. It is also called critical time period. As a result, if the closure time is less than 2L/a, it is considered rapid, and if it is larger than 2L/a, it is called gradual closure. Upstream closures are represented by a plus sign in the equation, whereas a minus sign means downstream pipeline closures.

Chaudhry (1987) explained the water hammer concept with the below figures and expressions. In Figure 3.1, a simple, frictionless piping system with a valve is indicated, and flow is in steady-state at the beginning. At time zero (t=0), the valve is supposed to be closed instantly. Flow behavior can be observed from the below figures for different time intervals. Minor losses and friction losses are not taken into account in the figures. The duration of $0 < t \leq L/a$ is represented in Figure 3.1.

Pressure head increases as $\Delta H = (a/g)V_0$ because of a sudden closure of valve and decrease of velocity to zero. In the pressure head rise equation, the wave speed is a, the gravitational acceleration is g, and the initial velocity is V_0.

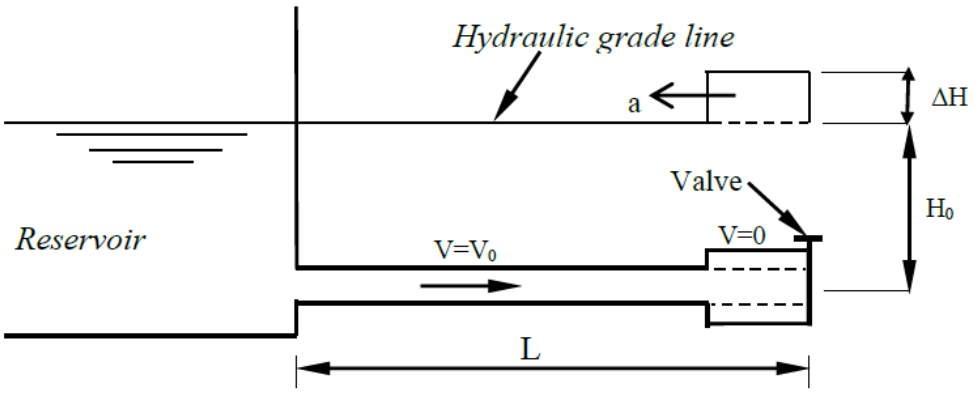

Figure 3.1 Water hammer effect in time between $0 < t \leq L/a$ (Chaudhry, 1987)

When the wave reaches the reservoir at t=L/a, the pressure head rise is felt, which is ΔH. Figure 3.2 indicates the status of the flow at $L/a < t \leq 2L/a$ time interval. The head of the reservoir does not change, which is H_0. There is inequality at the reservoir end at time t=L/a. As a result, flow occurs with a velocity $-V_0$ from pipe to reservoir. Therefore, head decreases from $H_0+\Delta H$ to H_0. Finally, the head of every section of the pipe is Ho when pressure wave is back to valve at t=2L/a

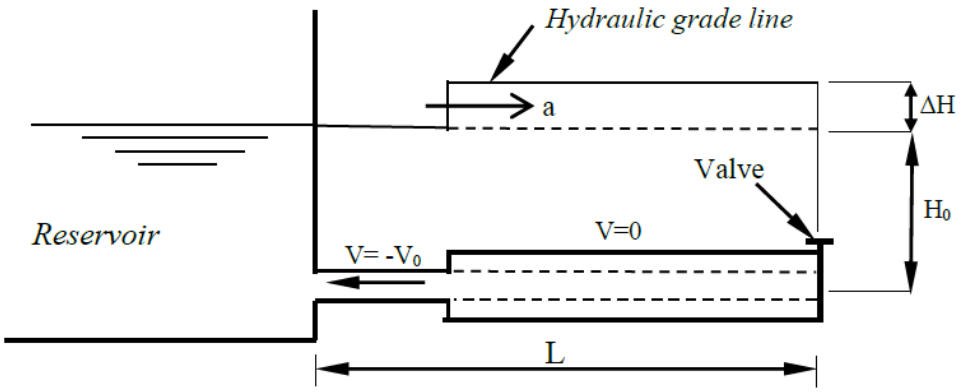

Figure 3.2 Water hammer effect in time between $L/a < t \leq 2L/a$ (Chaudhry, 1987)

In Figure 3.3, the flow conditions can be analyzed for the interval 2L/a <t ≤ 3L/a. At t=2L/a, the velocity decreases to zero as the reverse flow cannot be maintained any longer, which causes a sudden pressure decrease at the valve end by ΔH. Then, pressure head reduces to H_0-ΔH. Flow stops at time t=3L/a, and pressure head becomes H_0-ΔH.

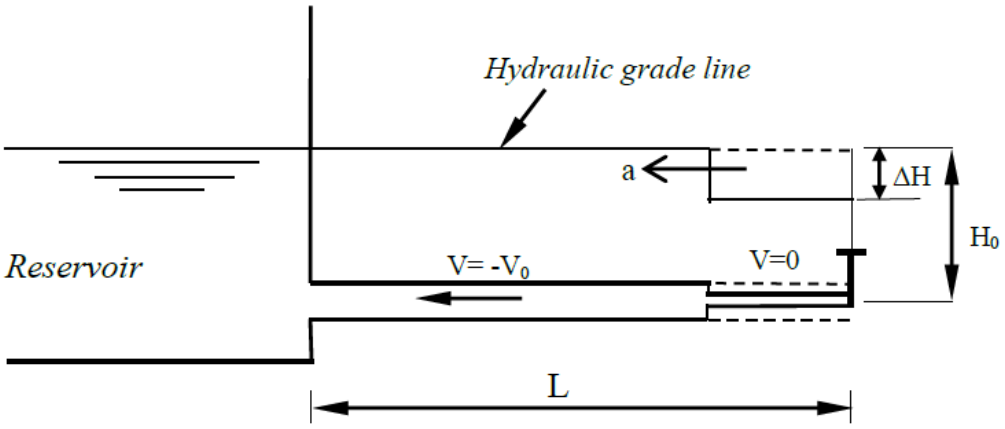

Figure 3.3 Water hammer effect in time between 2L/a < t ≤ 3L/a (Chaudhry, 1987)

Figure 3.4 indicates the conditions of the flow for the interval 3L/a < t ≤ 4L/a. The negative pressure head that occurs at the valve end breaks the balance at the reservoir end. The pressure at the pipe is lower than the pressure at the reservoir end. As a result, flow returns to the pipe with V_0, and pressure head becomes H_0.

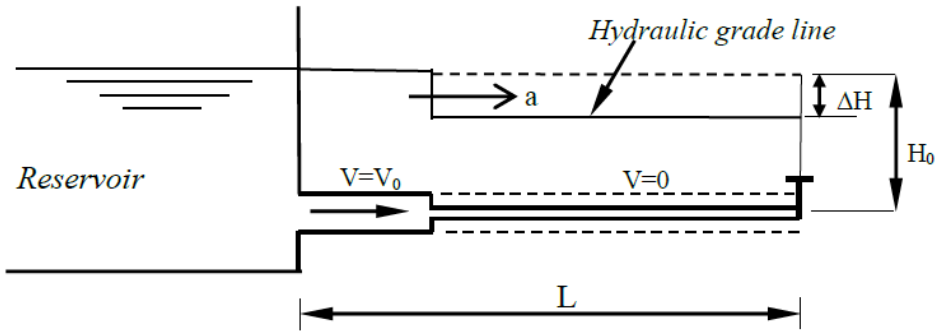

Figure 3.4 Water hammer effect in time between 3L/a < t ≤ 4L/a (Chaudhry, 1987)

This phenomenon repeats itself for every 4L/a time period, and if there is no friction or head losses in the system, it can proceed forever. Consequently, a sudden valve closure results in variations in the pressure head and velocity of the flow. The above explanations and figures can help to understand the water hammer concept.

3.3 Derivation of The Acoustic Wave Speed Equation

The momentum equation, Equation 3.2, for unsteady conditions is applied to the control volume, as shown in Figure 3.5. After starting of transient flow conditions in the control volume, it is observed that the wave is traveling to the left from right at a velocity of (a-V_0).

Velocity variation, ΔV, is directly related to pressure head increase, ΔH. The change in pressure head and velocity results in the formation of a force whose magnitude is ρgΔHA in the negative x-direction.

$$\sum \vec{F} = \frac{\partial}{\partial t}\int_{C.V.} \vec{V}\rho d\forall + \int_{C.S.} \vec{V}\,\rho(\vec{V}.\vec{n})dA \qquad (3.2)$$

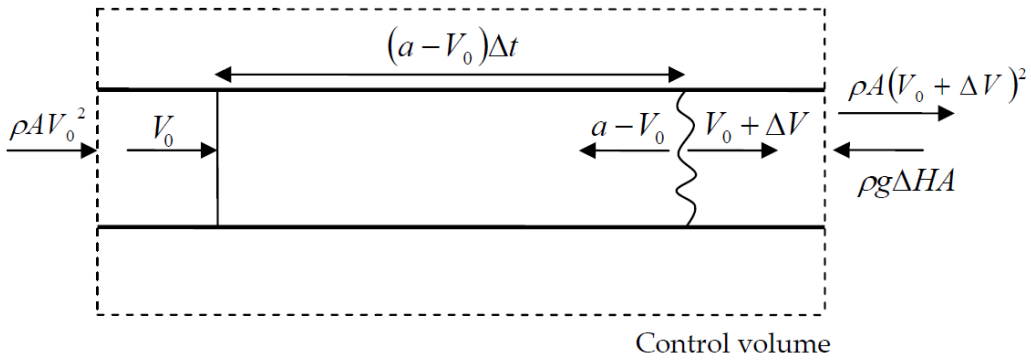

Figure 3.5 Control volume and momentum equation components (Calamak, 2010; Wylie et al., 1993)

After simplifying the momentum equation, the equation becomes:

$$-\gamma \Delta H A = \rho A(a - V_0)\Delta V + \rho A(V_0 + \Delta V)^2 - \rho A V_0^2 \qquad (3.3)$$

where;

γ	:	specific weight of fluid (N/m^3)
ρ	:	mass density of fluid (γ/g) (kg/m^3)
g	:	acceleration of gravity (m/s^2)
A	:	cross-sectional area of pipe (m^2)
V_0	:	initial velocity (m/s)
ΔV	:	increment of flow velocity (m/s)
a	:	wave speed to be determined (m/s)
ΔH	:	increment of head change (m)

From Equation 3.3, the negligible terms can be removed as the term ΔV^2 has a very small value. Then, we obtain;

$$\Delta H = -\frac{a\Delta V}{g}\left(1 + \frac{V_0}{a}\right) \cong -\frac{a\Delta V}{g} \qquad (3.4)$$

Acoustic speed is much larger than the initial velocity of the fluid. Therefore, Vo/a is also a negligible component of the equation. If the flow stops entirely because of the full closure of the valve, the final velocity will be zero, ΔV will be equal to – Vo, and ΔP will equal aV_0/g. If incremental closure pattern is defined to the valve which is at the end of the pipe, the equation can be arranged as below;

$$\sum \Delta H = -\frac{a}{g}\sum \Delta V \qquad (3.5)$$

The equation can be used for closure times up to the time t = 2L/a, which defines the time before the pressure waves reach the valve end after they are reflected from the reservoir end.

Since the velocity changes, a sudden pressure increase will affect the pipeline length as deformation per support type of the pipes. If it is assumed that the stretching of the pipe is ΔS at L/a seconds with a velocity of ΔSa/L, ΔV will be ΔSa/L-V_0. The mass of the fluid that entered the pipe is $\rho A V_0 L/a$ during t= L/a. This mass is accounted for by three components, namely, the mass filling the increased cross-sectional area ΔA, the mass filling the pipe extension ΔS, the mass increase in the entire pipe due to $\Delta\rho$, compression of the liquid density. This is shown in Figure 3.6 and expressed by the continuity equation, Equation 3.6 below;

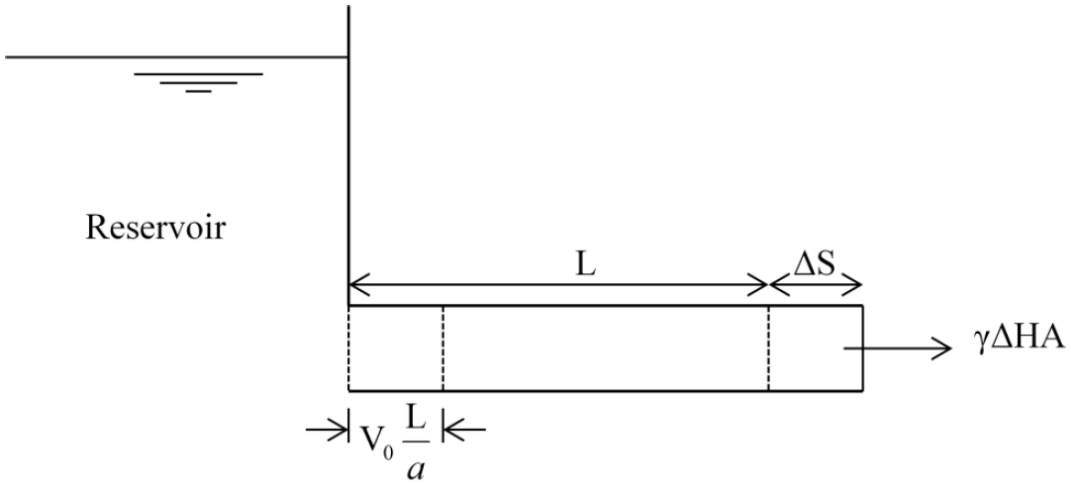

Figure 3.6 Parameters of continuity equation (Dursun, 2013; Streeter & Wylie, 1967)

$$\rho A V_0 \frac{L}{A} = \rho L \Delta A + \rho A \Delta s + L A \Delta \rho \tag{3.6}$$

ΔV= ΔSa/L-V_0 equality is used for simplification of equation and elimination of V_0,

$$-\frac{\Delta V}{a} = \frac{\Delta A}{A} + \frac{\Delta \rho}{\rho} \tag{3.7}$$

$\Delta V=V_f - V_i$ equality can be written into Equation 3.7,

$$a^2 = \frac{g\Delta H}{(\Delta A/A) + (\Delta\rho/\rho)} \tag{3.8}$$

Equation 3.8 can be rearranged by using the definition of the bulk modulus of elasticity of the fluid, K, as below;

$$K = \frac{\Delta p}{\Delta\rho/\rho} = -\frac{\Delta p}{\Delta\forall/\forall} \tag{3.9}$$

Equations 3.7 and 3.8 becomes by using bulk modulus of elasticity definition;

$$a^2 = \frac{K/\rho}{1 + (K/A)(\Delta A/\Delta p)} \tag{3.10}$$

$\Delta A/\Delta p$ will be very small for very thick-walled pipes resulting in $a \approx \sqrt{K/\rho}$ expression. On the other hand, the 1 on the denominator of Equation 3.10 becomes unimportant for very flexible pipes, resulting in Equation 3.11.

$$a \approx \sqrt{\frac{A}{\rho}\frac{\Delta p}{\Delta A}} \tag{3.11}$$

Regarding thin-walled pipes, supporting type is becoming a significant factor for wave speed equation. Using circumferential tensile forces, which are indicated at the end of the section and stresses acoustic speed equation is finalized as below;

$$a = \frac{\sqrt{K/\rho}}{\sqrt{1 + [(K/E)(D/E)]c_1}} \tag{3.12}$$

The support type of the pipe is defined with a constant c_1, and conditions are determined with the help of Poisson's ratio μ. When the pipe is anchored at its upstream end only, $c_1=1-\mu/2$, if pipe is anchored throughout against axial movement, then c_1 equals $1-\mu^2$, and if the pipe is anchored with expansion joints throughout, $c_1=1$.

Poisson's ratio depends on the axial (σ_1) and lateral (σ_2) unit stress in the pipe wall, also called Hoop Stresses. Lateral unit stress can be found from circumferential tensile force per unit length of pipe (T_f). Figure 3.7 indicates the forces on the semi-cylinder of pipe segment.

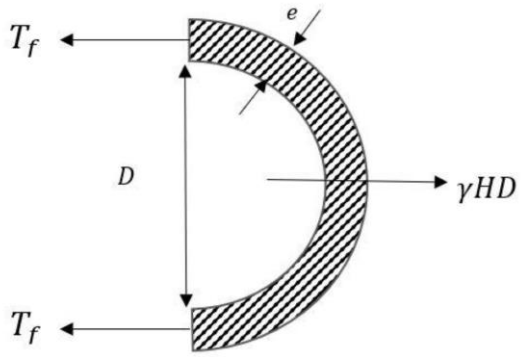

Figure 3.7 Free-body diagram of semi-cylinder of a pipe

In order to obtain the stresses that occur because of the water hammer, the free-body diagram is used. According to Figure 3.7, Hoop stresses can be written as below;

$$\sigma_2 = \frac{T_f}{e} = \frac{\gamma HD}{2e} \quad or \quad \Delta\sigma_2 = \frac{\gamma D\Delta H}{2e} = \frac{D\Delta p}{2e} \tag{3.13}$$

$$\sigma_1 = \frac{\gamma HA}{\pi De} = \frac{p\pi r^2}{2\pi re} = \frac{Dp}{4e} \tag{3.14}$$

where e is the thickness of pipe wall, D is the pipe inside diameter, and A is the pipe flow area.

3.4 Governing Equations of Transient Flow

The transient flow analysis aims to determine the main parameters such as velocity, V or discharge, Q and pressure, P or piezometric head, H at a specific location and

time while water hammer phenomena proceed. In order to find these variables, momentum and continuity equations have an essential role. The Law of mass conservation is used for the continuity equation, and Newton's second law of motion is used for the momentum equation. All the variables for the momentum equation are indicated in Figure 3.8. Pressure is assumed to be distributed uniformly over the control surfaces, flow is assumed to be slightly compressible, and flow is one-dimensional, and pipe walls can be deformed as they are assumed to be elastic.

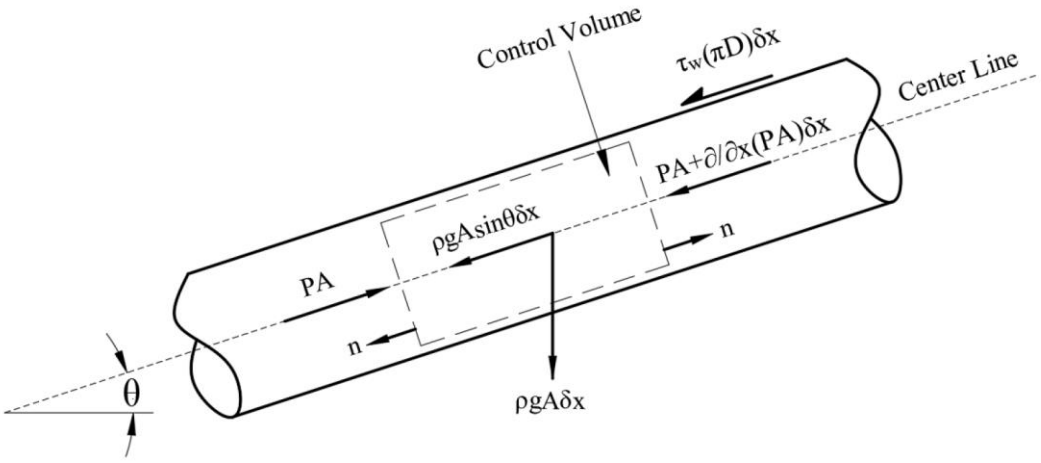

Figure 3.8 Control volume that indicates parameters for momentum equation

Applying the conservation law of mass and Newton's second law of motion to the above control volume, continuity and momentum equations of unsteady flow in a pipe in partial differential forms can be obtained as below;

Continuity Equation:
$$\frac{\partial P}{\partial t} + V\frac{\partial P}{\partial x} + \rho a^2 \frac{\partial V}{\partial x} = 0 \qquad (3.15)$$

Momentum Equation:
$$\frac{\partial V}{\partial t} + V\frac{\partial V}{\partial x} + \frac{1}{\rho}\frac{\partial P}{\partial x} + g\sin\theta + \frac{4\tau_w}{\rho D} = 0 \qquad (3.16)$$

where,

ρ	:	Mass density of fluid (kg/m^3)
P	:	Pressure (N/m^2)
V	:	Velocity of the fluid (m/s)
a	:	Acoustic wave speed (m/s)
τ_w	:	Wall shear stress (N/m^2)
D	:	Diameter of the pipe (m)
g	:	Gravitational acceleration (m/s^2)

The continuity and momentum equations cannot be solved by using a closed-form solution. Next, these equations will be transformed into four ordinary differential equations by the Method of Characteristics which is also used in the Bentley HAMMER software.

3.5 Solution of Transient Flow Equations by Method of Characteristics

Method of characteristics transforms partial differential equations into four ordinary differential equations and enables numerical solutions by integrating the equations for two dependent variables: velocity and pressure. (Wylie et al., 1993).

Since the method of characteristics can model simulation of steep wavefronts correctly, illustrate wave propagation, easy programming of the systems and computations, analyzing one-dimensional water hammer events can be understood with method of characteristics without any obligation. (Chaudhry, 1987)

The continuity equation is denoted with L_1, and the momentum equation is denoted with L_2 to put them in the following form.

$$L_1 + \lambda L_2 = 0 \tag{3.17}$$

After specifying the F term in the momentum equation as $\frac{4\tau_\omega}{\rho D} + gsin\theta$, Equation 3.17 can be described as below;

$$\frac{\partial P}{\partial t} + V\frac{\partial P}{\partial x} + \rho a^2 \frac{\partial V}{\partial x} + \lambda\left(\frac{\partial V}{\partial t} + V\frac{\partial V}{\partial x} + \frac{1}{\rho}\frac{\partial P}{\partial x} + F\right) = 0 \qquad (3.18)$$

The re-arranged form of Equation 3.18 is,

$$\left[\frac{\partial P}{\partial t} + \left(V + \frac{\lambda}{\rho}\right)\frac{\partial P}{\partial x}\right] + \lambda\left[\frac{\partial V}{\partial t} + \left(V + \frac{\rho a^2}{\lambda}\right)\frac{\partial V}{\partial x}\right]\lambda F = 0 \qquad (3.19)$$

Below mathematical expression is known from calculus as chain rule for a function θ of x and t,

$$\frac{d\theta}{dt} = \frac{\partial \theta}{\partial t} + \frac{\partial \theta}{\partial x}\frac{dx}{dt} \qquad (3.20)$$

If the below constraints are satisfied, chain rule can be applied for P and V,

$$\frac{dx}{dt} = V + \frac{\lambda}{\rho} = V + \frac{\rho a^2}{\lambda} \qquad (3.21)$$

As a result, Equation 3.19 can be written as,

$$\frac{dP}{dt} + \lambda\frac{dV}{dt} + \lambda F = 0 \qquad (3.22)$$

"λ" can be found from Equation 3.21,

$$\lambda = \pm\rho a \qquad (3.23)$$

Then, "λ" is substituted into constraints of Equations 3.21. Since the magnitude of velocity is much smaller than the magnitude of wave speed, velocity is neglected,

$$\frac{dx}{dt} \cong \pm a \qquad (3.24)$$

Equation 3.24 demonstrates two straight lines, which are called characteristics lines, and they are demonstrated in Figure 3.9. The slope of characteristics lines are "+1/a" and "-1/a" and represent the change in wave location per change in time. By substituting Equation 3.23 into Equation 3.22, the final form of characteristics and compatibility equations are found as below,

$$C^+: \quad \frac{1}{\rho}\frac{dP}{dt} + a\frac{dV}{dt} + aF = 0 \quad if \quad \frac{dx}{dt} = +a \tag{3.25}$$

$$C^-: \quad \frac{1}{\rho}\frac{dP}{dt} - a\frac{dV}{dt} - aF = 0 \quad if \quad \frac{dx}{dt} = -a \tag{3.26}$$

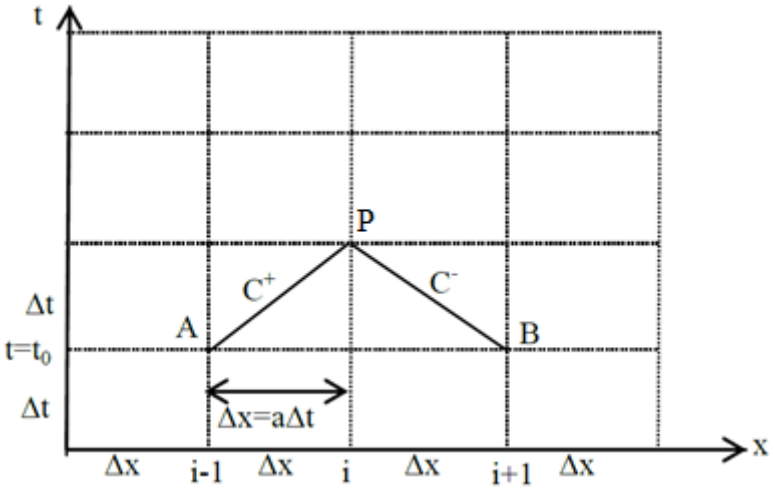

Figure 3.9 Characteristics Lines in x-t solution domain

Figure 3.9 indicates the characteristics lines in x-t plane. C+ characteristics line has the slope of "+1/a," and C^- characteristics line has the slope of "-1/a" representing Equations 3.25 and 3.26. These lines demonstrate the path of the transient flow physically. Pipe is divided into many nodes and reaches with a length of Δx. The time step, Δt, should satisfy Courant Condition, which is $\Delta x/\Delta t \leq a$.

Compatibility equations can be solved if the dependent variables pressure, P and velocity, V, are known at locations A and B from either initial conditions for $t=t_0$ or previous step computations. Then, pressure and velocity at point P are calculated for $t=t_0+\Delta t$ by integrating compatibility equations simultaneously along characteristics lines.

$$C^+: \quad \int_A^P \frac{1}{\rho a}dP + \int_A^P dV + \int_A^P F dt = 0, \qquad \int_A^P dx = \int_A^P a dt \tag{3.27}$$

$$C^-: \quad -\int_B^P \frac{1}{\rho a} dP + \int_B^P dV + \int_B^P F dt = 0, \qquad \int_B^P dx = -\int_B^P a dt \quad (3.28)$$

It is assumed that quasi-steady friction is valid in transient conditions, and the term with the shear stress is expressed by Equation 3.29 by replacing the wall shear stress with its equivalent of $\frac{f}{8}\rho V^2$ to write it in terms of velocity. V^2 term is written $V|V|$ to account for the reverse flow.

$$\frac{4\tau_w}{\rho D} = f\frac{V|V|}{2D} \quad (3.29)$$

In Equations 3.27 and 3.28, "F" is integrated, and Equation 3.29 is substituted into these equations,

$$C^+: \quad \int_{t_A}^{t_P} F dt = g \sin\theta \Delta t + \frac{f}{2D} V_A|V_A|\Delta t \quad (3.30)$$

$$C^-: \quad \int_{t_B}^{t_P} F dt = g \sin\theta \Delta t + \frac{f}{2D} V_B|V_B|\Delta t \quad (3.31)$$

Compatibility equations can be simplified, which are Equations 3.25 and 3.26, by taking integrals of them and naming Equation 3.30 as G_A and Equation 3.31 as G_B,

$$C^+: \quad (P_P - P_A) + \rho a(V_P - V_A) + \rho a G_A = 0 \quad (3.32)$$

$$C^-: \quad -(P_P - P_B) + \rho a(V_P - V_B) + \rho a G_B = 0 \quad (3.33)$$

After arranging Equations 3.32 and 3.33,

$$V_P = \frac{1}{2}\left[(V_A + V_B) + \frac{1}{\rho a}(P_A - P_B) - (G_A + G_B\right] \quad (3.34)$$

$$P_P = \frac{1}{2}[(P_A + P_B) + \rho a(V_A - V_B) - \rho a(G_A - G_B] \quad (3.35)$$

Additionally, Equations 3.25 and 3.26 (compatibility equations) can be written in terms of piezometric head, H, and discharge Q instead of pressure, P, and velocity, V, respectively. After Courant Condition is satisfied for Δt, Equation 3.29 is substituted into compatibility equations by multiplying these equations with "$a\frac{dt}{g} = \frac{dx}{g}$". Integral of the equation can be taken along C^+ line with using pipe area to write the equation in terms of discharge.

$$\int_{H_A}^{H_P} dH + \frac{a}{gA}\int_{Q_A}^{Q_P} dQ + \frac{f}{2gDA^2}\int_{x_A}^{x_P} Q|Q|dx = 0 \qquad (3.36)$$

Then, Equation 3.26 is integrated similarly along the C^- line, and Equation 3.36 is simplified,

$$C^+: \quad H_P = H_A - B(Q_P - Q_A) - RQ_A|Q_A| \qquad (3.37)$$

$$C^-: \quad H_P = H_B + B(Q_P - Q_B) + RQ_B|Q_B| \qquad (3.38)$$

where,

$$B = \frac{a}{gA} \qquad and \qquad R = \frac{f\Delta x}{2gDA^2}$$

These equations must hold for steady flow, which is a special case of unsteady flow. For steady conditions the flows are equal, $Q_A = Q_P = Q_B$, and $RQ_A|Q_A|$ is the steady-state friction head loss over the reach Δx.

The equations are also written for section *i* in general form,

$$C^+: \quad H_{Pi} = C_P - BQ_{Pi} \qquad (3.39)$$

$$C^{-}: \quad H_{Pi} = C_M + BQ_{Pi} \tag{3.40}$$

where,

$$C_P = H_{i-1} + BQ_{i-1} - RQ_{i-1}|Q_{i-1}| \tag{3.41}$$

$$C_M = H_{i+1} - BQ_{i+1} + RQ_{i+1}|Q_{i+1}| \tag{3.42}$$

By using the general formula of the characteristics lines equation above, transient flow behavior is computed for many time steps, and the piezometric head and discharge values can be obtained for any point. While time steps decrease, computations provide more accurate information about the transient event.

CHAPTER 4

COMPUTER SOFTWARE

4.1 Necessity of Computer Program

The continuity and momentum equations, which are hyperbolic, quasi-linear partial differential equations, describe transient flow in closed conduits. Although many methods are developed to solve the equations and understand the behavior of the transients, results can be obtained manually only for simple pipeline systems. Solving the equations needs complex mathematical calculations, and it is a time-consuming event because of iterations. As a result, computer software enables users to decrease computational errors and save time from calculations for complex pipeline systems and boundary conditions.

In this study, Bentley HAMMER is used to solve the continuity and momentum equations and simulate the hydropower plant model. Computer software solves method of characteristics equations that convert non-linear, hyperbolic partial differential equations into ordinary differential equations for large and complicated pipeline systems. Using Bentley HAMMER has many advantages, which are expressed as below;

- Since model can be formed and analyzed before the construction of the systems, appropriate precautions can be suggested in order to prevent any damage after operation of the plants.
- HAMMER has many properties that enable users to import drawings and form models on existing projects.
- Each element can be analyzed one by one with necessary results and parameters so that a problem can be simplified and solved quickly.
- Since the data input system is simple, a hydropower plant can be modeled without missing members, and protective measures can be applied for

different scenarios. HAMMER leads to comparison of all scenarios and alternatives in one window.

- Results can be observed with graphical representations with animations that indicate hydraulic head, pressure, turbine speed, etc.

Because HAMMER has many advantages, it contributes this study to analyze hydropower plant with turbines for many critical scenarios. Modeling hydraulic turbines is simple, and results help find any system problem. After validating the model in HAMMER with measured data in the field, critical cases are observed to suggest any protective measure so that the hydropower plant is covered from many risks in the future.

4.2 Interface and Toolbars of the Bentley HAMMER

Bentley HAMMER has an easy-to-use interface, and toolbars can be adjustable per user requirements. Users can access every necessary element in one window if the location of the lay-outs, members, result screen, and short-cuts are adjusted and personalized. Figure 4.1 indicates interface of the software in the beginning.

Toolbars enable users to reach many features in developing the model or comparing results. All the toolbars will be explained one by one in the below part. However, there is a toolbar that has been added to HAMMER recently. “Home” toolbar is available in the last versions of the computer program. It can be explained as the summary of all the toolbars because commonly used features from different toolbars are collected into one window. Therefore, users can develop the model and compare the results without using other tabs. Elements can be observed in “Home” toolbar from Figure 4.1.

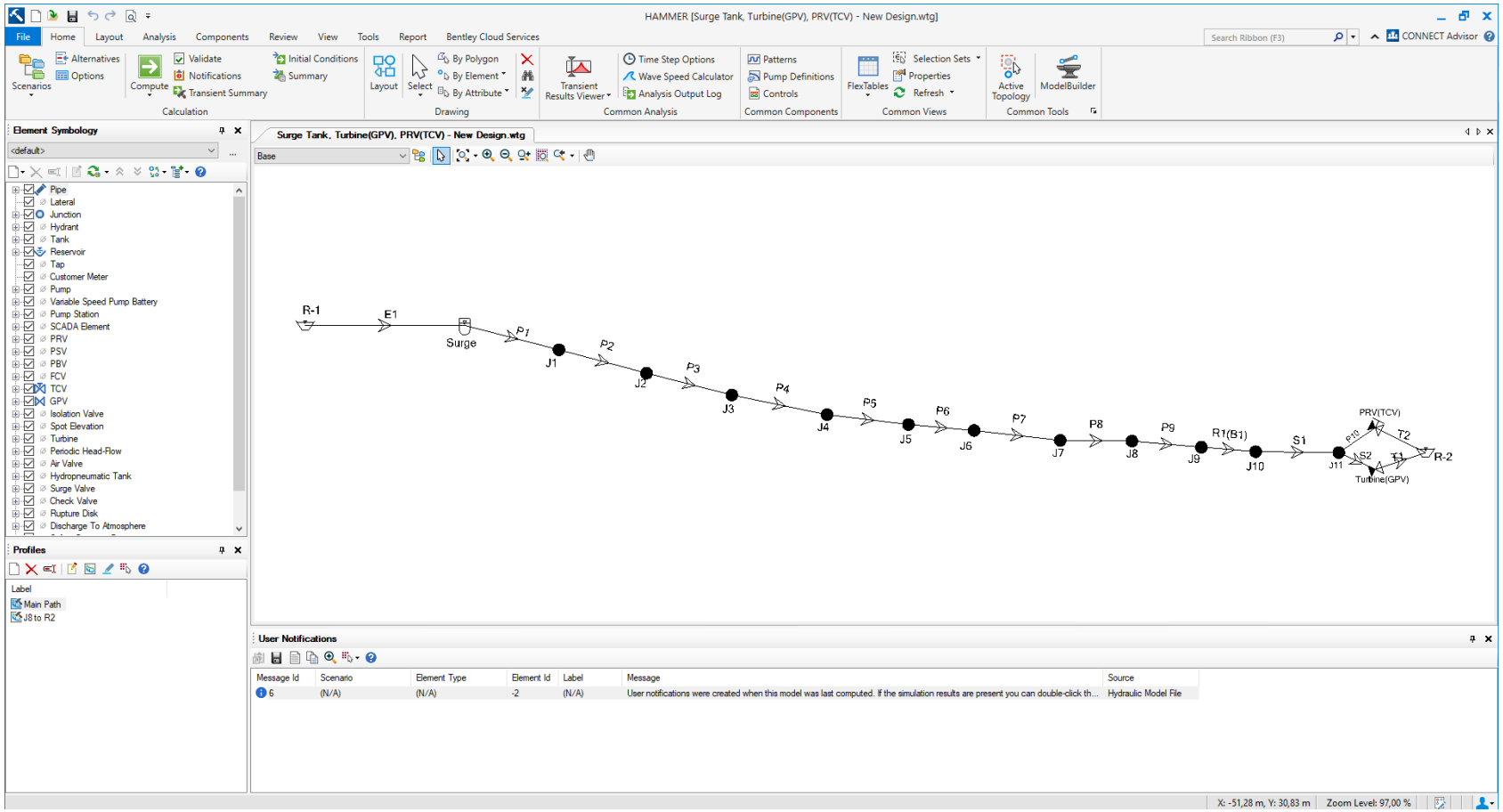

Figure 4.1 Default Interface of HAMMER

In HAMMER, there are eight different toolbars, and every toolbar is categorized per its properties. The first toolbar is named “File” from left to right. Users can create or open a new project, save or print the file and use export or import commands.

“Layout” toolbar includes all the members such as pipe, junction, PRV, turbine, for a hydropower system to develop a HAMMER model. Users can construct a model easily by using the features in this toolbar.

Scenarios, alternatives, and calculation options can be arranged from the “Analysis” toolbar. Analysis toolbar enables users to compare the results for different scenarios or cases and different models with different members, such as protective measures.

“Calculation Options Property” is under the analysis toolbar, and it helps to arrange steady-state and transient conditions, determines report period and time step. Figure 4.2 indicates details of the calculation options window for transient and steady-state conditions.

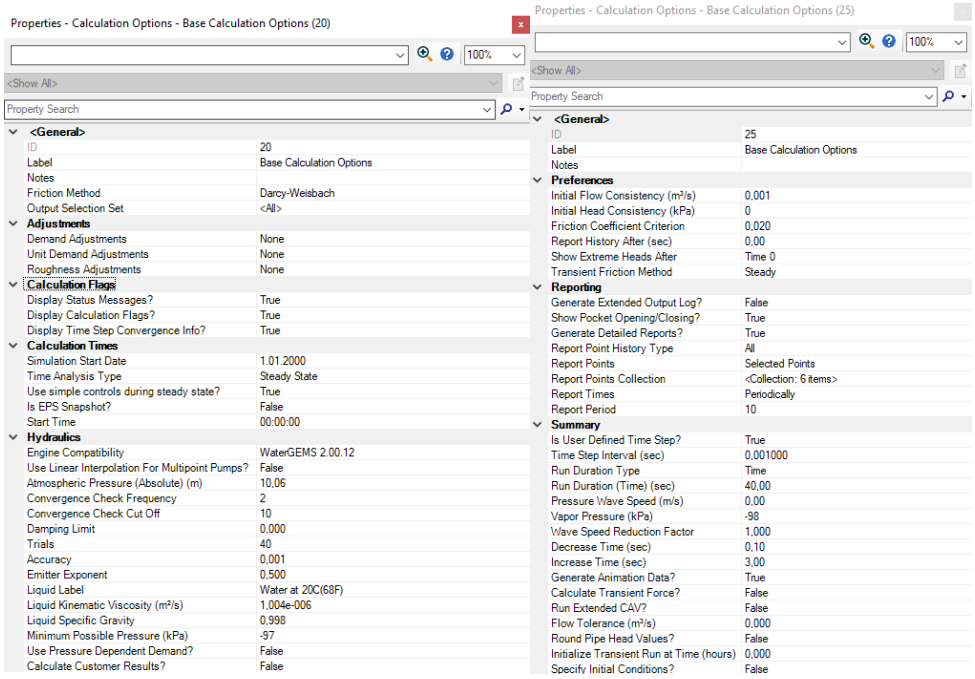

(a) (b)

Figure 4.2 Calculation options window for (a) initial conditions and (b) transient analysis

Analysis toolbar also includes transient results viewer which is shown in Figure 4.3, which provides graphical representations of the results. There are many types of showing the results in HAMMER. Users can analyze the results such as hydraulic grade, pressure on profile with a sketch or view the results directly on a graph with respect to time. Additionally, properties of the specific elements such as turbine speed, wicket gate closure can be observed from "Extended Node Data."

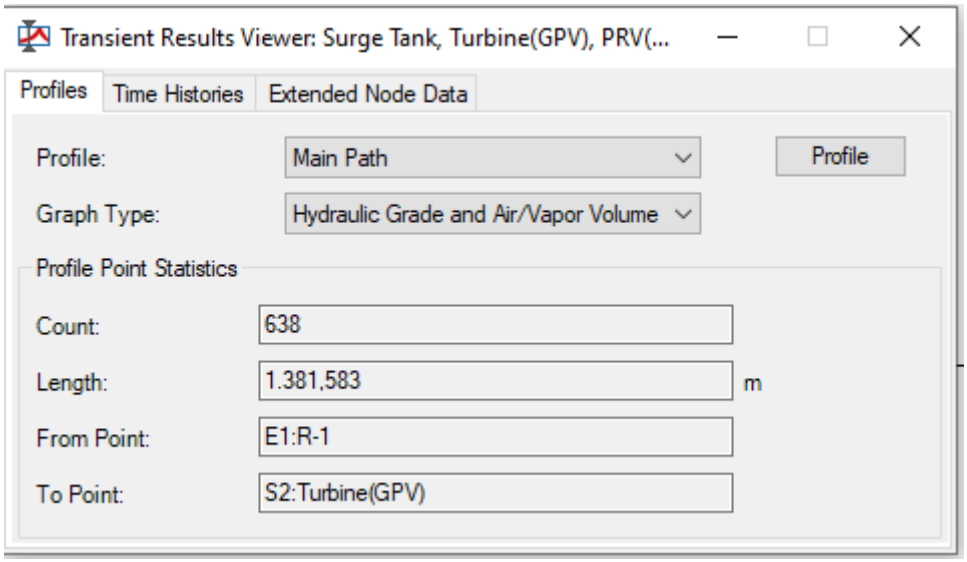

Figure 4.3 Transient Results Viewer

User can illustrate many graphics by using "Transient Results Viewer. In water hammer analysis, in order to understand transient flow behavior, different types of graphics are analyzed and observed, such as pressure versus time graphs, discharge versus time graphs, hydraulic grade variation along the penstock. These graphics lead to understanding the phenomenon in the hydropower plant and realization of the critical points in the penstocks or other members. HAMMER provides animations in the graphics, and it enables users to open different graphs and analyze all the variations in separate windows simultaneously. There are many different alternatives that indicate the hydraulic grade, pressure, velocity, vapor pressure for determined flow paths in "Profile" section. "Time Histories" indicates the pressure, flow, hydraulic grade versus time graphs for specified points. Figure 4.4 indicates an example of pressure and flow versus time graph at a point which is on turbine inlet.

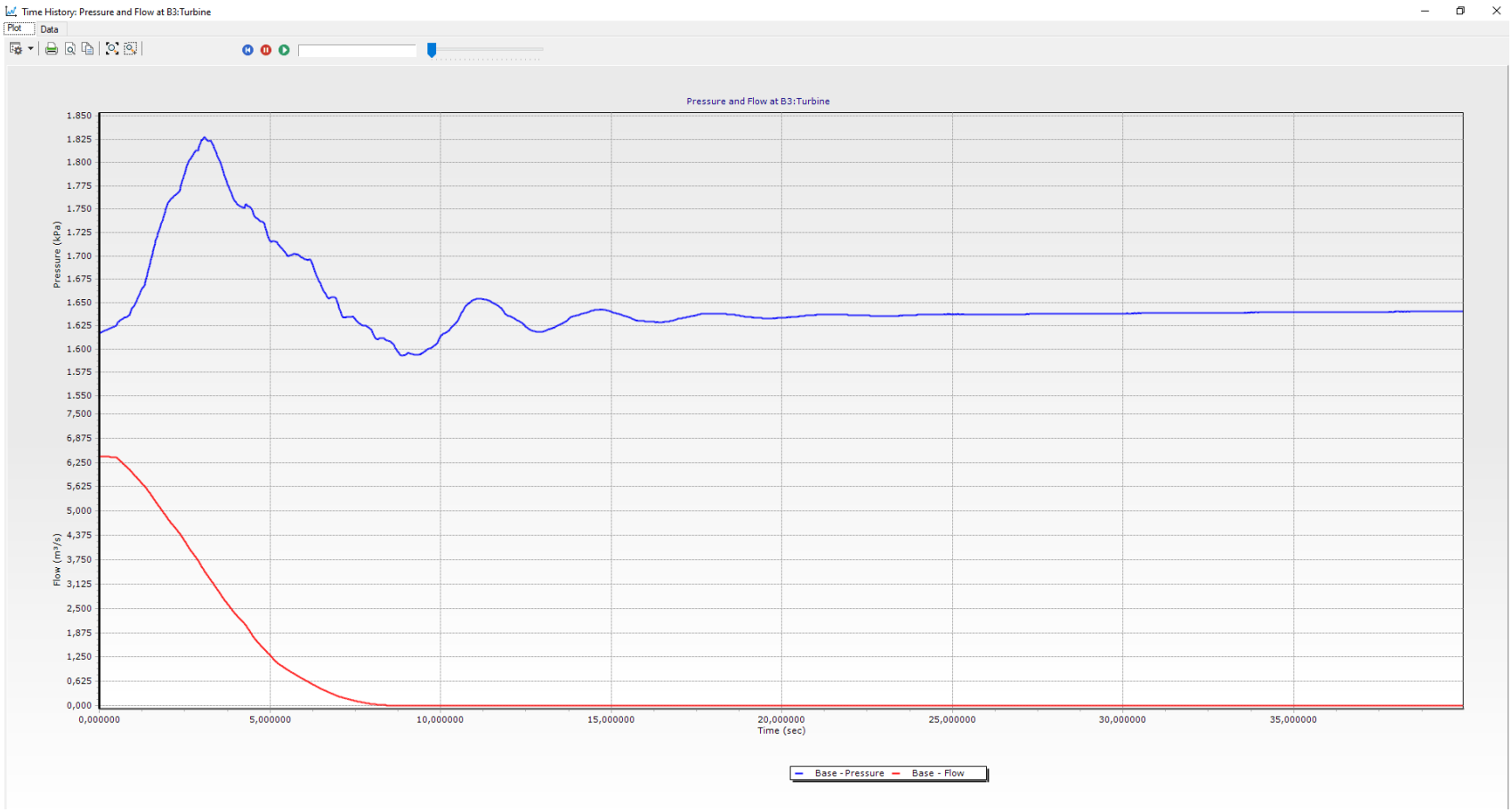

Figure 4.4 Pressure and Flow versus Time graph

Calculation summary is another property under the analysis tool that summarizes demanded, supplied, and stored flow. Transient calculation summary indicates the results of the simulations. After simulation and calculations are finished, this window opens automatically and enables users to see the summary of the operation such as time step, total simulated time, initial condition results, maximum and minimum pressures in transient analysis. Figure 4.5 presents an example of transient calculation summary property.

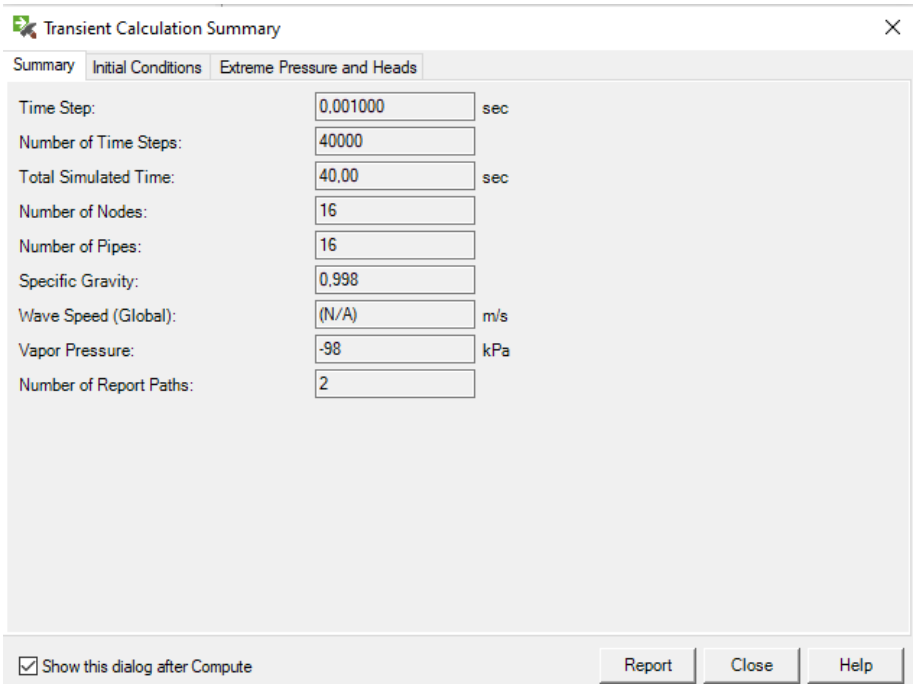

Figure 4.5 An example of Transient Calculation Summary

In order to reveal errors in input data before running initial or transient computations, "Validate" tool can be used in the analysis section. After validation of the model is completed, a user runs the model using compute initial conditions and compute buttons.

One of the other toolbars is "Components." Controls feature enables to check whether an element is working and the status of the in the simulation. Elements can be separated section by section, and changes can be defined for many model elements using the "Zones" tool. Generally, it is used in modeling water supply systems with

water demand amounts. Patterns property leads to regulate valve closure or opening such as wicket gate, PRV, TCV. Users can define %relative closure or %opening versus time graphs to arrange the operating rule of the valves. Since every pipe has its minor loss, coefficients can be entered into the program as input data from the "Minor Loss Coefficients" tool. HAMMER helps to find related material coefficients from its library.

View toolbar includes graphs, profiles, and flextables properties. Flextables indicate many parameters and results of elements such as pipes, junctions in a table. The table columns can be adjusted per user requirements, and values of the properties can be changed from flextables whose example is given in Figure 4.6.

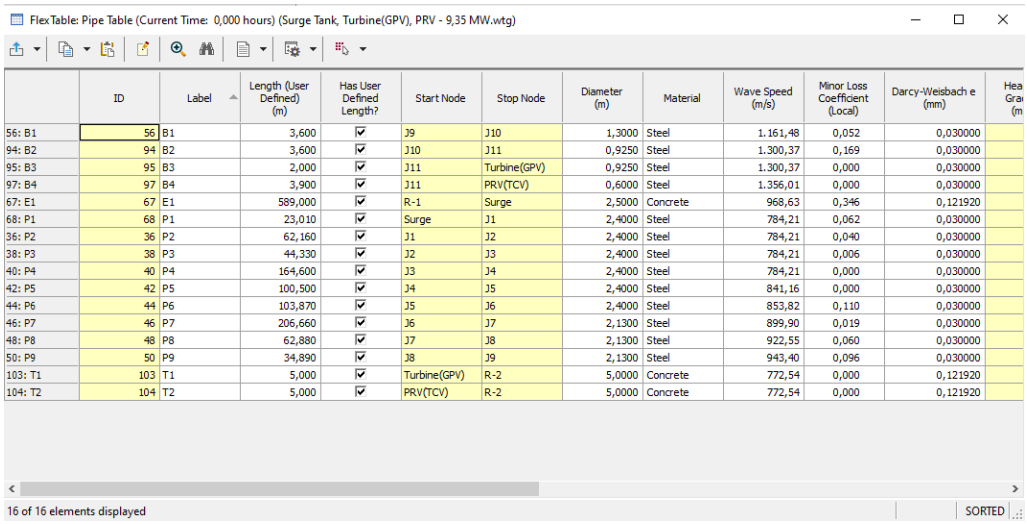
FlexTable: Pipe Table (Current Time: 0,000 hours) (Surge Tank, Turbine(GPV), PRV - 9,35 MW.wtg)

	ID	Label	Length (User Defined) (m)	Has User Defined Length?	Start Node	Stop Node	Diameter (m)	Material	Wave Speed (m/s)	Minor Loss Coefficient (Local)	Darcy-Weisbach e (mm)	Hea Gra (m
56: B1	56	B1	3,600	☑	J9	J10	1,3000	Steel	1.161,48	0,052	0,030000	
94: B2	94	B2	3,600	☑	J10	J11	0,9250	Steel	1.300,37	0,169	0,030000	
95: B3	95	B3	2,000	☑	J11	Turbine(GPV)	0,9250	Steel	1.300,37	0,000	0,030000	
97: B4	97	B4	3,900	☑	J11	PRV(TCV)	0,6000	Steel	1.356,01	0,000	0,030000	
67: E1	67	E1	589,000	☑	R-1	Surge	2,5000	Concrete	968,63	0,346	0,121920	
68: P1	68	P1	23,010	☑	Surge	J1	2,4000	Steel	784,21	0,062	0,030000	
36: P2	36	P2	62,160	☑	J1	J2	2,4000	Steel	784,21	0,040	0,030000	
38: P3	38	P3	44,330	☑	J2	J3	2,4000	Steel	784,21	0,006	0,030000	
40: P4	40	P4	164,600	☑	J3	J4	2,4000	Steel	784,21	0,000	0,030000	
42: P5	42	P5	100,500	☑	J4	J5	2,4000	Steel	841,16	0,000	0,030000	
44: P6	44	P6	103,870	☑	J5	J6	2,4000	Steel	853,82	0,110	0,030000	
46: P7	46	P7	206,660	☑	J6	J7	2,1300	Steel	899,90	0,019	0,030000	
48: P8	48	P8	62,880	☑	J7	J8	2,1300	Steel	922,55	0,060	0,030000	
50: P9	50	P9	34,890	☑	J8	J9	2,1300	Steel	943,40	0,096	0,030000	
103: T1	103	T1	5,000	☑	Turbine(GPV)	R-2	5,0000	Concrete	772,54	0,000	0,121920	
104: T2	104	T2	5,000	☑	PRV(TCV)	R-2	5,0000	Concrete	772,54	0,000	0,121920	

16 of 16 elements displayed SORTED

Figure 4.6 Flextable of pipes

In order to examine results such as hydraulic grade, pressure for different water paths in the model, user forms profiles and decides which elements will be included with the help of Profiles tools. This tool indicates the location of the components in case of elevation and illustrates a sketch of the model. Horizontal axis indicates the distance from reservoir, and vertical axis shows the elevation. Users can select all the points in the model to have a general thought about the difference between hydraulic grade line and elements in the system. Figure 4.7 shows an example of a profile.

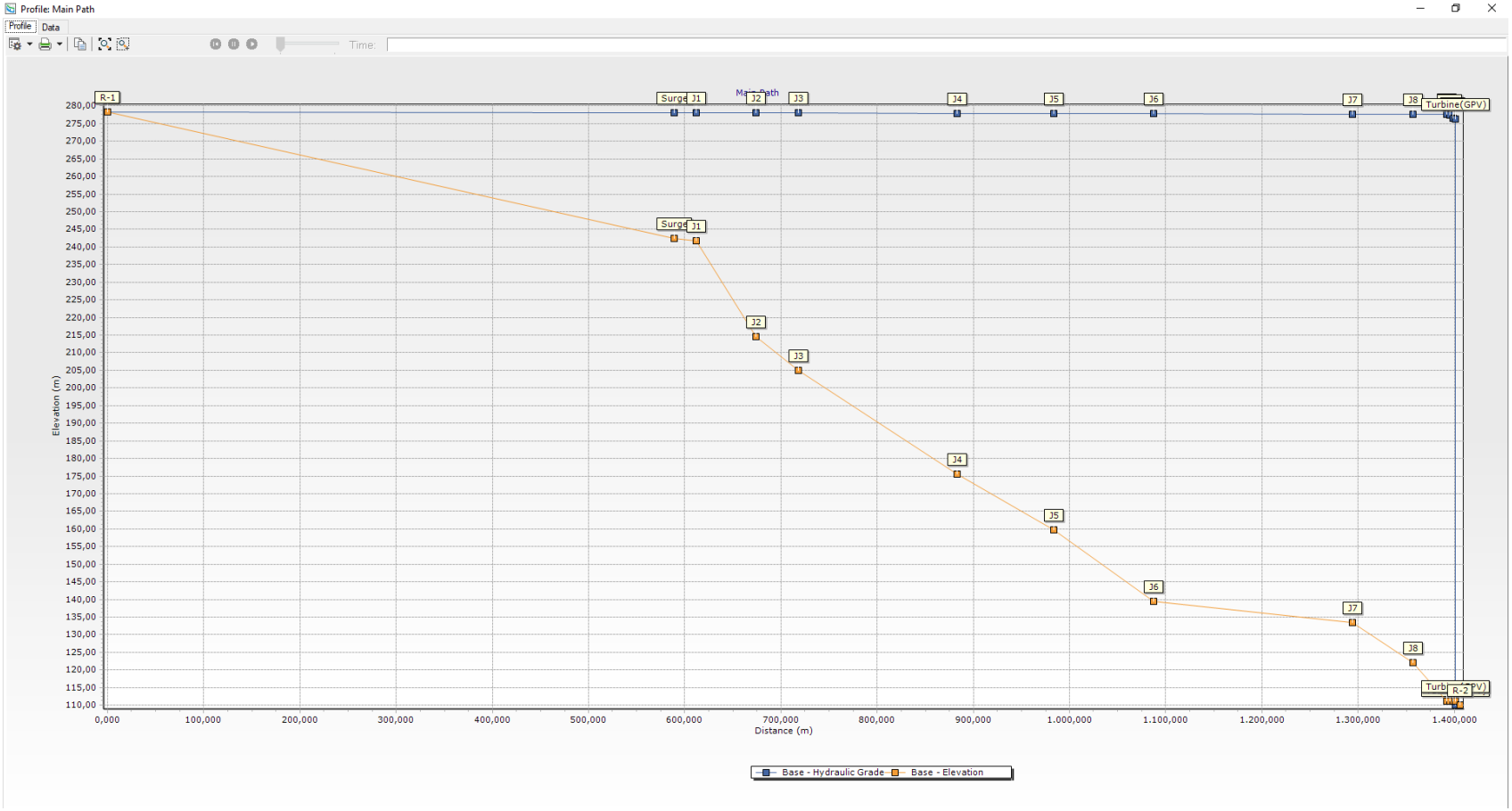

Figure 4.7 Profile that illustrates the water flow path and hydraulic grade line along the penstock

There is “Properties” menu for every element that includes details of the selected one. The user can see input data, transient analysis results, initial conditions, labels, etc. In addition to that, many variables can be changed or entered for a single selected element. Figure 4.8 indicates the properties menu for a turbine and a pipe.

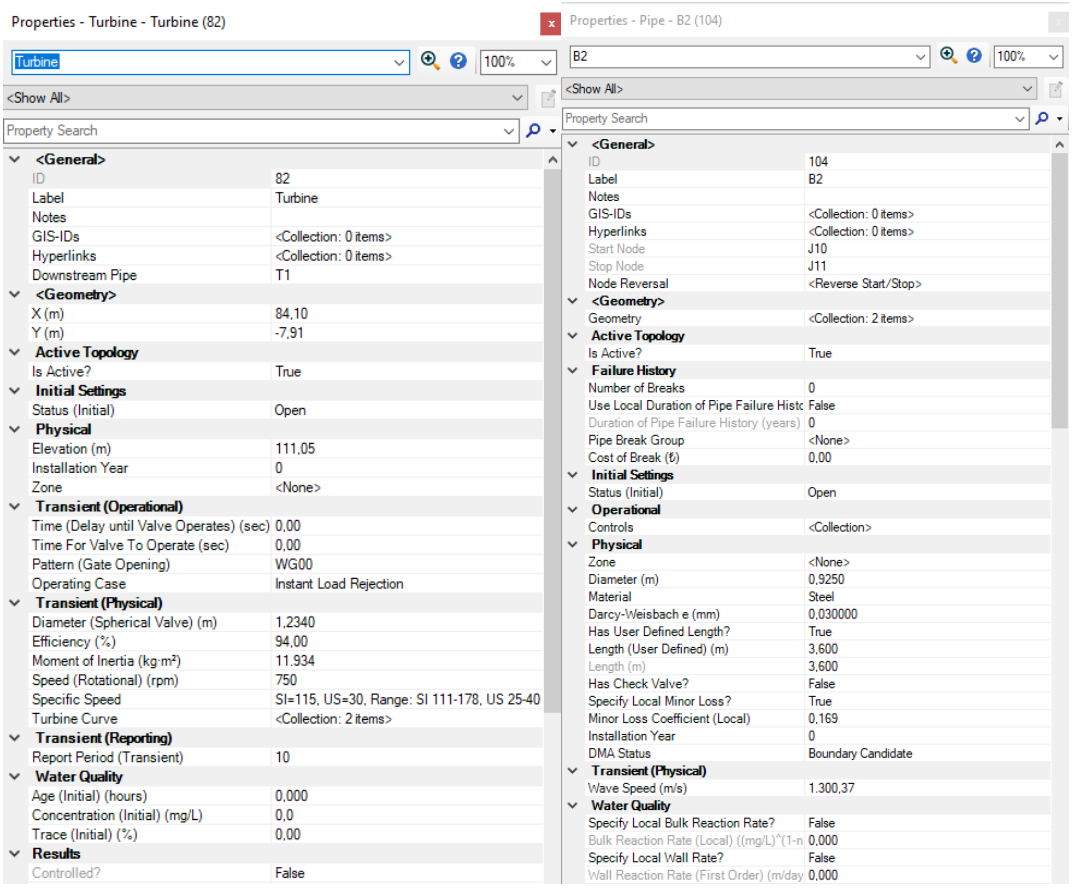

Figure 4.8 Properties menu for a pipe and a pipe

CHAPTER 5

CASE STUDY AND DISCUSSION OF RESULTS

In this chapter, the transients in KEPEZ – I Hydropower plant are studied. Firstly, the hydropower plant is introduced briefly, and information about the structure of the facility is given. Then, validation of the HAMMER model is presented with the methodology of the process. The results of the validated model and measured field data are compared and discussed for different scenarios. Finally, simulations are held without PRV to investigate the PRV effect on the system.

5.1 Information about KEPEZ-I Hydropower Plant

Kepez – I Hydropower Plant is located in Kepez, Antalya. This HPP is founded on the Duden river, which poured into the Mediterranean Sea. Flow comes from Kepez – II Hydropower Plant's tailwater to Kepez – I HPP's forebay. The Hydropower plant started its operation in 1961, and Kepez – II HPP was commissioned for energy production in 1986, which is located upstream of Kepez – I HPP. KEPEZ – I has three Francis type turbines, each having an installed capacity of 8.8 MW amounting to total installed capacity of 26.4 MW. Kepez – I HPP produces 114,008,133 kWh of electricity daily, and it can meet all electrical energy needs of 34,444 people in their daily life.

Kepez – I HPP is investigated and analyzed to improve the facility's conditions and efficiency. A rehabilitation project is developed for this purpose, named MILHES Project by TUBITAK and TOBB University of Economics and Technology. MILHES Project aims to change the turbines with more efficient ones so that the efficiency and power capacity is increased in the hydropower plant with new design approaches of turbines. Design of the turbine, calculation of the fluid mechanics and

transient analysis, testing, and manufacturing of the turbine model is performed by TOBB University of Economics and Technology. MILHES Project started in 2015 to design and produce a Francis turbine, generator, speed regulator, and SCADA systems with local means.

FENSU Engineering Construction Energy Company visited the KEPEZ – I HPP site to investigate the components of the facility and control the status of structures. Then, they calculated the hydraulic losses, net heads, and gross heads for each turbine by using provided data in the field and projects. It was observed that inside of the penstocks were covered with a layer of lime due to the working conditions over time. However, since the calcination in penstocks is cleared before the tests, it is not considered in the calculations of the study.

KEPEZ – I HPP forebay is fed directly from the water coming from Kepez – II HPP. Firstly, water accumulates in the artificially created pond before the forebay, and it is rested in the pond to prevent any unnecessary energy loss for the system. The water is supplied to the forebay with a rack system. There is a lateral spillway in order to evacuate the oscillations out of headpond that may occur in the case of shutdown due to turbine operating conditions in the forebay. In addition, since fluctuations can be dissipated by decreasing the energy of the flow, there are energy-breaking structures in the canal. After water reaches the headpond, it is conveyed to the energy tunnel with an intake structure which is illustrated in Figure 5.1. One of the canals was canceled after an artificial pond had been constructed because this canal directly conveys the water from KEPEZ – II HPP downstream to KEPEZ – I headpond without resting the flow in the created pond. The rack system in the intake structure has a 35 mm space between them. After water is transmitted to the energy tunnel, it is transferred to the turbines through the penstocks for energy production. A ventilation pipe is placed at the entrance of the penstock system to prevent pressure going below vapor pressure.

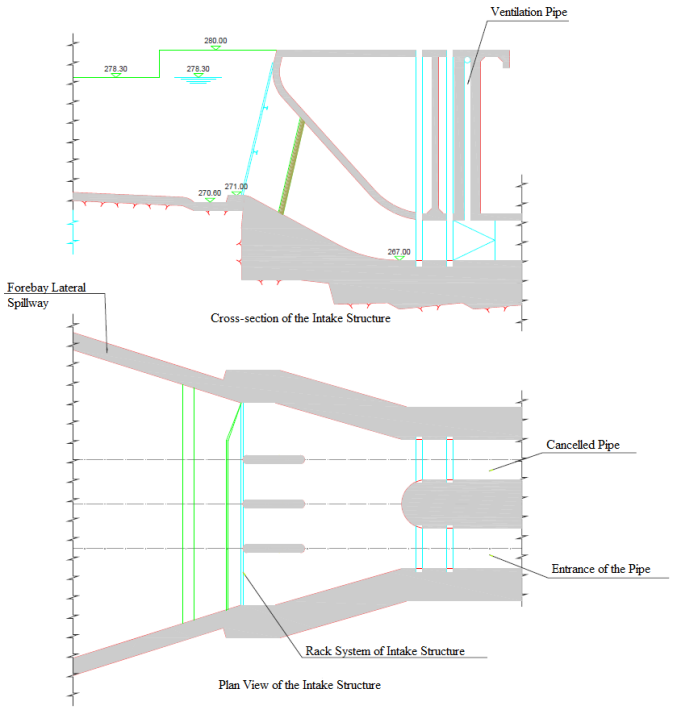

Figure 5.1 Plan view and Cross-Section of Intake Structure

Energy tunnel transports the water from forebay to surge tank. It has a concrete circular cross-section with a 2.5 m diameter and 589 m length with one vertical bend in its direction.

There is a surge tank at the connection of the energy tunnel and the penstock. Surge tank is constructed to prevent any pressure increase or negative pressure because of transient events. However, since the pressure relief valve is directly mounted to the turbines' spiral case, pressure waves that occur in sudden shutdown situations are damped directly near the turbine region before reaching the surge tank. On the other hand, the surge tank is more functional for load acceptance cases since it speeds up the water supply to the turbines and would theoretically prevent pressures from going below dangerously low values. The structure has a 5 m internal diameter at the connection point with energy tunnel and penstock below the ground level, and the total height of the tank is 55.55 m from the foundation level. Because of the land elevations, it has 50.05 m height from the ground level. The inner diameter of the surge tank is 5 m from ground level to 39.05 m height. The inner diameter becomes

9 m from 39.05 m height to the top of the surge tank. The diameter of energy tunnel increases slightly and is connected to the inner section of surge tank with a slight slope. Figure 5.2 indicates a photograph of the surge tank.

Figure 5.2 Surge Tank of Kepez – I HPP

After the surge tank, a steel penstock starts with 2.4 m diameter and 499 m length. Then, the diameter decreases to 2.13 m along 305 m in length. Penstocks convey the water to the powerhouse, and turbines extract the energy of the flow before being conveyed to tailwater canal with a draft tube. In the powerhouse, penstock is separated by a branch to distribute water to three turbines. Then, the second branch divides the water for PRV and turbine. Table 5.1 includes the pipe parameters for the system.

Table 5.1 Pipe parameters

	Material	**Diameter (m)**	**Length (m)**
Energy Tunnel	Concrete	2.5	589
Penstock 1	Steel	2.4	499
Penstock 2	Steel	2.13	305
Branch 1	Steel	1.3	3.6
Branch 2	Steel	0.925	5.6
Tailwater Tunnel	Concrete	5	5

There are three Francis type turbines in the powerhouse. The design discharge of the turbines is 6.05 m^3/s, but the system flow rate changes per operating power of the turbines. In this study, validation of the model process is held for 8.5 MW and 9.35 MW power generation. As a result, the discharge is 5.82 m^3/s for 8.5 MW and 6.41 m^3/s for 9.35 MW. Turbine characteristics are shown in Table 5.2. Additionally, pressure relief valve is in the powerhouse. It is mounted to the turbine spiral case with a by-pass pipe. There is a branch in turbine spiral case, and pipeline is separated for turbine and PRV. The downstream of the PRV is connected to the tailwater channel, so discharged water is conveyed downstream of HPP.

Table 5.2 Basic Characteristics of Turbines in HPP

Type	Francis Turbine
Number of Turbine Units	3
Installed Capacity (MW)	3 x 8.8
Rated Speed (rpm)	750
Rated Discharge (m^3/s)	3 x 6.1
Nominal Gross Head (m)	168.28
Moment of Inertia ($kg.m^2$)	11.394

The tailwater channel width is 4 m, and the bottom elevation of the tailwater is 108.85 m. If only one turbine is operated, the water level is 110.04 m in the channel and 278.3 m in the reservoir. The gross head of the turbine is calculated as 168.26 m. Since the net head depends on the minor and friction losses in the system, it changes according to wicket gate opening, generated energy, or operated discharge. FENSU computed minor and friction losses, and calculations are gathered into a hydraulic loss report, (FENSU, 2015). In the present study, those loss calculations are used in the model.

5.2 Model Development and Validation Methodology

Three different steps are followed to validate the simulation results with measured data and form the scenarios. A different model is developed for each step. Firstly, input data are gathered for the model from the KEPEZ – I HPP projects. Figure 5.3 indicates the HAMMER model that includes all the components of the system.

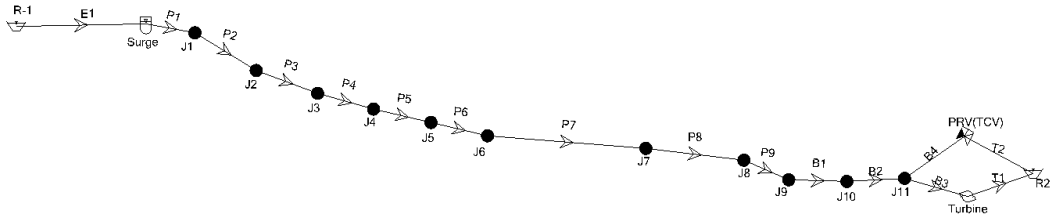

Figure 5.3 HAMMER Model

Flow is conveyed from reservoir having a water surface elevation of 278.3 m to surge tank by concrete energy tunnel. Corresponding surge tank steady-state water surface elevation is 278.04 m. Then, steel penstock transmits the water to the turbine whose center elevation is 111.05 m, and water reaches the tailwater level with 110.04 m elevation after energy dissipation is completed in the turbine. Table 5.3 indicates the elevations for the main nodes.

Table 5.3 Elevations of Main Nodes in Model

Node	**Elevation (m)**
Reservoir 1	278.3
Surge Tank (bottom)	242.5
Turbine	111.05
PRV	111.05
Reservoir 2	110.04

According to design drawings of the HPP, pipe nodes are determined per bends, expansions, contractions, and branches in the pipeline system. Therefore, the model has 11 junctions between the surge tank and the rehabilitated turbine. All the pipe parameters are collected from the design drawings, and wave speed for each pipe is

calculated accordingly. Table 5.4 shows the pipe parameters. Although there are three turbines with PRV in the facility, simulations are done for only one turbine operation. Since the rehabilitation project is applied on one turbine, tests are held for that turbine, and results are collected.

Table 5.4 Pipe characteristics

Pipe Name	Length (m)	Diameter (mm)	Thickness(mm)	Wave Speed (m/s)
E1	589.00	2500	200.0	968.63
P1	23.01	2400	9.0	784.21
P2	62.16	2400	9.0	784.21
P3	44.33	2400	9.0	784.21
P4	164.60	2400	9.0	784.21
P5	100.50	2400	11.0	841.16
P6	103.87	2400	11.5	853.82
P7	206.66	2130	12.0	899.90
P8	62.88	2130	13.0	922.55
P9	34.89	2130	14.0	943.40
B1	3.60	1300	10.0	1161.48
B2	3.60	925	300.0	1300.37
B3	2.00	925	300.0	1300.37
B4	3.90	600	300.0	1356.01
T1	5.00	5000	200.0	772.54
T2	5.00	5000	200.0	772.54

Since the PRV is mounted onto spiral case of the turbine with a by-pass pipe, branch is determined as “Junction 11,” and pipe is divided for the PRV and the turbine. The PRV is modeled as a throttle control valve in HAMMER model because it is operated without a set pressure limit in the field. It works with an algorithm that depends on the wicket gate pattern. Turbine governor controls the turbine wicket gates and the PRV, and servomotor closing or opening rate is entered to the governor by users during the field tests. User defines a behavior manually to the wicket gates and PRV in order to decrease pressure waves, and governor system works per this behavior. PRV and wicket gates have different hydraulic proportional valves in the governor that control the speed of the servomotors. These valves are working with pressurized oil, and pressure is regulated per required speed for servomotors that control the

opening or closing of PRV and wicket gates. PRV is directly connected to a servomotor, but guide vanes are connected to a regulating ring with small shafts. Every blade of the wicket gate has a shaft, and shafts are connected to the regulating ring that is controlled by servomotors. Figure 5.4 indicates the working principle of servomotors and regulating ring. There are two different servomotors to hold the mechanism. As one piston moves forward, the other moves back, and regulation ring turns in order to open or close wicket gate blades. All the system is connected to each other in the governor system. Therefore, servomotors of the wicket gates and PRV work together in order to control water hammer pressures. There are location sensors on the servomotors that warn the proportional valves to regulate the oil pressure in the governor. Governor arranges the pressure in the oil pipes according to the described algorithm, and controls the speeds of servomotors for PRV and wicket gate simultaneously. As a result, when the water pressure increases in the hydropower plant, PRV and wicket gate patterns work together. PRV directly starts to open soon after the wicket gate closure is initiated to prevent high pressures to be generated. Since different proportional valves control the components, their behavior may not be the same because of operation differences.

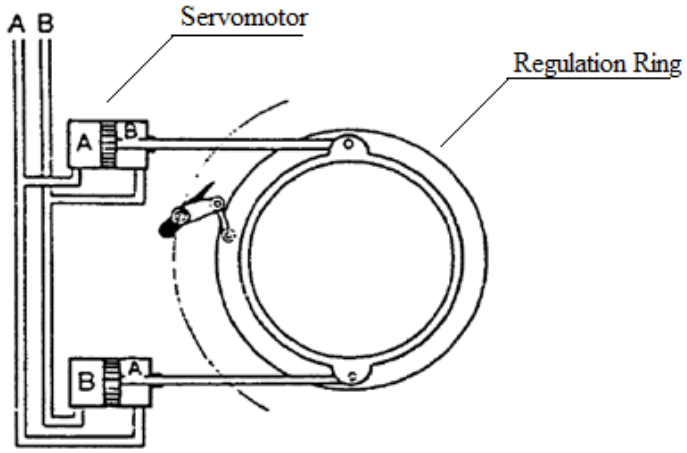

Figure 5.4 Operation Principle of Wicket Gate (Krivchenko, 1994)

Since pistons or servomotors control the wicket gates and PRV, there is a difference in measured data patterns and model operating rules. Location sensors are mounted to pistons that control the opening or closing of the PRV and wicket gate in the tests, so collected data give linear behavior for the operating rules of the wicket gate and PRV. Since pistons move forward or backward along a line, provided data can not reflect the valve pattern correctly. Piston movement regulates the wicket gate blades' position with angular motion. In addition, PRV and wicket gate are modeled as a circle valve in HAMMER. While a circle valve is opening or closing, the percentage of the pattern can not increase or decrease linearly. Therefore, this difference between the measured data and simulations is applied approximately.

As mentioned before, in order to validate the HAMMER model, three different models are developed to reach a final model whose results are close to measured data in the field tests.

- Case-1: HAMMER model has surge tank and General Purpose Valve (GPV) simulating the Turbine only but considering the PRV effect in its behavior.
- Case-2: HAMMER model has surge tank, GPV simulating the turbine only, and Throttle Control Valve (TCV) simulating PRV only.
- Case-3: HAMMER model has surge tank, Turbine, and TCV simulating PRV.

In the field, tests are held for different generated power values. However, two powers of 8.5 MW and 9.35 MW are used for this study. The discharge determines these operating capacities because turbine power is directly proportional to discharge. Flow rate is regulated with the wicket gate opening percentage in the field. However, since the discharge data are not measured in the field, Case-1 is developed to find the reference flow rate data for the next steps of validation methodology. Although pressure, turbine speed, wicket gate, and PRV pattern data are available for the tests, discharge should be determined to understand the system response. Therefore, Case-1 is formed only with GPV simulating the turbine in the HAMMER. PRV is not added to the system in that case, but its effect, that is, releasing water from the system

is considered. Then, by using the reference discharge data obtained from Case-1, wicket gate and PRV pattern approximations are determined in Case-2. Therefore, GPV remains as acting like the turbine, and PRV is added to the model by using TCV in the second case. Finally, all the inferences and results are collected and applied to the model in Case-3. Model results are checked with the turbine speed, pressure variation, wicket gate, and PRV operating rules of measured data. In Case-3, because the turbine feature is added to the mode, rotational speed of the turbine is validated with field test results as a final step. According to the data taken from the field tests, the maximum turbine speed is 995 rpm for 8.5 MW test and 1035 rpm for the 9.35 MW test. On the other hand, HAMMER does not collect data for extended nodes after wicket gate opening drops below 20%. Therefore, results are obtained until that point, and maximum rotational speeds are determined according to the graphic pattern in the simulations of Case-3. Maximum turbine speed is found as 990 rpm for the 8.5 MW test and 1030 rpm for the 9.35 MW test.

Since the model of Case-3 reflects the hydropower plant more realistically and directly, after the results of the simulations are satisfied with the measured data, validation of the model is completed. All cases are simulated for 8.5 MW and 9.35 MW tests, and results are compared with measured data for these tests.

In order to understand the differences between two tests in the field, comparison of the pressure variation, operating rules, turbine speed is executed before developing a model. Figure 5.5 shows the pressure variation and opening rules of PRV and wicket gate for measured data in 8.5 MW and 9.35 MW tests in the field.

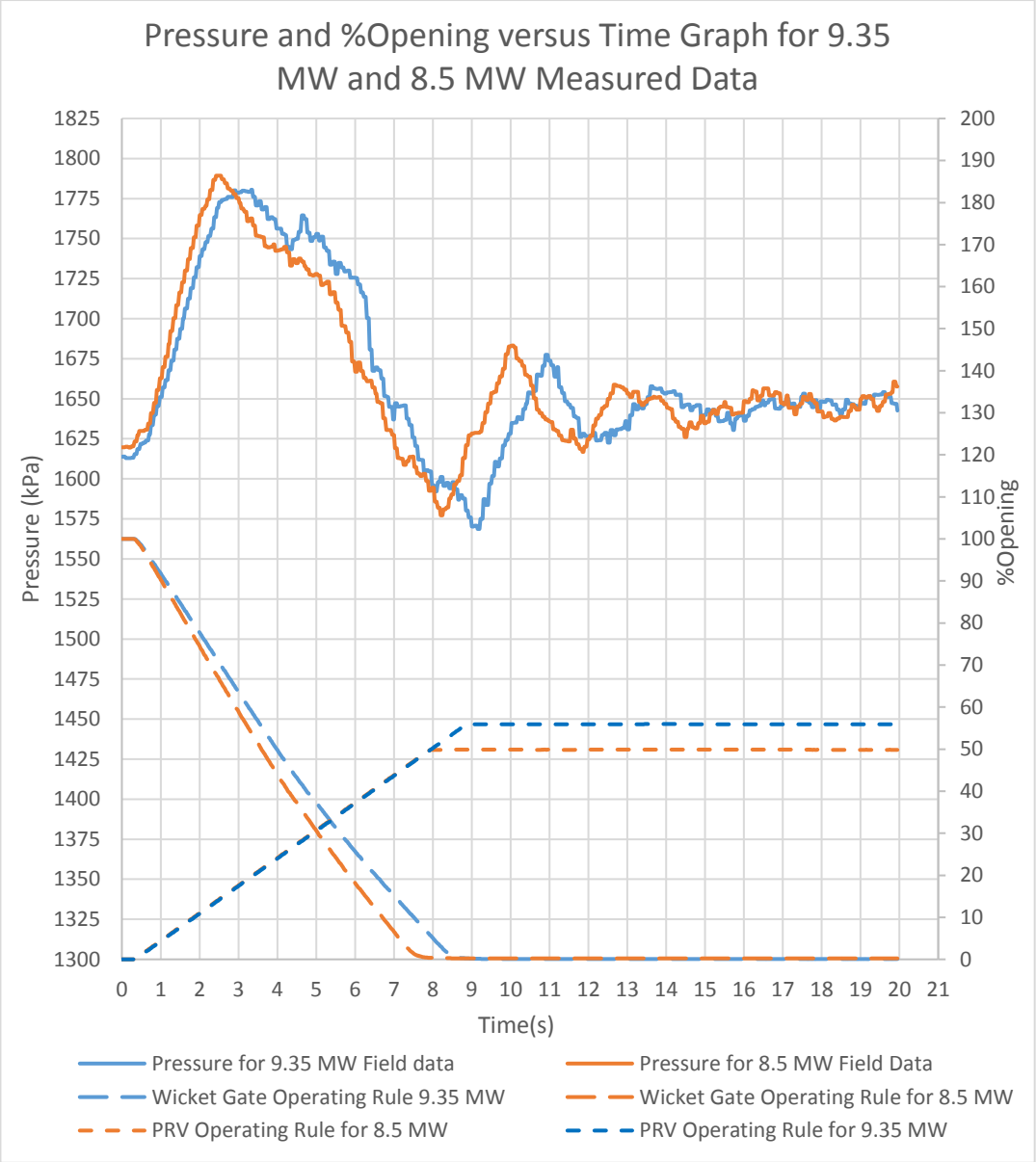

Figure 5.5 Pressure Variation and Operating Rules of 9.35 MW and 8.5 MW Tests in the Field

It can be observed that although discharge and turbine power is greater in the 9.35 MW test, pressure results are similar to the 8.5 MW test. In fact, the maximum pressure value is larger in 8.5 MW. The main reason for this phenomenon is the operating rules of PRV and wicket gate. Since the magnitude of pressure increase or decrease is related to the velocity change in the flow, if the closing speed of the wicket gates is the same for different tests, change in discharge and velocity will not

differ dramatically. In addition, PRV opens with wicket gate motion simultaneously and starts to discharge pressurized flow out of the system in the same pattern for two tests. Therefore, pressure results do not indicate large differences for 8.5 MW and 9.35 MW tests. Table 5.5 shows the differences between the field test parameters.

Table 5.5 Measured Data Comparison for 8.5 MW and 9.35 MW Tests

Turbine Power (MW)	8.5	9.35
Wicket Gate Opening (%)	74	83
Wicket Gate Closure Time (s)	7.70	8.55
PRV Opening Time (s)	7.90	8.85
Maximum PRV Opening (%)	49.85	55.92
Maximum Pressure (kPa)	1789	1781
Maximum Turbine Speed (rpm)	995	1035

It can be observed that although maximum pressure is larger, maximum turbine speed is smaller in the 8.5 MW test. Since discharge in the 9.35 MW test is bigger, the closing time of the wicket gate is longer because of the equality of closing slopes. Turbine is affected from pressurized flow with larger velocity values for a longer time in the 9.35 MW test, and the turbine speed increases.

PRV opening percentage and time duration are larger in 9.35 MW because discharge is more than 8.5 MW. Since different hydraulic proportional valves control the PRV and wicket gate, they start their operation simultaneously, but PRV continues to open after the wicket gate is closed totally. Although an algorithm is determined for both patterns, there may be differences in the operation stage.

Tests were held for instant load rejection case in the field. Firstly, hydraulic proportional valve behaviors are defined for PRV and wicket gate. Then, the system starts to work in the initial condition, which is steady-state. Finally, an emergency shut down procedure is used to start instant load rejection case. After this step, the connection between the generator and the electricity grid breaks, and the electrical load decreases to zero suddenly. In order to prevent a sudden increase in turbine speed, wicket gate begins to close. At the same time, PRV starts to open. Since

electrical load decreases to zero, turbine does not have any torque to resist water velocity. Therefore, wicket gate closure should be regulated not to cause damage to the turbine components. In the following sections, three cases used in validation will be explained in detail for 8.5 MW and 9.35 MW tests.

5.2.1 Case 1: HAMMER Model with only GPV

A HAMMER model is created with surge tank and GPV. GPV is used to model turbine, and PRV is removed from the system. This case aims to simplify the system and find the discharge variation (to be used as a reference discharge later) that causes a transient event that would be close to that obtained with the measured data. Therefore, GPV in place of turbine is regulated to mimic the combined effect of the turbine closure and PRV opening simultaneously in controlling the flow. Figure 5.6 shows the model development for Case 1.

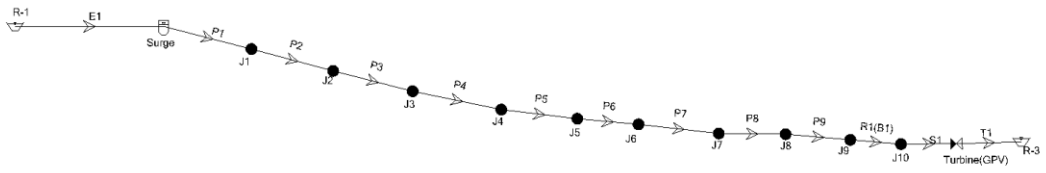

Figure 5.6 HAMMER Model for Case 1

Regarding the 8.5 MW field test, wicket gate opening percentage is 74% in the field, and calculated flow rate is 5.82 m^3/s for this generated power. After hydraulic losses are extracted from the energy equation, the net head of the turbine is found as 166.66 m. Since PRV stays open after wicket gate is closed completely, GPV stays open at the end of the pattern. Another essential point is that the PRV continues to increase its opening rate after wicket gate operation is completed, so that flow rate increases slightly after it reaches minimum value. This phenomenon can be defined with a GPV pattern.

Because the computer program does not allow introducing a starting percentage different from 100%, at the beginning of the valve pattern wicket gate percentage at the starting point is accepted as 100% instead of 74% for the 8.5 MW test. Therefore, the wicket gate opening rates are calculated by taking this ratio per initial opening. This procedure is applied to field data and simulations. Figure 5.7 demonstrates the comparison of GPV pattern in the model and wicket gate, PRV operating rules in the field. Although wicket gate closure is completed in 7.7 seconds, the GPV pattern continues until the PRV operation is finished at about 7.9 seconds.

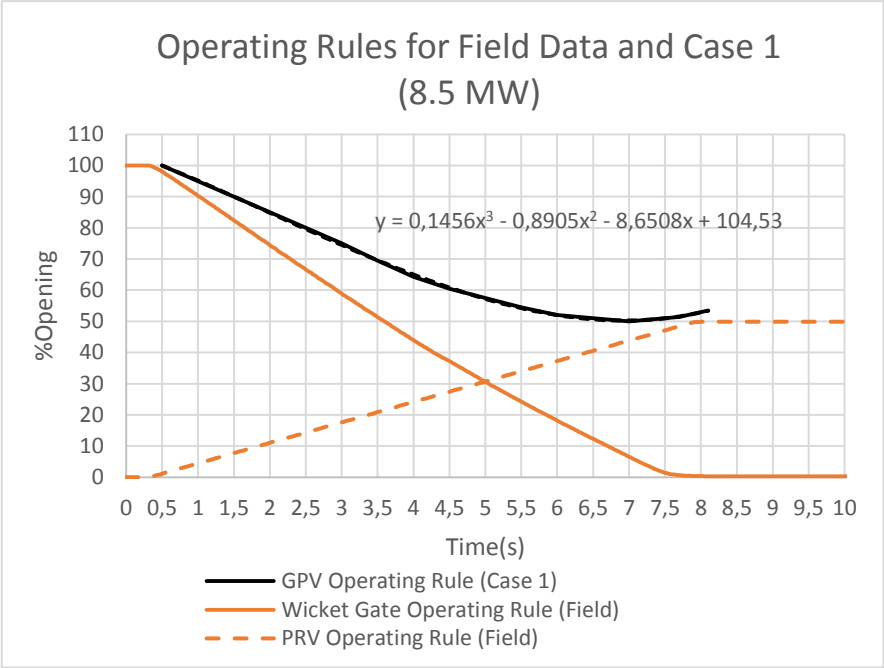

Figure 5.7 Comparison of Operating Rules for GPV in Case 1 and Wicket Gate, PRV in Field for 8.5 MW Test

In order to decrease breaking points (to smooth out the curve) in the GPV operating rule, 3rd ordinary curve is fit to the pattern, and the equation of the curve is added to the graphic in Figure 5.7. It should be noted that if the slope of pattern is not smooth in operating a valve or gate, discharge and pressure results fluctuate because any sudden change in velocity results in sudden changes on discharge and pressure. In fact, time intervals should be decreased to receive more precise data for pressure and discharge results.

However, as it can be observed from Figure 5.8, which shows the pressure and discharge variation for simulation and measured data, input data are enough for GPV pattern because the results do not have large fluctuations. Results are taken from Junction 11, which is the branch for the pipes that convey the water to PRV and turbine. Since flow is divided in the branch, total discharge can be controlled from Junction 11. As there is only one pipe with 2 m length and negligible minor loss between the junction and turbine, discharge and pressure results do not change for these two points.

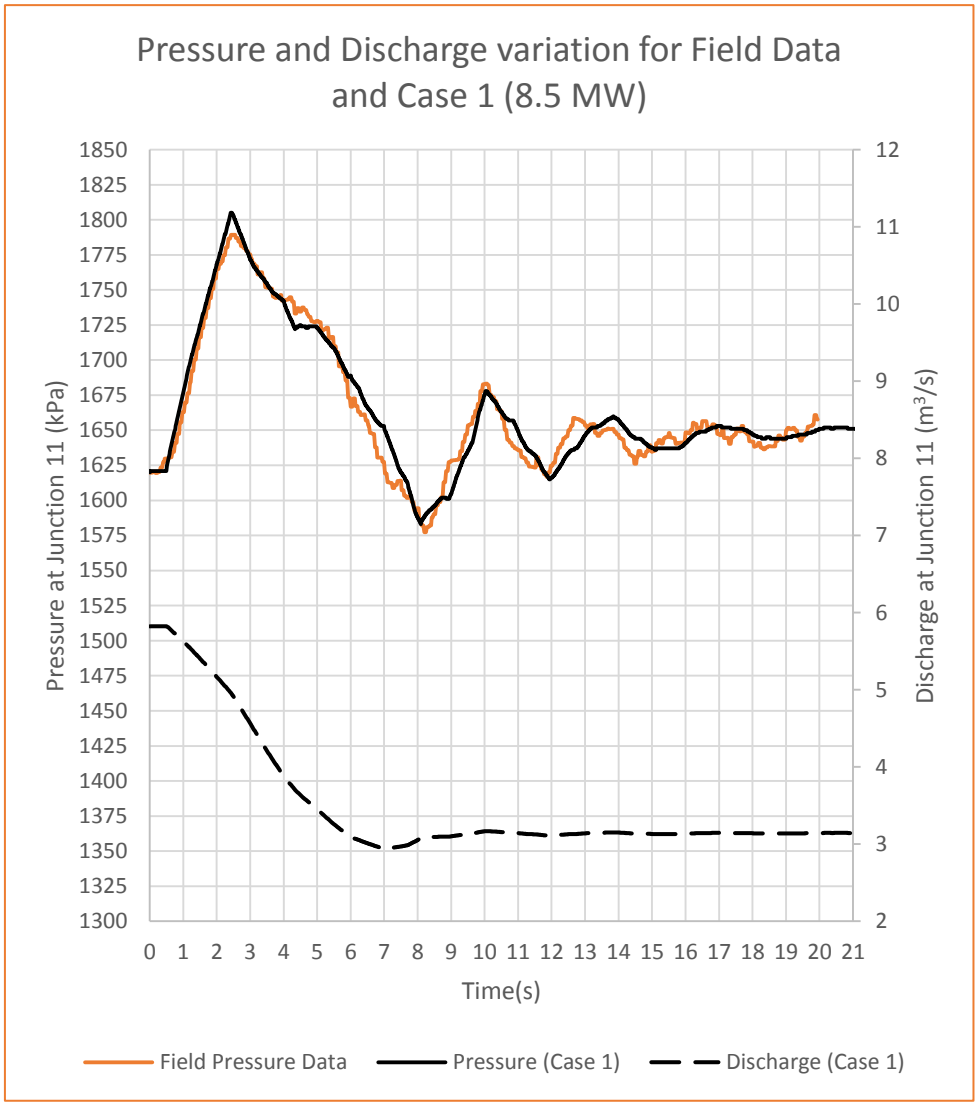

Figure 5.8 Comparison of Pressure Variation between Field data (8.5 MW Test) and Case 1 with Flow Variation

As seen in Figure 5.8, the magnitude of the pressure peaks and their occurrence times are predicted overall very closely.

Regarding the 9.35 MW field test, wicket gate opening percentage is 83% in the field, and calculated flow rate is 6.41 m^3/s for this generated power. The net head is calculated as 166.3 m because minor and friction losses increase as discharge increases. The same steps are followed in this test as in the 8.5 MW test. The methodology starts with defining a GPV pattern which is indicated in Figure 5.9.

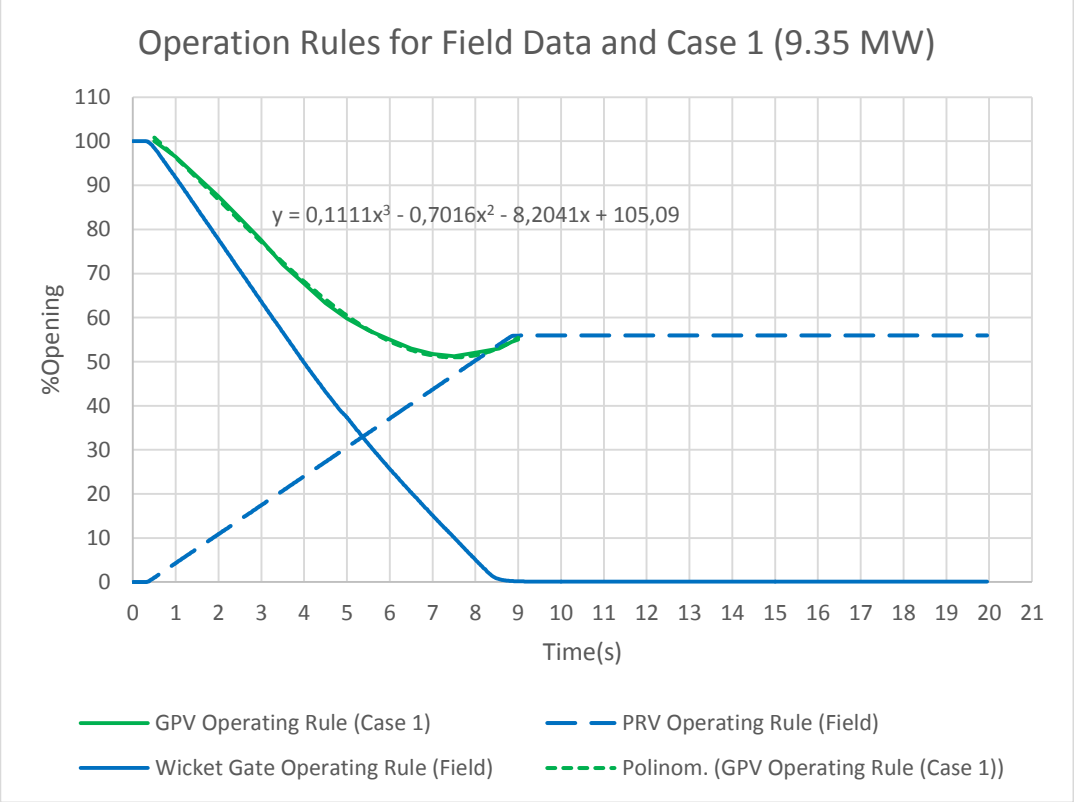

Figure 5.9 Comparison of Operating Rules for GPV in Case 1 and Wicket Gate, PRV in Field for 9.35 MW Test

In the 9.35 MW test, wicket gate closure time and PRV opening time are different from the 8.5 MW test. PRV opening time is increased from 7.9 seconds to 8.85 seconds, and wicket gate closure is increased from 7.7 seconds to 8.55 seconds. Discharge is larger than 8.5 MW test because the wicket gate opening is larger at the

beginning of the tests as 83%. PRV final opening percentage is increased from 50.15% to 55.85%. Since these precautions are taken at the beginning of the test, the pressure increase is smaller than the one obtained at the 8.5 MW test. Figure 5.10 indicates the pressure and flow variations for simulation and pressure values for measured data.

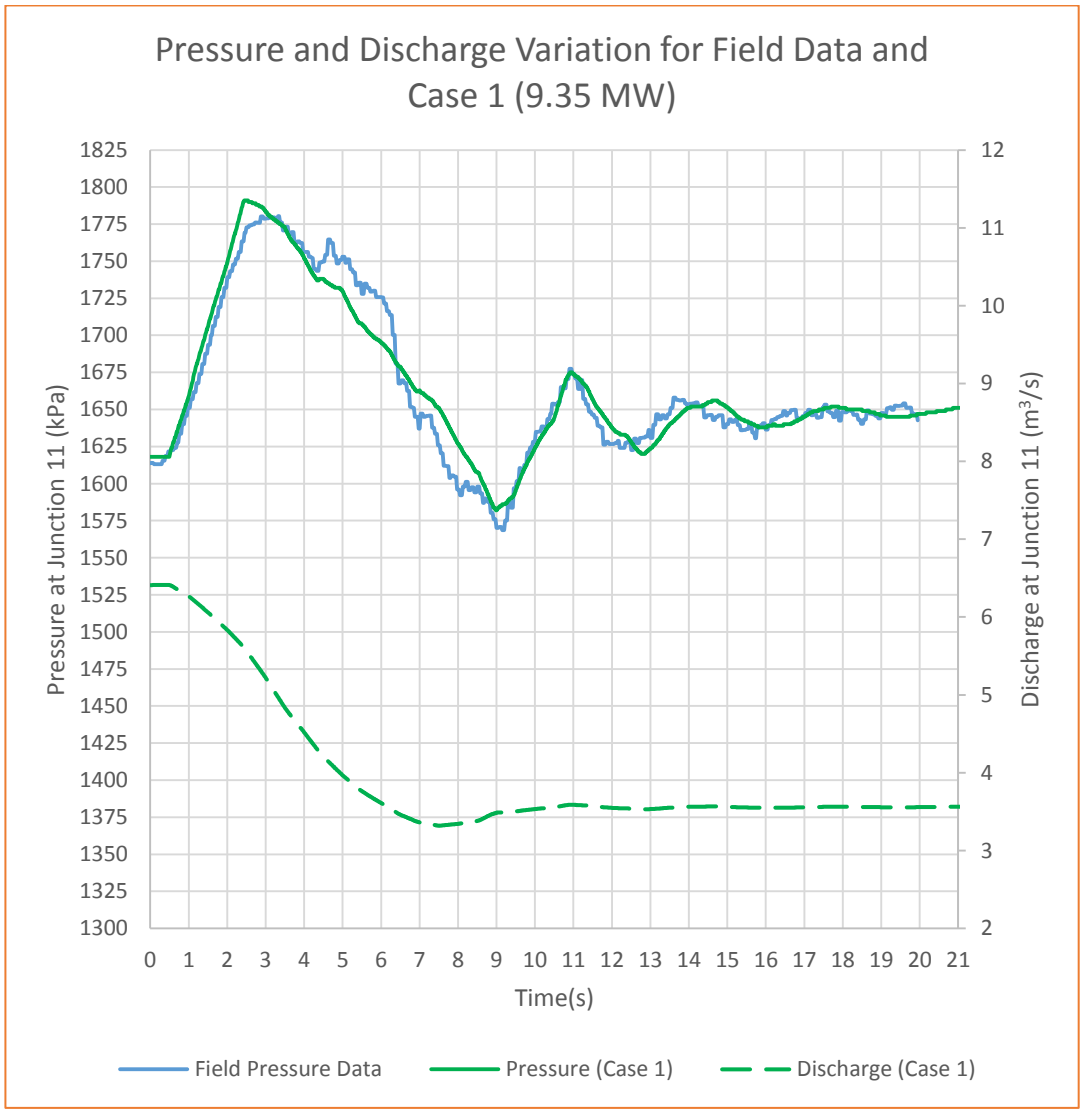

Figure 5.10 Pressure and Discharge Variation for Field data and Case 1 and Flow variation for Case 1 in 9.35 MW Test

The above part of the graph in Figure 5.10 shows the pressure comparison of field test and Case 1 simulation for 9.35 MW. The below part of the graph demonstrates

the discharge variation of Case 1 simulation of the HAMMER model. Since discharge versus time values are not measured in the field, discharge needs to be determined to be used as a reference in other cases. There are small phase and amount differences between the simulation results and measured data, but the flow behavior is simulated accurately with related discharge. As a result, in order to assess PRV and GPV behavior in Case 2, the reference discharge obtained at this stage will be used in the following cases, and necessary calibrations will be applied. Once again, the magnitude of the pressure peaks and their occurrence times are predicted overall very closely for this power as well.

5.2.2 Case 2: HAMMER Model with GPV and PRV

This time, a HAMMER model is created with surge tank, GPV, and PRV. GPV is used to model the turbine only, and PRV is added to the system with a by-pass pipe from Junction 11. This case aims to simplify the turbine effects and determine the wicket gate and PRV patterns by using the reference discharge variations obtained in Case 1. PRV and GPV will control the flow together, so the flow rates per unit time will be determined for the pipes that convey water to PRV and GPV separately. Therefore, operating rules are arranged per measured patterns, GPV rule is regulated as wicket gate closure, and TCV pattern is arranged as PRV operating rule. Figure 5.11 illustrates the model development for Case 2.

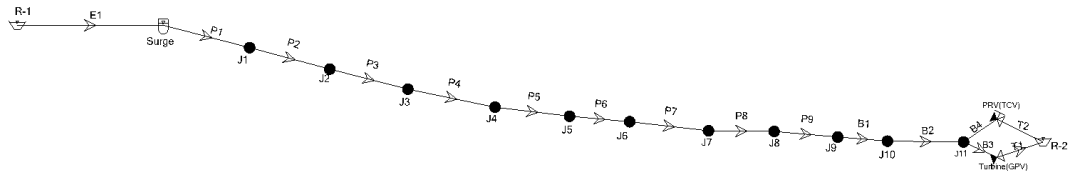

Figure 5.11 HAMMER Model for Case 2

Simulations are done for 5.82 m^3/s and 166.66 m net head for the 8.5 MW test. Comparisons of patterns are analyzed separately for PRV and GPV in Figure 5.12 and Figure 5.13.

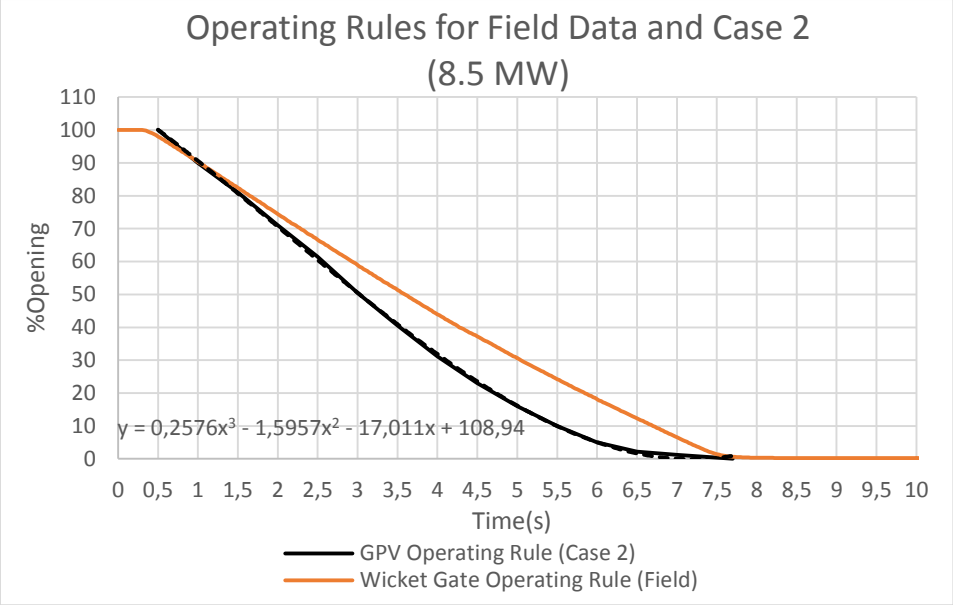

Figure 5.12 Comparison of Operating Rules for GPV in Case 2 and Wicket Gate in Field for 8.5 MW Test

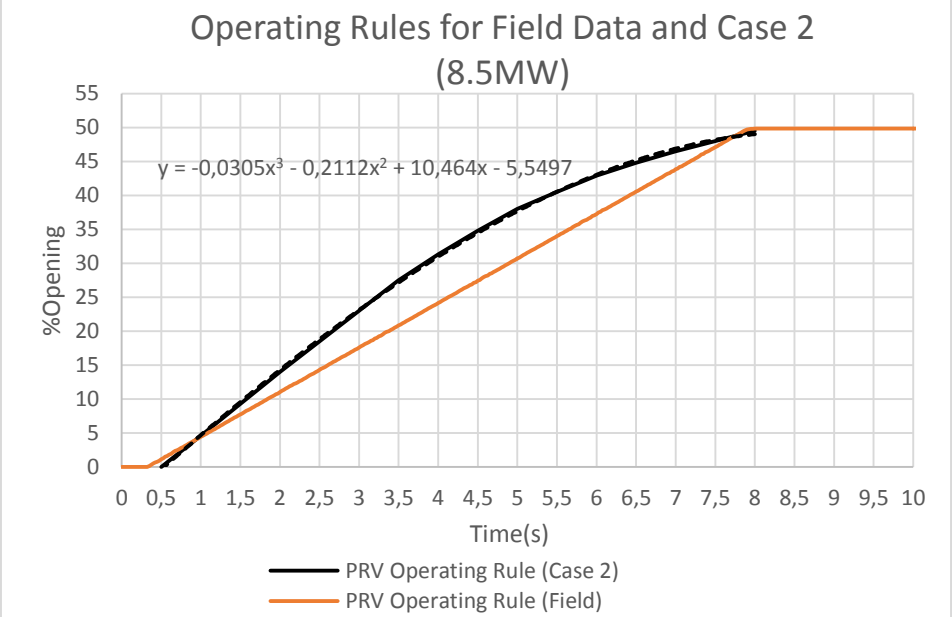

Figure 5.13 Comparison of Operating Rules for PRV in Case 2 and measured data for 8.5 MW Test

Figure 5.12 indicates the differences between measured data for PRV operating rule and simulated PRV pattern. Figure 5.13 shows the differences between measured data for PRV behavior and simulated TCV opening percentage per unit time used to model PRV in the simulations. Curve equations for the operating rules are added to the comparison graphs. After smooth curves are shaped, pressure and discharge variations are compared for measured data and simulation results in Figure 5.14. As seen in Figure 5.14, the magnitude of the pressure peaks and their occurrence times are predicted overall very closely.

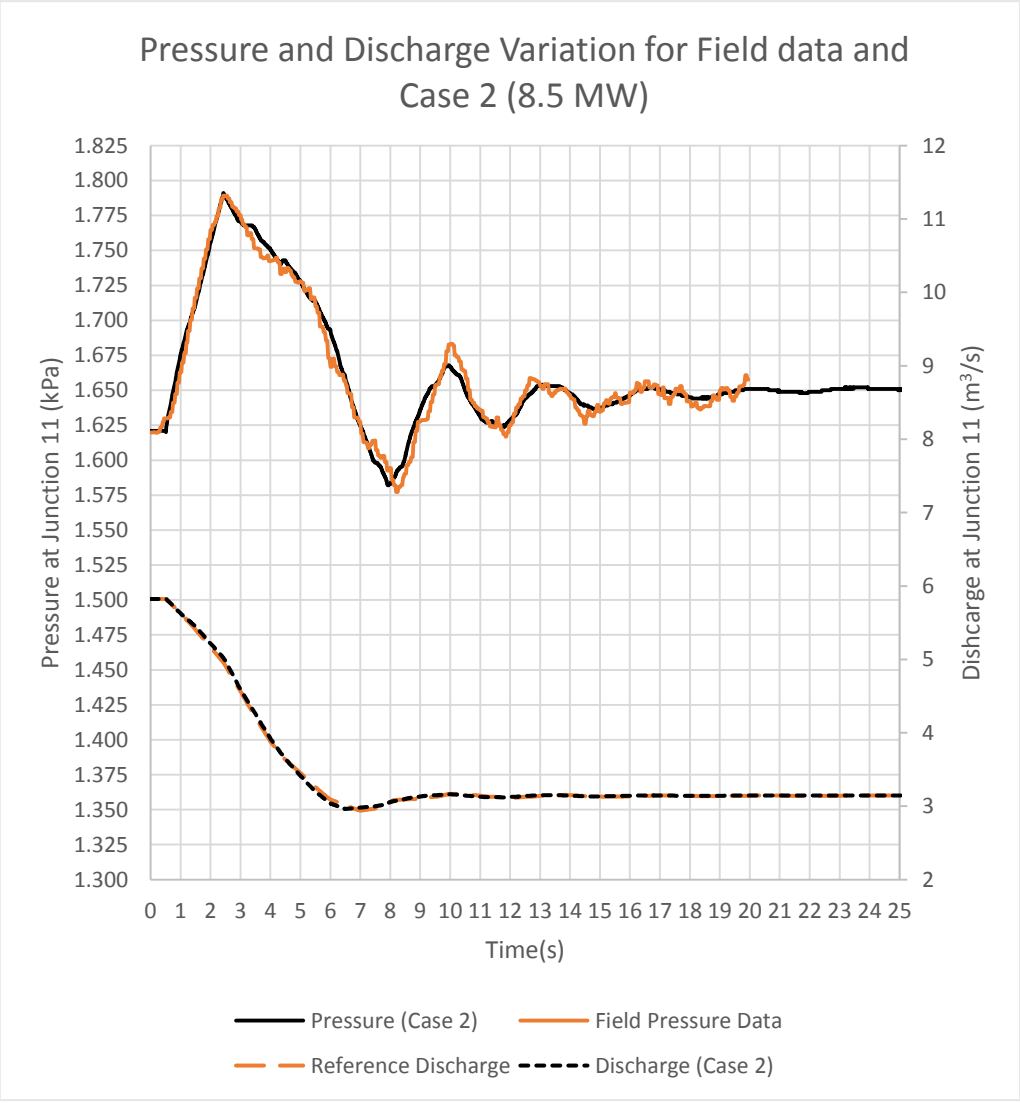

Figure 5.14 Pressure and Discharge Variation for Field data and Case 2 in 8.5 MW Test

Since reference discharge values are defined in Case 1 using only GPV in the system, it is accepted as field discharge values. All the calculations and approximations are made per reference data which represent flow behavior in the field. This acceptance is done by using measured values of pressure, PRV, and wicket gate operating rules.

Regarding the 9.35 MW test, wicket gate opening percentage at the beginning, closing time, PRV opening time, and PRV final opening percentage values increases per 8.5 MW Test. As calculated before, the flow rate is 6.41 m^3/s, net head 166.3 m, and wicket gate opening percentage at the beginning is 83%. Figure 5.15 demonstrates the GPV operating rule with curve equation used to gather a more smooth pattern for GPV in the simulations.

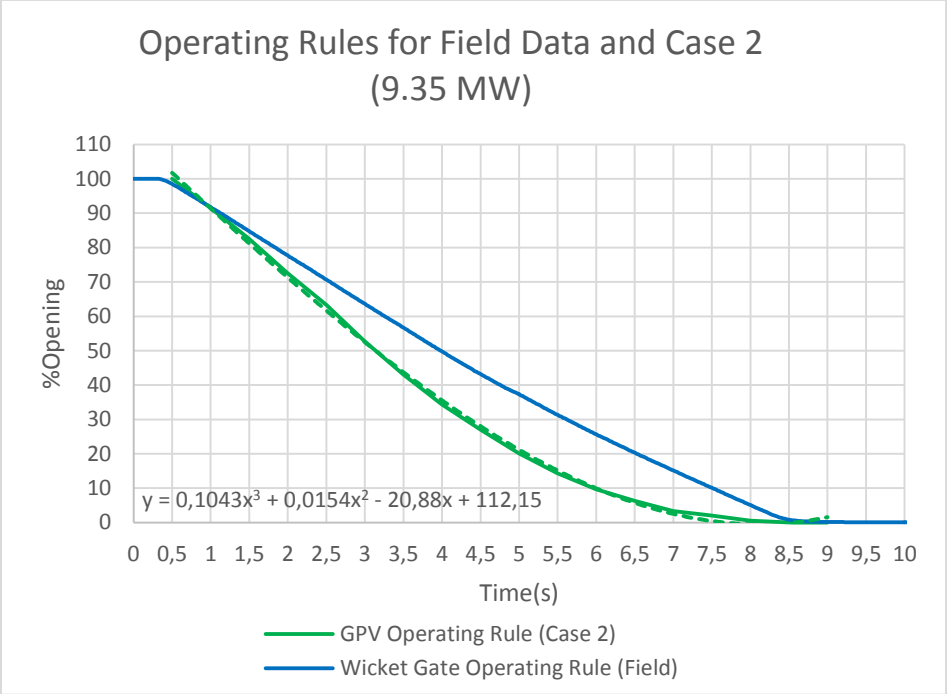

Figure 5.15 Comparison of GPV Operating Rule in Case 1 and Wicket gate Operating Rule in Measured Data for 9.35 MW Test

Figure 5.16 indicates the PRV pattern of the measured data and Case 2 simulation. In order to obtain a smooth curve to prevent sudden pressure and discharge changes in the system, 3rd ordinary curve is fit to the pattern, and necessary arrangements are proceeded without affecting general flow behavior.

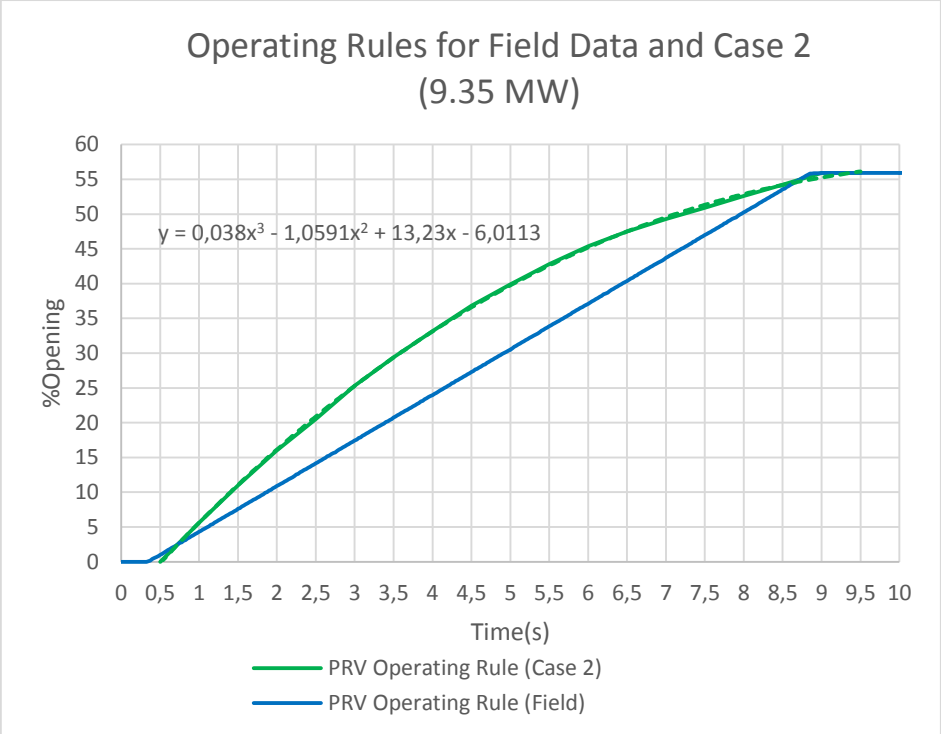

Figure 5.16 Comparison of PRV Operating Rules in Case 2 and measured data for 9.35 MW Test

If there is only one element to control the flow in the system, it is easy to understand behavior and arrange the pattern with respect to pressure. Optimization of the discharge with the pattern and pressure can be organized, and transient behavior can be obtained. However, controlling the flow with two or more elements causes many different parameters to understand the system. This phenomenon makes the behavior more complex. Therefore, while the number of controlling elements increases, the error percentage between pattern and smooth curve increases slightly. Still, it is resulted that since these errors do not cause significant fluctuations in the flow attitude and do not change the main points for pressure, discharge, or other parameters, errors and breakpoints are within acceptable limits. If there were large differences in the behavior, the time step for the pattern definitions could be decreased to obtain more smooth curves.

After related arrangements are completed, simulations are held for the 9.35 MW test. Results are compared with field pressure data and reference discharge in Figure 5.17 for Junction 11 to see the total flow rate in the system. As seen in Figure 5.17, the magnitude of the pressure peaks and their occurrence times are predicted sufficiently well.

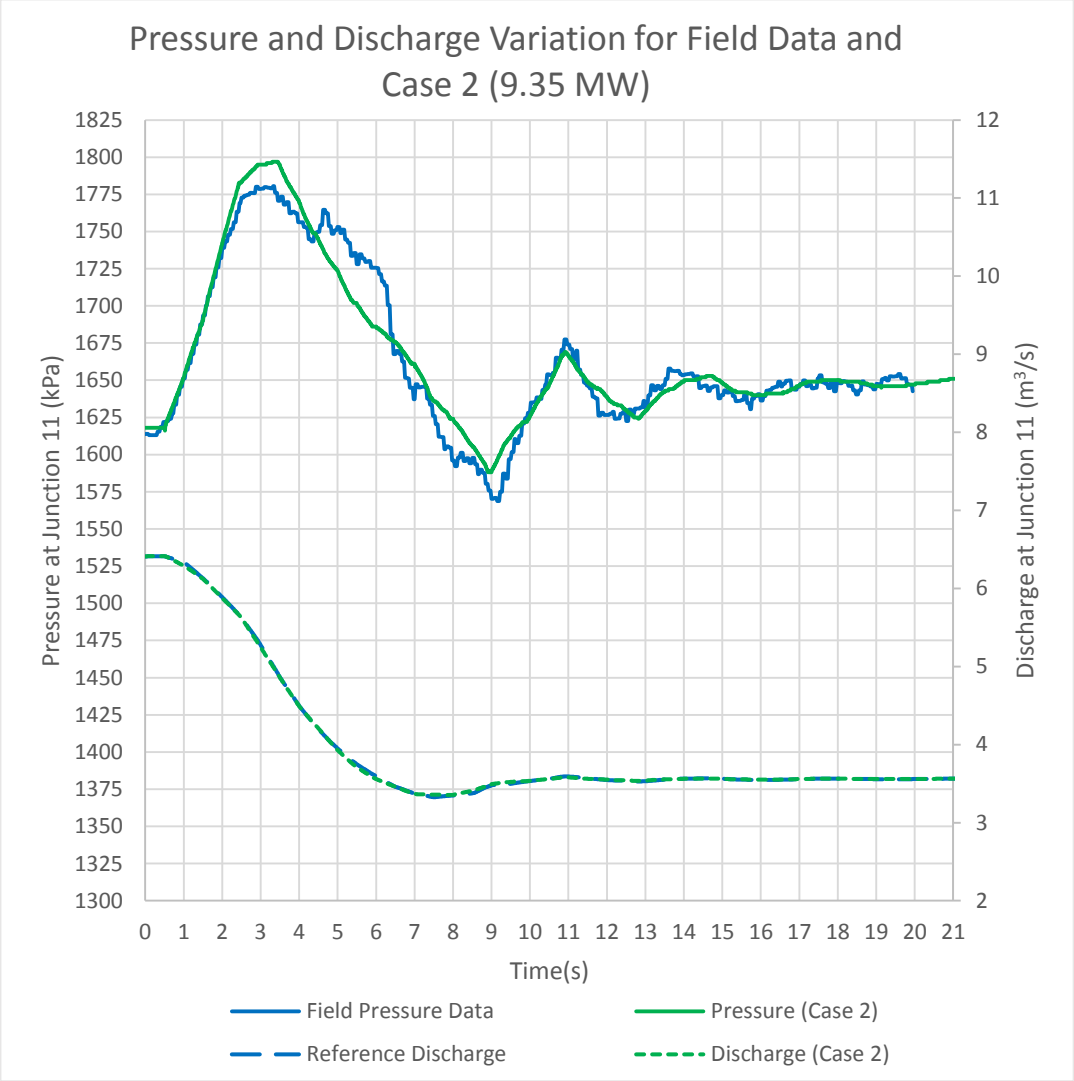

Figure 5.17 Pressure and Discharge Variation for Field data and Case 2 in 9.35 MW Test

The PRV and GPV operating rules for the HAMMER models are calculated using reference discharge and measured data in the field for pressure and patterns in Case 2. These patterns will be used to find wicket gate behavior by adding turbine model into the system in Case 3.

5.2.3 Case 3: HAMMER model with Turbine and PRV

Case 3 is the final step for validating the model with measured data. All the simulations for scenarios will be performed with Case 3 model. Since the HAMMER model is developed using the KEPEZ – I HPP, results reflect the reality. Only PRV is modeled as TCV in the model, but PRV behaves as a throttle control valve in the field because it does not work per set pressure limit. Therefore, there is not any significant difference between HPP system in the field and the numerical model.

Essential information is collected from Case 1 and Case 2, and the model is arranged for the final version. Reference discharge, GPV, and PRV patterns are used to obtain pressure results. Turbine parameters taken from manufacturers are entered as input data. Simulations are held for 8.5 MW and 9.35 MW field tests separately.

Regarding the 8.5 MW test, after model is developed, patterns are arranged according to measured operating rules in the field. Wicket gate opening at the beginning is 74%, and it is closed in 7.70 seconds, resulting in 5.82 m^3/s discharge and 166.66 m net head in turbine. PRV gate opening at the end is 50.15%, and opening time is 7.90 seconds. The comparisons of the wicket gate operating rules for field data and simulation results are shown in Figure 5.18.

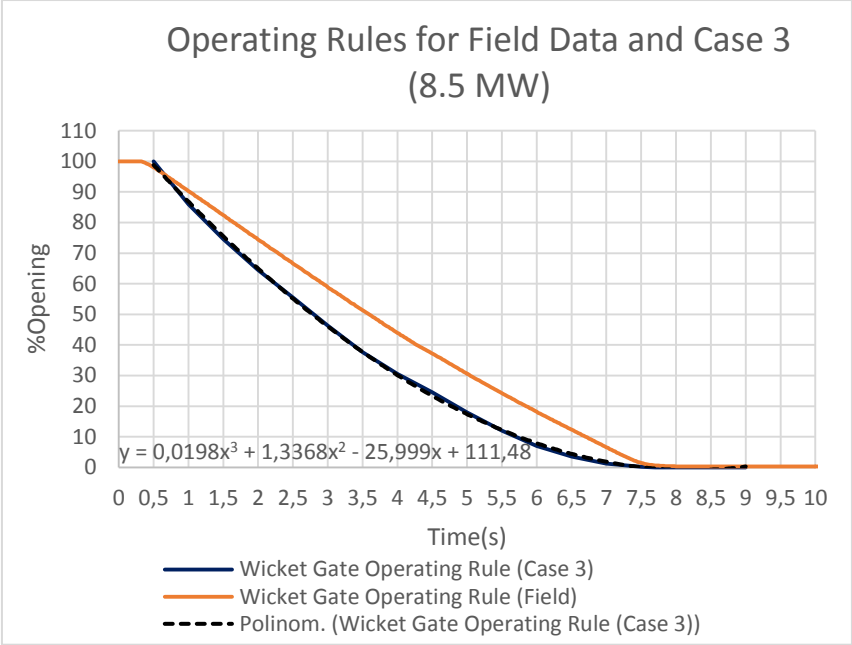

Figure 5.18 Comparison of Wicket Gate Operating Rules in Case 3 and measured data for 8.5 MW Test

Figure 5.19 indicates the comparison of PRV operating rules for Case 3 model and field measured data from the servomotor of the PRV.

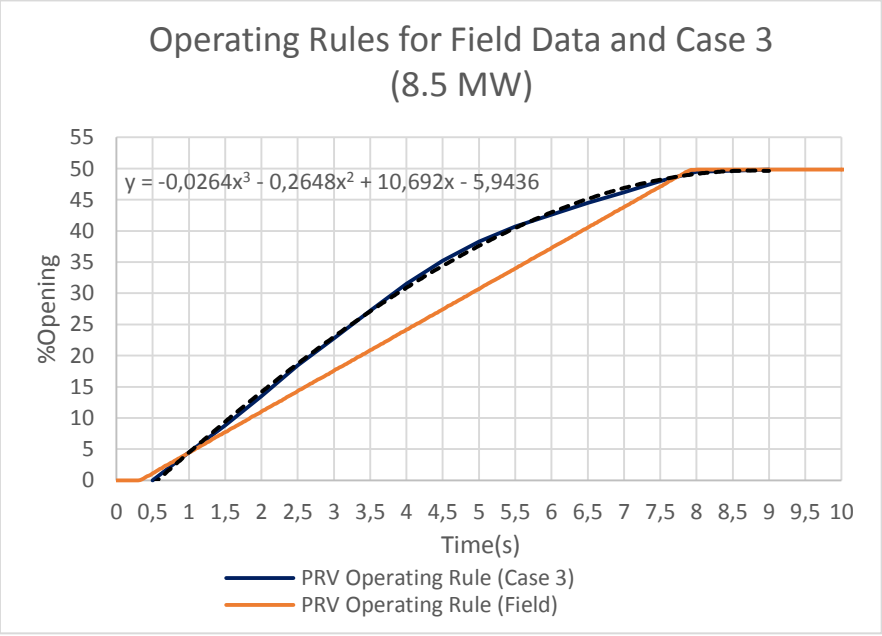

Figure 5.19 Comparison of PRV Operating Rules in Case 3 and measured data for 8.5 MW Test

Finally, after all the steps are finished, field data are fully modeled, and pressure is compared with simulation results. Since GPV is a simple valve that helps regulate the water amount transmitted in the pipeline system, there is no extra parameter that affects the pressure or discharge. In contrast, turbine is a complex system, and turbine parameters affect the flow behavior in different ways. As a result, 3rd ordinary curves do not fit exactly, which causes fluctuations in the pressure results. In some of the parts, changes can be observed easily, but it is not valid for every point of simulation results. In order to decrease sudden pressure changes in the graphs, time interval is reduced to 0.5 seconds while determining the valve and wicket gate patterns.

Pressure variatıons and flow changes are compared with field data for the 8.5 MW test in Figure 5.20. There are slight differences between the field pressure data and model results.

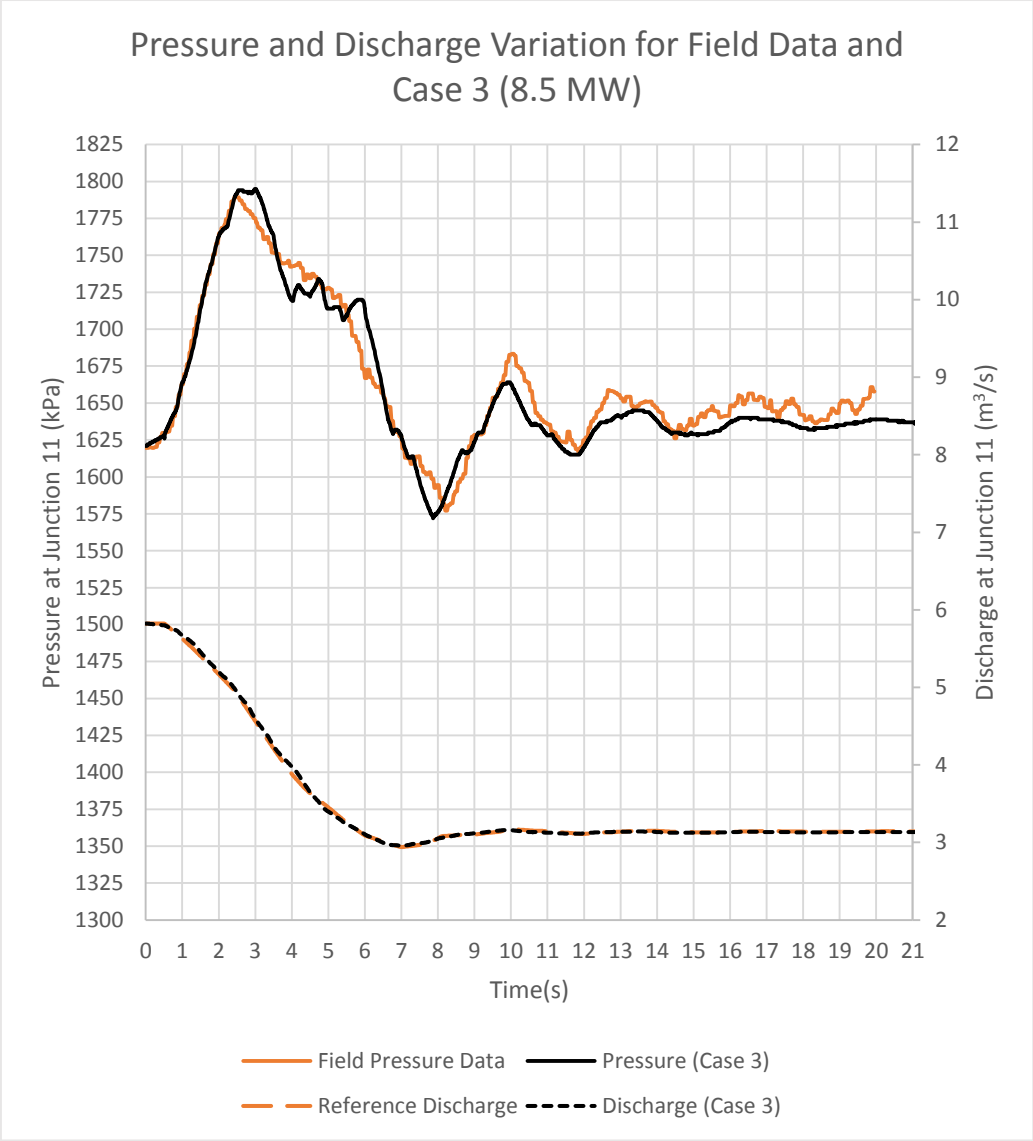

Figure 5.20 Pressure and Discharge Variation for Field data and Case 3 for 8.5 MW Test

Maximum pressure is 1794 kPa between 2.53 seconds and 2.66 seconds for model, and it is 1789 kPa between 2.425 and 2.55 seconds for measured data. Minimum pressure is 1572 kPa at 7.87 seconds for model, and it is 1577 kPa between 8.2 seconds and 8.25 seconds for field. The pressure amount of the second peak is 1683.3 kPa between 10.025 seconds and 10.075 seconds in the field, and it is 1664 kPa between 9.9 seconds and 9.98 seconds for model. As a result, after the comparisons, it is decided to use model for 8.35 MW testing scenarios in the next section.

Regarding the 9.35 MW test, the same methodology is followed, and wicket gate, PRV patterns are defined per the information collected from Case 1 and Case 2. Wicket gate opening at the beginning and closure time is changed as 83% and 8.55 seconds resulting 6.41 m^3/s discharge and 166.3 m net head at turbine. As mentioned before, wicket gate opening at the starting point is accepted as 100% because of computer program restrictions, and calculations are proceeded by taking the ratio of initial opening for field and simulations. Since discharge amount in the initial conditions is regulated for the system, the wicket gate and discharge relationship remains the same as field data indicated in Figure 5.21.

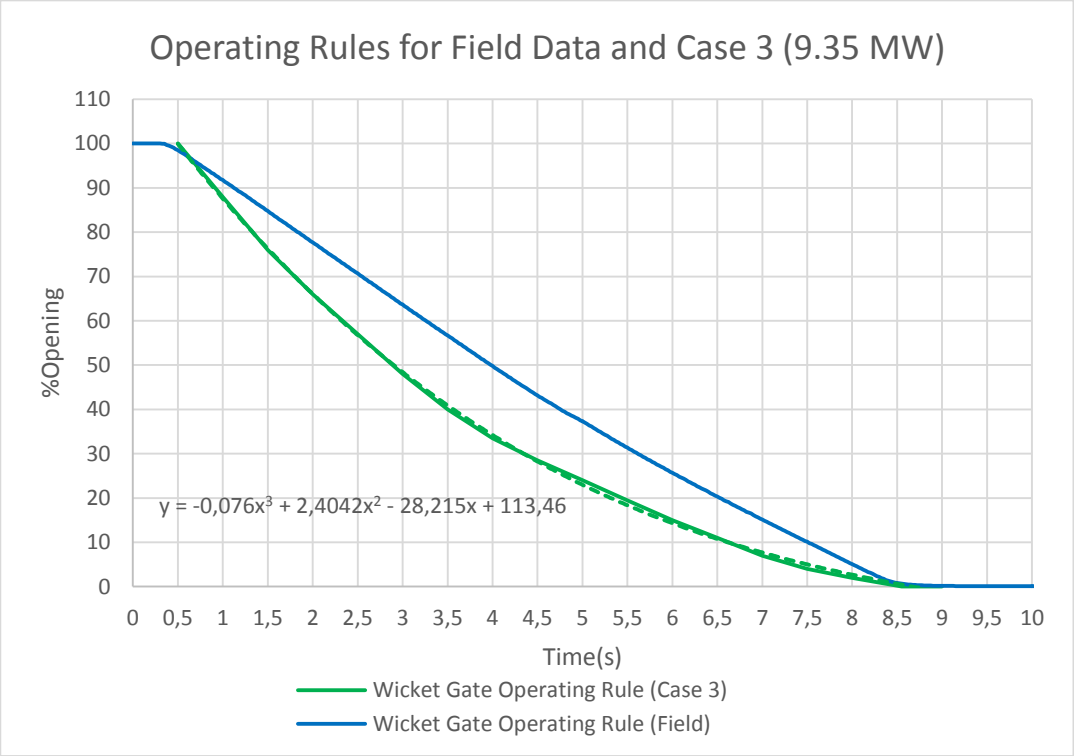

Figure 5.21 Comparison of Wicket Gate Operating Rules in Case 3 and measured data for 9.35 MW Test

PRV opening at the end and opening time are changed as 55.85% and 8.85 seconds. Therefore, arrangements are applied by considering these changes, and field comparison is shown in Figure 5.22.

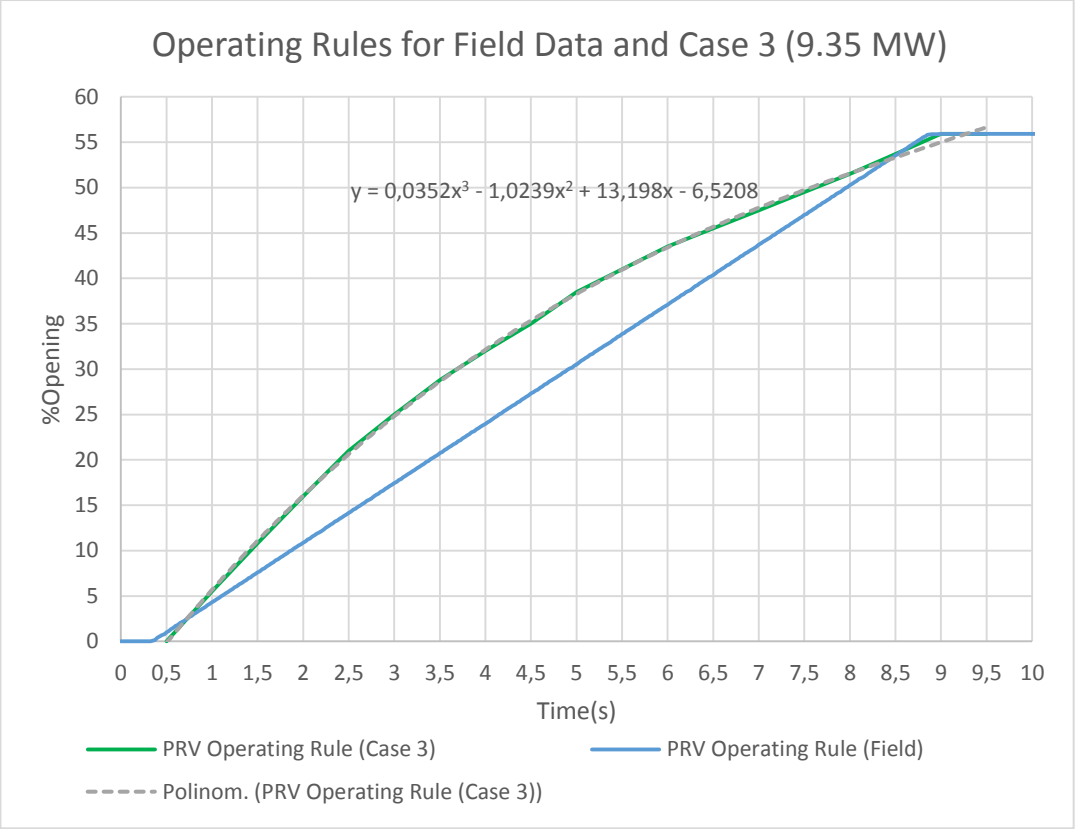

Figure 5.22 Comparison of PRV Operating Rules in Case 3 and measured data for 9.35 MW Test

The curves of the operating rules are organized as parallel in 8.35 MW and 9.35 MW tests because operating rates are equal or close to each other in the field test results. Since the opening or closing rates are close to each other for the field tests and simulations, obtained results for flow behavior are also close to each other such as pressure and discharge since closing or opening rates in operating rules directly affect pressure variations in the system. Figure 5.23 shows the pressure and flow rate variation of the Case 3 simulation and field measured data with reference discharge

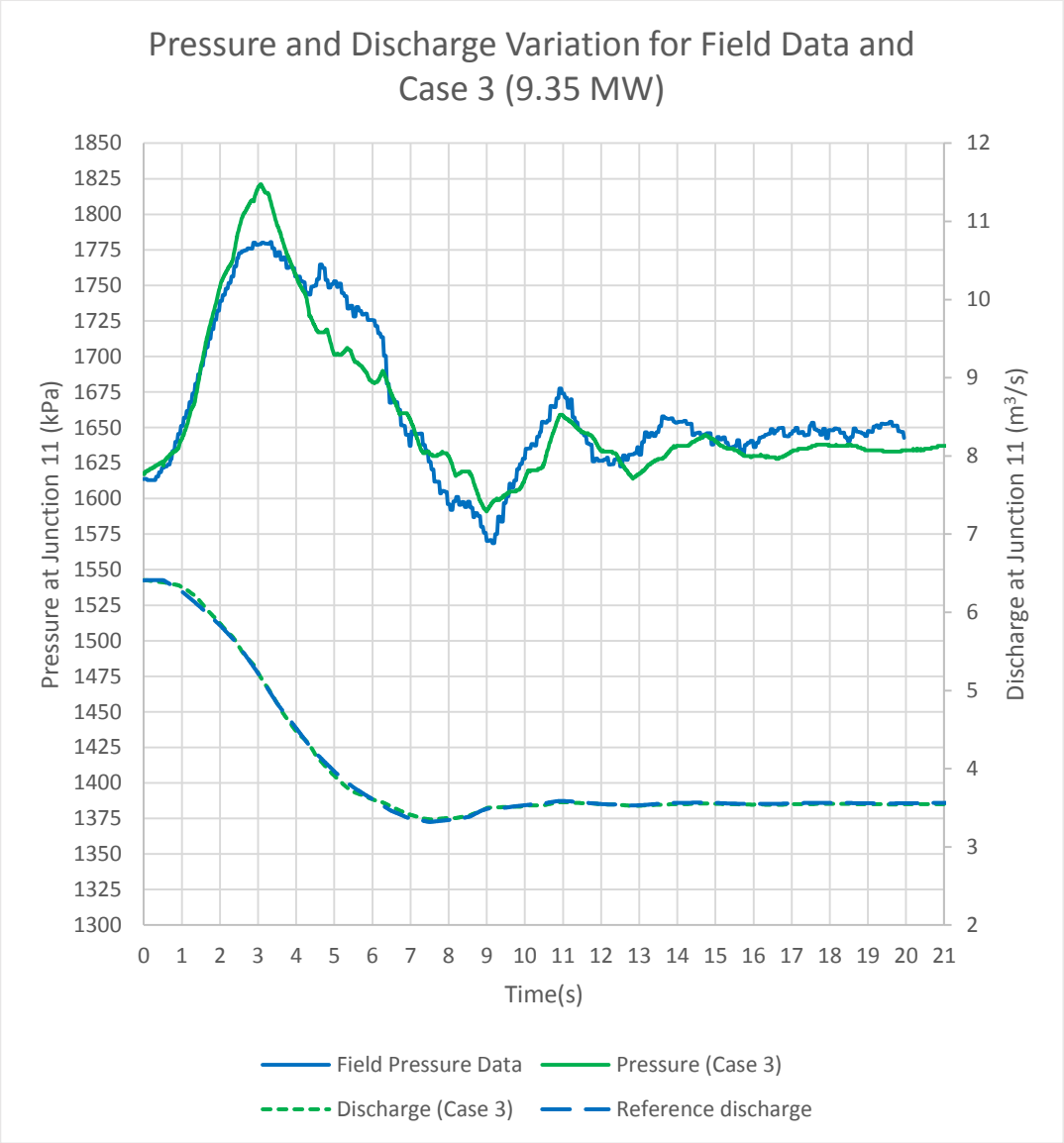

Figure 5.23 Pressure and Discharge Variation for Field data and Case 3 for 9.35 MW Test

Maximum pressure is 1,825 kPa between 3,05 seconds and 3,08 seconds for model, and it is 1,780 kPa between 3,1 and 3,15 seconds for field. Minimum pressure is 1,590 kPa at 8,99 seconds for model, and it is 1,568 kPa between 9,15 seconds and 9,2 seconds for field. The pressure amount of the second peak is 1677,4 kPa between 10,9 seconds and 10,95 seconds in field, and it is 1659 kPa between 10,91 seconds and 10,99 seconds for model.

Finally, the validation process is completed for the model because results are close enough to field test measured data. Therefore, scenarios can be formed and simulated with the HAMMER model developed in Case 3. In this section, the discharge values are estimated with a GPV controlled system in Case 1. Then, GPV and PRV patterns are determined by using reference discharge values. In the end, a model is developed the same as field structures, and validation process is finalized by using reference discharge from Case 1 and patterns from Case 2, Case 3.

5.3 Transient Analysis for KEPEZ – I Hydropower Plant

In this study, transient analyses are investigated for different scenarios. After the validation stage, the HAMMER model, which is developed in Case 3, is used to obtain results for the scenarios. In order to investigate PRV effect on the system, different scenarios are applied to the model for two different cases. One of the cases includes PRV in the system, and the other one does not include it because the protection of the system is satisfied by surge tank and PRV in hydropower plant. Surge tank is constructed with plant, and PRV is mounted in recent days. Since surge tank is approximately 800 m away from the turbine, protective effects are not significant. Therefore, surge tank is included in every scenario, and only PRV is excluded or included. In this section, four different scenarios is investigated to understand the transient events and effect of protective measure.

- Scenario 1: Instant Load Rejection
- Scenario 2: Load Rejection
- Scenario 3: Load Acceptance
- Scenario 4: Load Variation

Simulations are held, and the most critical cases are analyzed for listed scenarios in order to give advice on operation limits of the facility and observe the protective measure effects. Since the highest pressure or head values are expected just before the turbine, simulation results are taken from that point. Although results are

controlled from the branch to analyze the discharge, investigations will be done just upstream of the turbine in this section. In the last part, the differences between the results of Junction 11 and just before turbine points are minimal and negligible. Therefore, in order to observe total discharge in the system, simulation results are taken from that point in the validation stage.

5.3.1 Scenario 1: Instant Load Rejection

In this scenario, the electrical load which comes from the grid drops to zero instantly. Then, the connection between the generator and the grid breaks, and generator torque is rejected on the turbine. Turbine starts to turn without any resistance. Therefore, the governor closes the wicket gate rapidly to prevent damage to turbine components before reaching runaway speed. Field tests are executed for instant load rejection scenario, and wicket gate closure times are 7.70 seconds for the 8.5 MW test and 8.55 seconds for the 9.35 MW test. In order to prevent excessive pressure waves in the system, closure times should not be shorter than critical time, which is a time interval for returning a pressure wave to wicket gate after being reflected from the reservoir. Since the wave speeds and length of the pipes are known, critical time is calculated as 3.14 seconds from $T_c = 2L/a$ formula. As wicket gate closure times are larger than 3.14 seconds, system is closed gradually, so it is not affected by excessive pressures because of rapid closure. According to this information, the critical time calculation is applied for field tests, and valve and wicket gate operating rule speeds are arranged manually in the field. Although the critical time is calculated as 3.14 seconds, pressure decrease starts after 2.5 seconds in the field test results. Therefore, it is resulted that surge tank behaves like a reservoir and reflects the water hammer waves before the reservoir because the volume of the surge tank is large for the system.

Simulations are held for 8.5 MW and 9.35 MW field tests separately. Results are analyzed for two different system for each test. HAMMER models with PRV and without PRV are analyzed and compared to understand the effect of PRV in the HPP.

Same wicket gate and PRV operating rules are applied. Steady-state flow conditions of Case 3 in validation stage exist in Scenario 1. Therefore, pattern graphs will not be indicated in this section.

Regarding the 8.5 MW test, two different simulations are completed for unprotected and protected cases. Figure 5.24 indicates the pressure and discharge variations of the system without PRV at turbine inlet for 5.82 m^3/s discharge and 166.66 m net head in initial conditions. Since wicket gate closure and PRV behavior remain the same with Case 3 in the previous section, they are not included in this part.

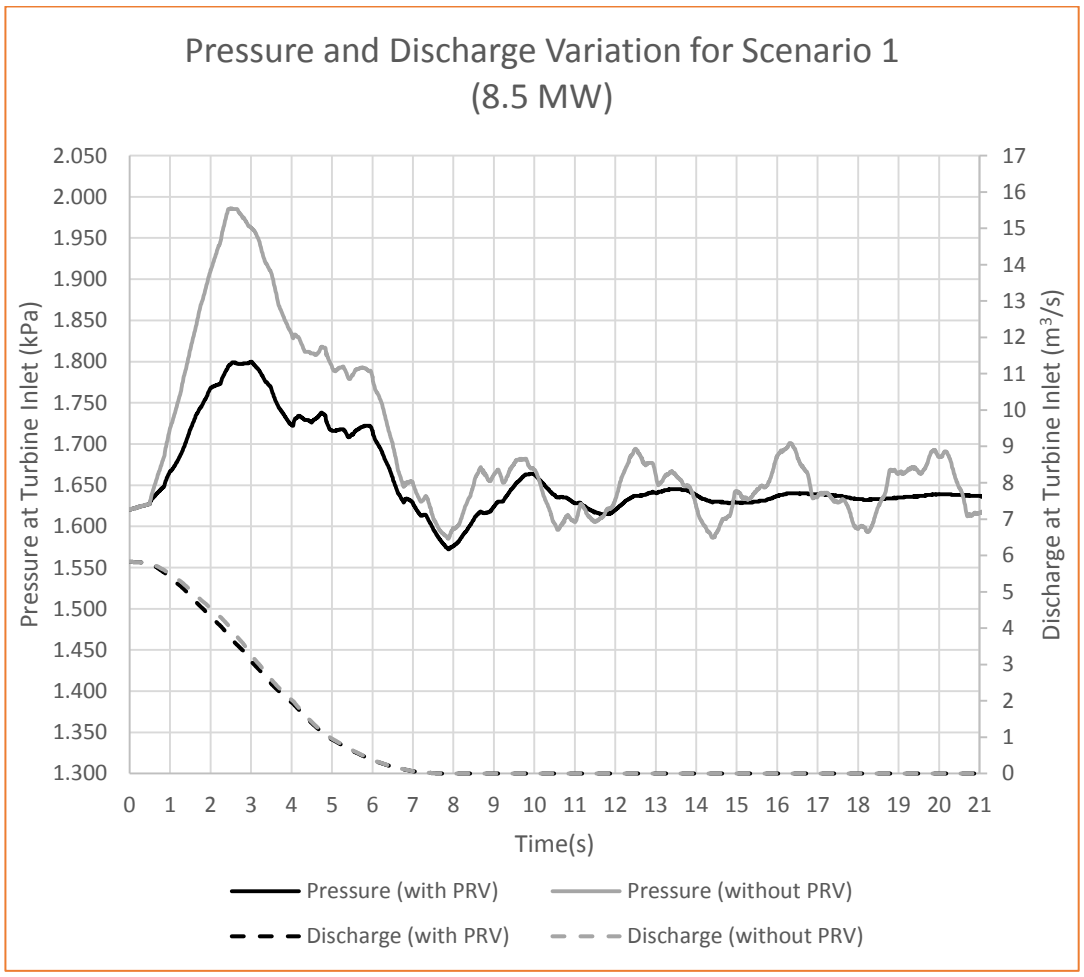

Figure 5.24 Pressure and Discharge Variation for Scenario 1 with and without PRV in 8.5 MW Test

Maximum pressure is 1799 kPa, and minimum pressure is 1572 kPa for protected system. There is 10.98% increase and 3.02% decrease in pressure.. It can be noted that maximum pressure is 1986 kPa and minimum pressure is 1585 kPa. Since initial pressure is 1621 kPa, 22.52% of rise and 2.22% decrease in pressure are observed for unprotected case in instant load rejection scenario. PRV reduces the pressure increase from 22.52% to 10.98%, i.e., 51.24% of the pressure rise is absorbed by PRV. Besides, although the flow rate is changing more slowly in unprotected case, since the water is not discharged from the system by PRV, pressure rise is more than in the protected case.

Pressure is not absorbed by the system after wicket gate is closed totally for the unprotected system in Figure 5.24. This phenomenon is analyzed and being investigated. Although the wave pressures continue to fluctuate in the system, because there is no flow in the pipeline or there is flow with small velocity, friction and minor losses can not decrease the energy of the waves. In addition, since the surge tank has a 5 m orifice at the entrance of the structure, it is not enough to dissipate the energy of the waves in short times. If the simulations are held for a longer time, it is observed that after approximately 5 minutes, the system absorbs the pressure waves and returns to the steady-state condition. It is understood that since PRV discharges the water after wicket gate is closed completely, wave pressures are absorbed, and system backs to steady-state condition earlier than unprotected case. PRV prevents the pipeline system from vibration because of the fluctuation of pressure waves for a long time after wicket gate is closed.

Hydraulic grade lines are presented in Figure 5.25. Piezometric heads are decreased by PRV effect in protected case. The most critical point is just before the turbine, according to Figure 5.25. Piezometric head increases after the surge tank, which is 589 m away from the reservoir, because the surge tank dissipates the energy and does not reflect the wave pressures to energy tunnel. Initial piezometric head is 276.7 m at turbine. Maximum piezometric head is 313.96 m, and minimum piezometric head is 272.99 m without PRV. Therefore, there is a 13% increase and a 1.34% decrease

in the piezometric head. Minimum pressure head is not below the pipeline anywhere, so there is no risk for negative pressure in the system.

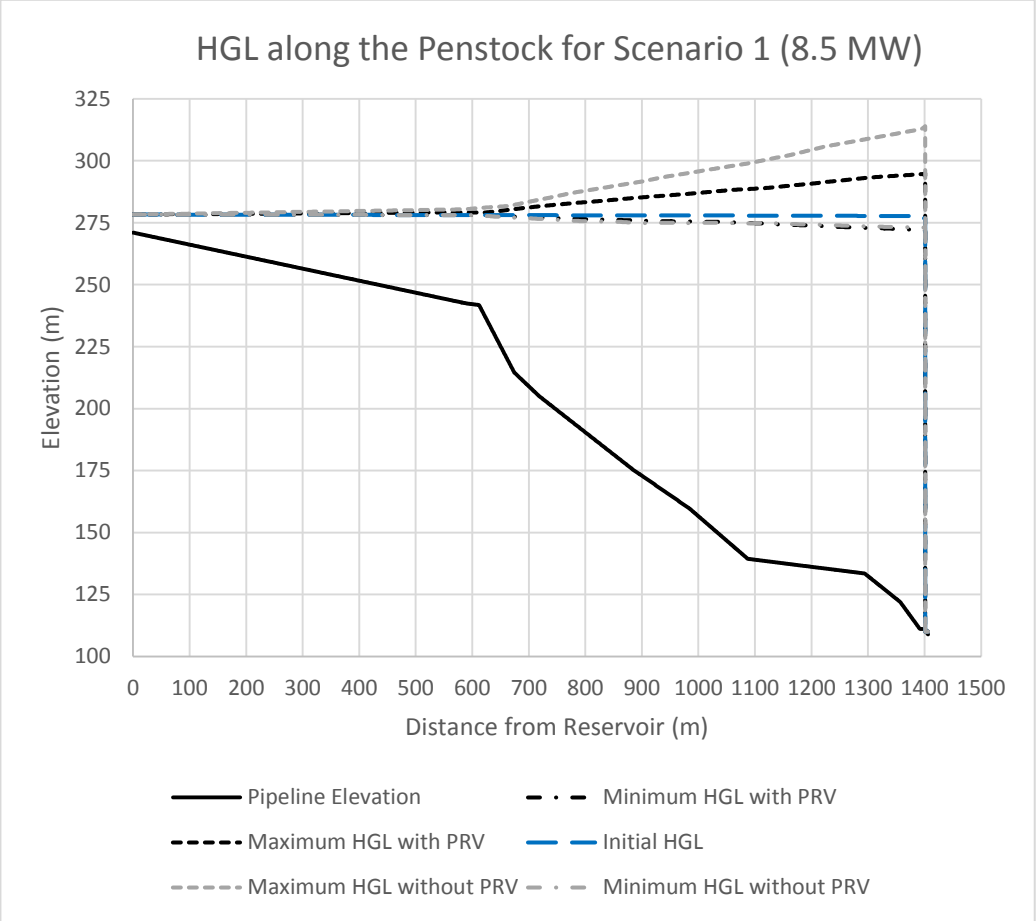

Figure 5.25 HGLs along the Penstock for 8.5 MW Test in Scenario 1 with and without PRV

In Figure 5.25, initial piezometric head is 276.7 m at turbine. When PRV is included in the system, maximum and minimum piezometric heads become 295.02 m and 271.76 m. Therefore, there is 6.6% increase and 1.78% decrease in piezometric head with PRV. Piezometric head rise is reduced approximately 50% by PRV. There is no significant effect on minimum pressure or hydraulic grade line values since PRV can not supply water or air into the system.

In the 9.35 MW test, simulations are held for systems with and without PRV for 6.41 m^3/s flow rate and 166.3 m net head at turbine. Then, a comparison for two different systems is investigated to understand the effect of PRV.

After collecting the required data from the computer program, pressure and discharge changes over the single turbine unit is obtained. The difference between protected and unprotected cases for the 9.35 MW test is analyzed by observing Figure 5.26.

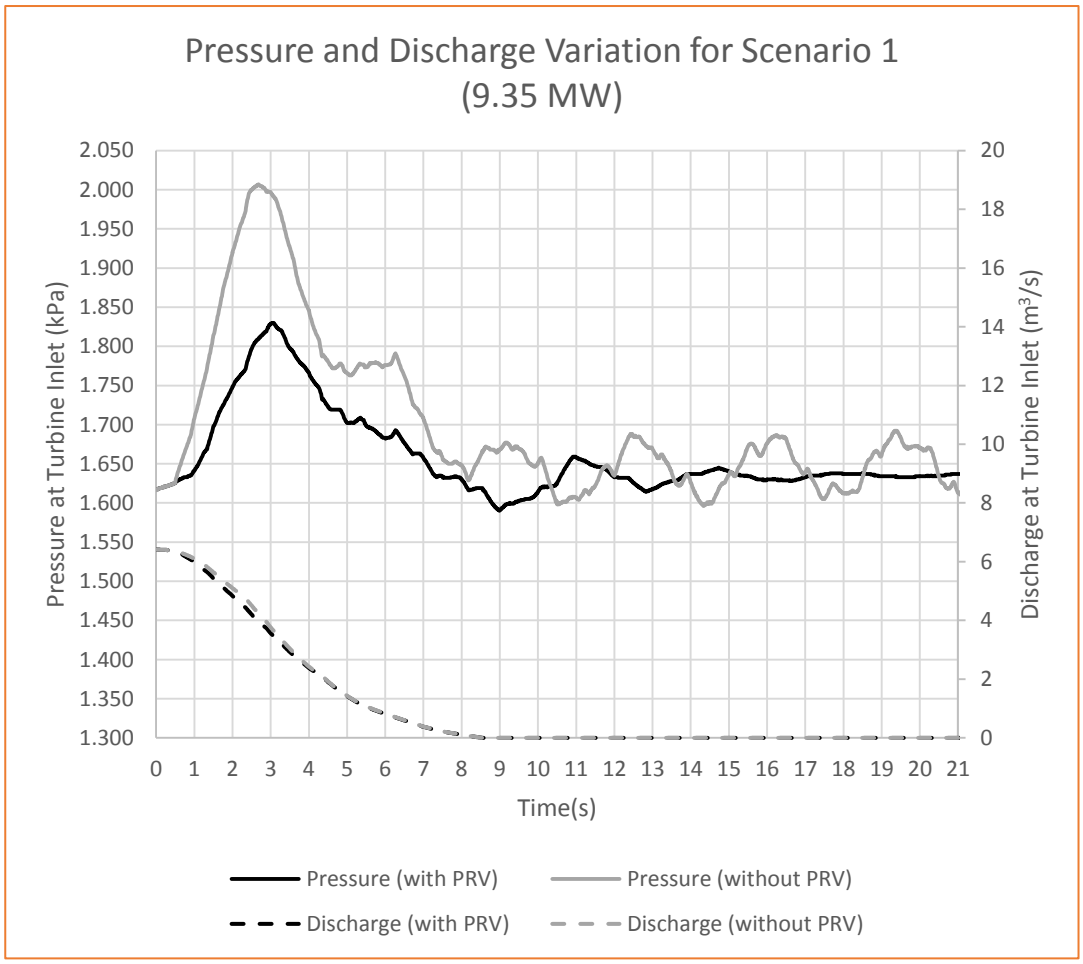

Figure 5.26 Pressure and Discharge Variation for Scenario 1 with and without PRV in 9.35 MW Test

From Figure 5.26, critical points are noted to study on the physical results of numerical values. Maximum pressures are 1830 kPa with %13.17 increase and 2007

kPa with 24.12% increase for the systems with and without PRV. The pressure rise is reduced 45.40% with the help of PRV.

Before summarizing the instant load rejection scenario results, PRV effects on hydraulic grade lines are investigated according to Figure 5.27, which indicates the piezometric heads of the points from reservoir to tailwater.

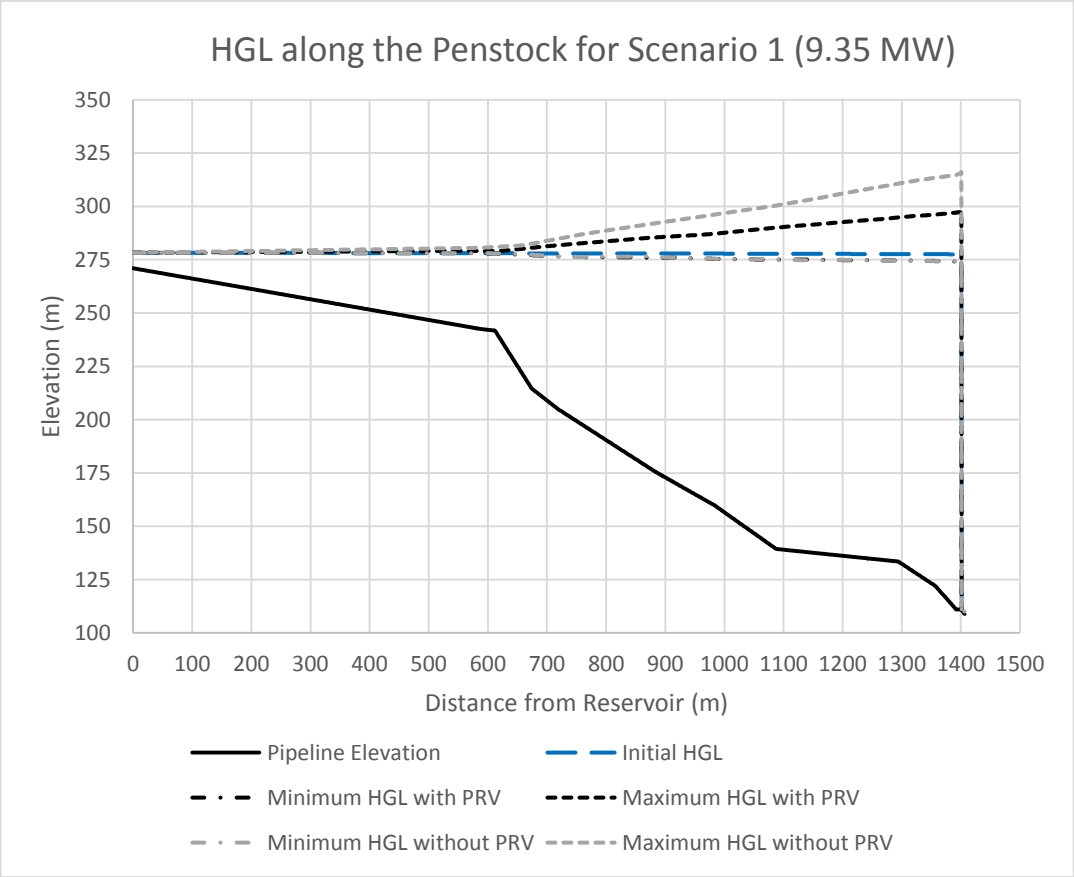

Figure 5.27 HGLs along the Penstock for 9.35 MW Test in Scenario 1 with and without PRV

As seen from Figure 5.27, the critical point is just before the turbine, and there is no significant change in minimum hydraulic grade lines between the two cases. Initial hydraulic grade line is marked with blue in Figure 5.27, and it is 276.36 m at turbine. Protected and unprotected systems' maximum piezometric heads are 297.67 m with 7.71% rise and 316.14 m with 14.39% rise at turbine inlet. PRV effect can be observed as 46.45% reduction on heads from the graphs and numerical results.

Pressure and piezometric head values are slightly higher in the 9.35 MW test without PRV, although initial pressure and piezometric heads are smaller than the 8.35 MW test. Since the flow rate is lower in the 8.35 MW test, friction and minor loss affect are less, so initial values are higher. In contrast, because the wicket gate closure times are the same in this scenario, the closing slope is steeper in the 9.35 MW test. Therefore, maximum pressure and hydraulic grade values increases. However, wicket gate operating rules are not the same in the field tests held with PRV, and closing rates are close to each other. Therefore, PRV absorbs excessive pressures, and 8.35 MW pressure values are slightly higher than the 9.35 MW test. This difference is sourced from PRV operating conditions.

5.3.2 Scenario 2: Load Rejection

Load rejection scenario is similar to instant load rejection. The main difference is that electrical load decreases with respect to time, and turbine frequency is synchronized with generator and grid in load rejection case. Therefore, governor regulates the wicket gate opening according to the electrical torque of the grid. However, electrical load directly drops to zero in instant load rejection case. Therefore, governor tries to close wicket gate rapidly.

Krivchenko (1994) proved that electrical torque decreases linearly by using angular momentum equation. He calculated the runner blade moments acting upon the liquid and equated the moment to turbine energy by multiplying with angular velocity. Therefore, electrical load versus time graph is defined as linear for the computer program in this scenario.

Simulations are done for 9,35 MW and 8,5 MW cases, and different wicket gate closure times are applied to find the critical pattern in the system. After the worst cases are determined, PRV effects are analyzed by simulating protected and unprotected systems.

Firstly, in order to find the most critical closure time for wicket gate, all the simulations are collected in one graph in Figure 5.28. Then, the most vital operating time is selected and analyzed in detail. This point is determined according to instant load rejection pressure values. Since the load rejection can not cause more pressure increase than instant load rejection, a case with pressure values close to field test results is selected. The maximum allowable stress of the pipes is calculated as 1900 kPa from the Hoop stress equation for cylindrical vessels in Chapter 3, Equation 3.8. Therefore, tests are performed with a pressure limit that does not exceed 1800 kPa with a safety factor to prevent any damage to components of the HPP. As a result, this pressure limit is accepted as the critical case for unprotected systems to suggest operating limits without PRV. In load rejection cases, PRV is not preferred to manage because there is enough time to close wicket gate gradually except emergency conditions. In order to suggest operating limits with PRV for emergency conditions, PRV is simulated for the worst case.

Regarding the 8.5 MW Test, in Figure 5.28, pressure and discharge variations are indicated for different wicket gate closure times. These simulations are run without PRV, so after wicket gate is closed, fluctuation of the pressure waves continues until approximately 5 minutes. It can be observed that while the operating time decreases, maximum pressure values increase in the system. If the slope of the wicket gate closure pattern becomes steep for a time interval, the difference between final and initial velocity rises for that time interval. This phenomenon causes a significant increment in pressure values in the system. As a result, the most critical time is selected as 15 seconds for operating rule of wicket gate. Although 12 seconds closure time has 1825 kPa for maximum pressure value, it is not taken as critical since it exceeds the pressure limit in HPP tests.

It is observed from Figure 5.28 while the slope of the discharge versus time graph is decreasing, pressure variation and maximum, minimum pressure values are decreasing.

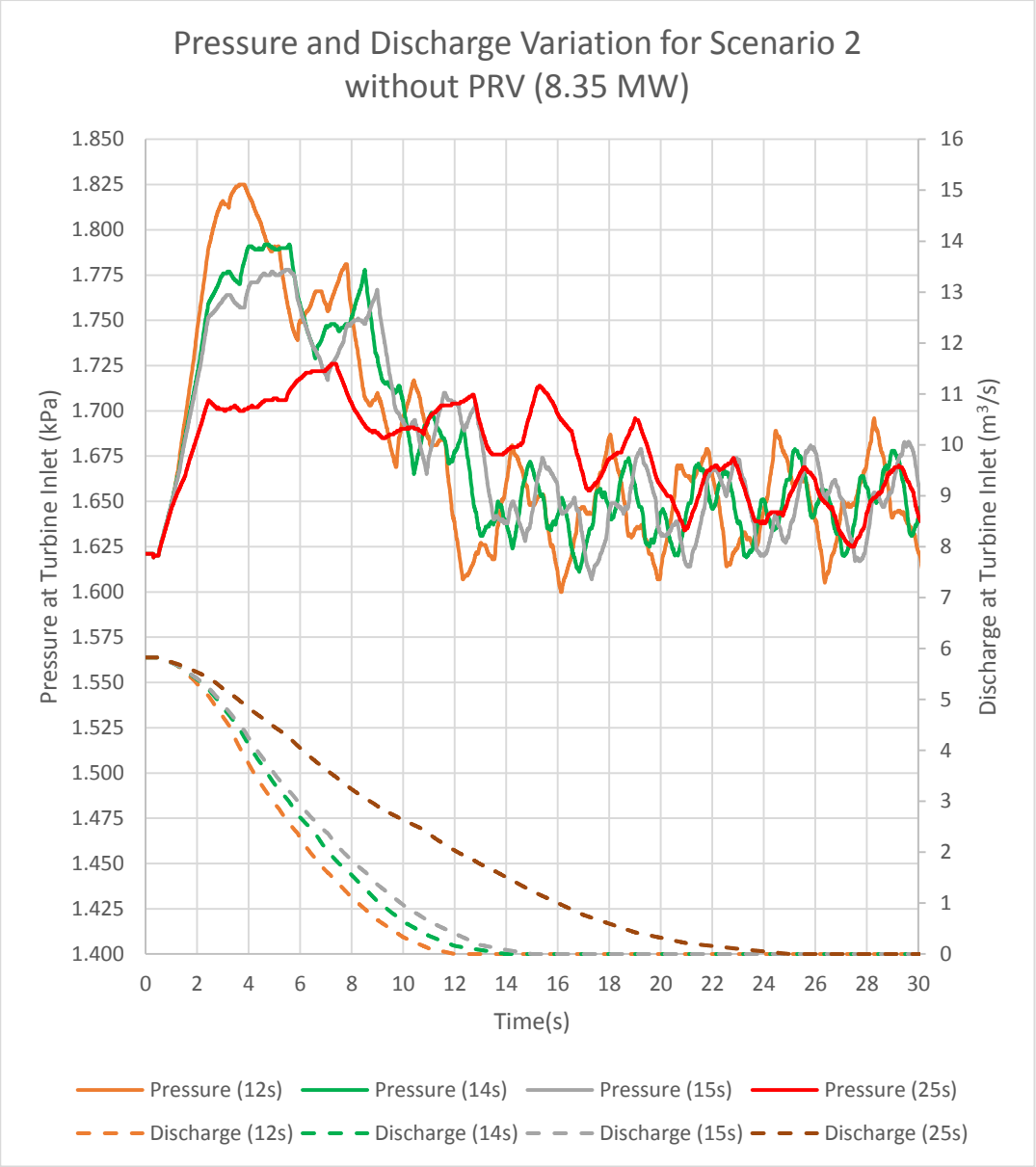

Figure 5.28 Pressure and Discharge Variations for different wicket gate closure times in Load Rejection Scenario for 8.35 MW

After determining the critical operating rule from Figure 5.28, the case is analyzed in detail, and simulations are held for protected and unprotected systems to see the PRV effects on the operation. Wicket gate closure and PRV opening patterns are arranged according to field measured data. Operating rules' closure rates are not changed, and finalization times are extended. Wicket gate closure is performed in 7.70 seconds in the field test, and PRV opening is performed in 7.90 seconds in 8.5

MW field test. Therefore, wicket gate and PRV operating rules are taken as 15 seconds and 15.5 seconds, as seen in Figure 5.29 with curve equations.

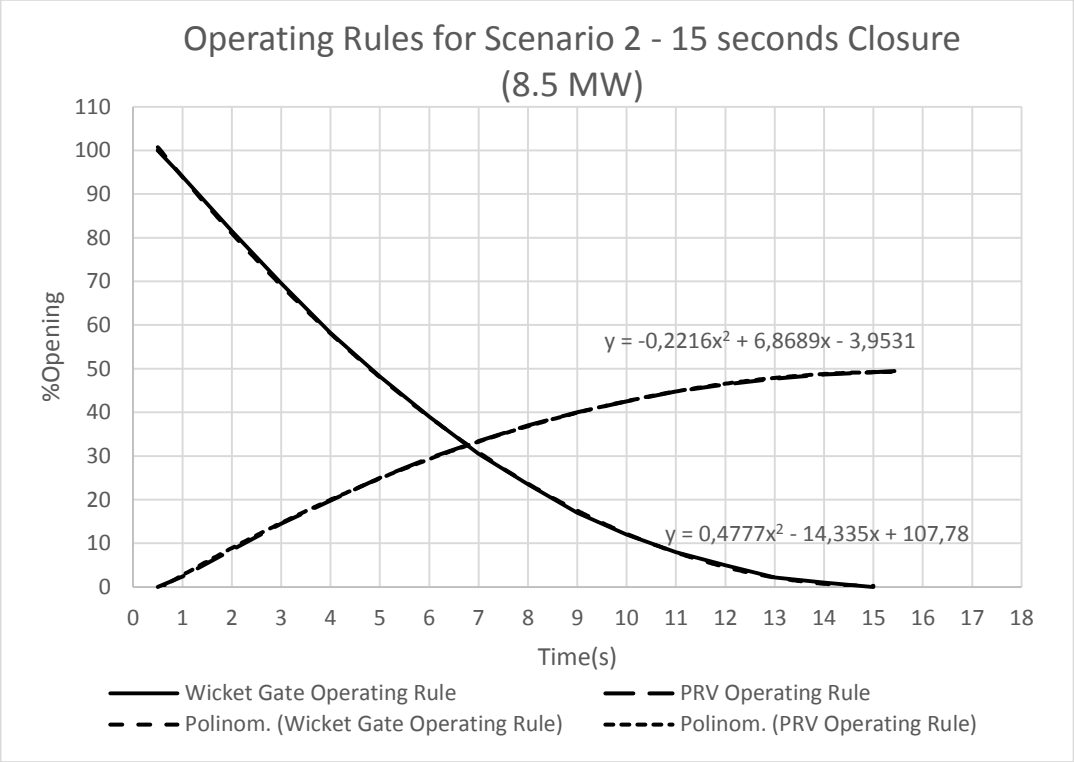

Figure 5.29 PRV and Wicket Gate Operating Rules for Load Rejection 8.5 MW Test 15 seconds closure

Since the PRV is opened while wicket gate is closed simultaneously in field tests, this behavior is applied to all the simulations. Patterns are arranged based on measured data taken from location sensors of servomotor, which controls the wicket gate and PRV.

Figure 5.30 indicates the pressure and discharge changes for load rejection scenario. The most critical closure time is selected as 15 seconds for the 8.5 MW test. There is a slight difference in discharge between 1 and 4 seconds. This difference causes an increase in velocity change so that pressure variation occurs for unprotected case. Initial pressure is 1621 kPa for both cases. Maximum pressure is 1778 kPa without PRV and 1703 kPa with PRV. As a result, 9.69% pressure rise is reduced to 5.06% by PRV. In other words, PRV decreases 47.78% of the pressure rise in the system.

In unprotected system, minimum pressure occurs after wicket gate is closed totally because system can not dissipate the energy of the water hammer pressures, and waves reflect from reservoir and wicket gate with a loop. Still, it is absorbed eventually since there is a flow with negligible velocity in the pipes. This phenomenon is explained in Section 5.3.1.

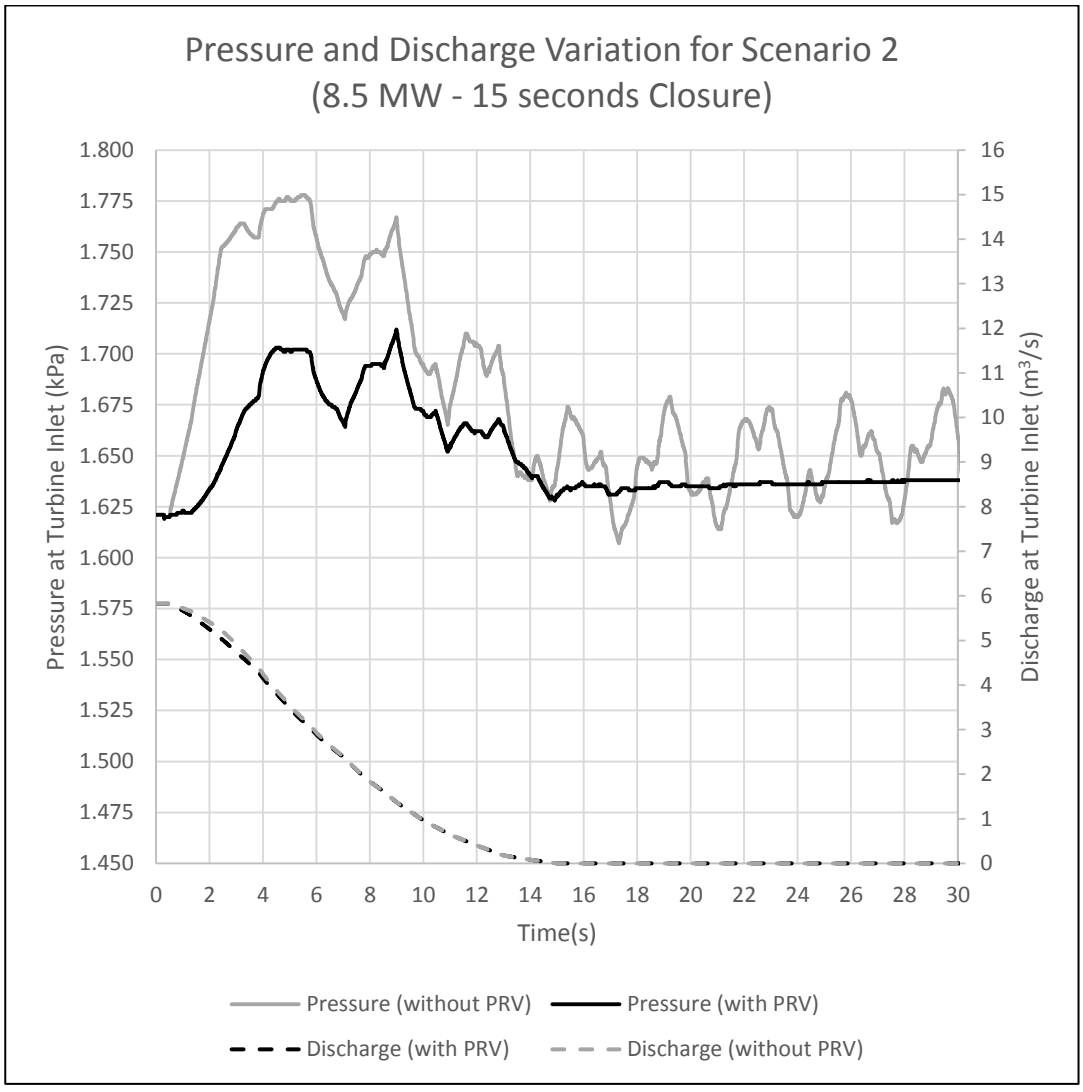

Figure 5.30 Pressure and Discharge Variation for Scenario 2 with and without PRV in 8.5 MW Test

The hydraulic grade line variation on the system is another essential point for understanding the flow behavior and effects of the components along the penstock. Figure 5.31 represents the piezometric heads in the penstocks

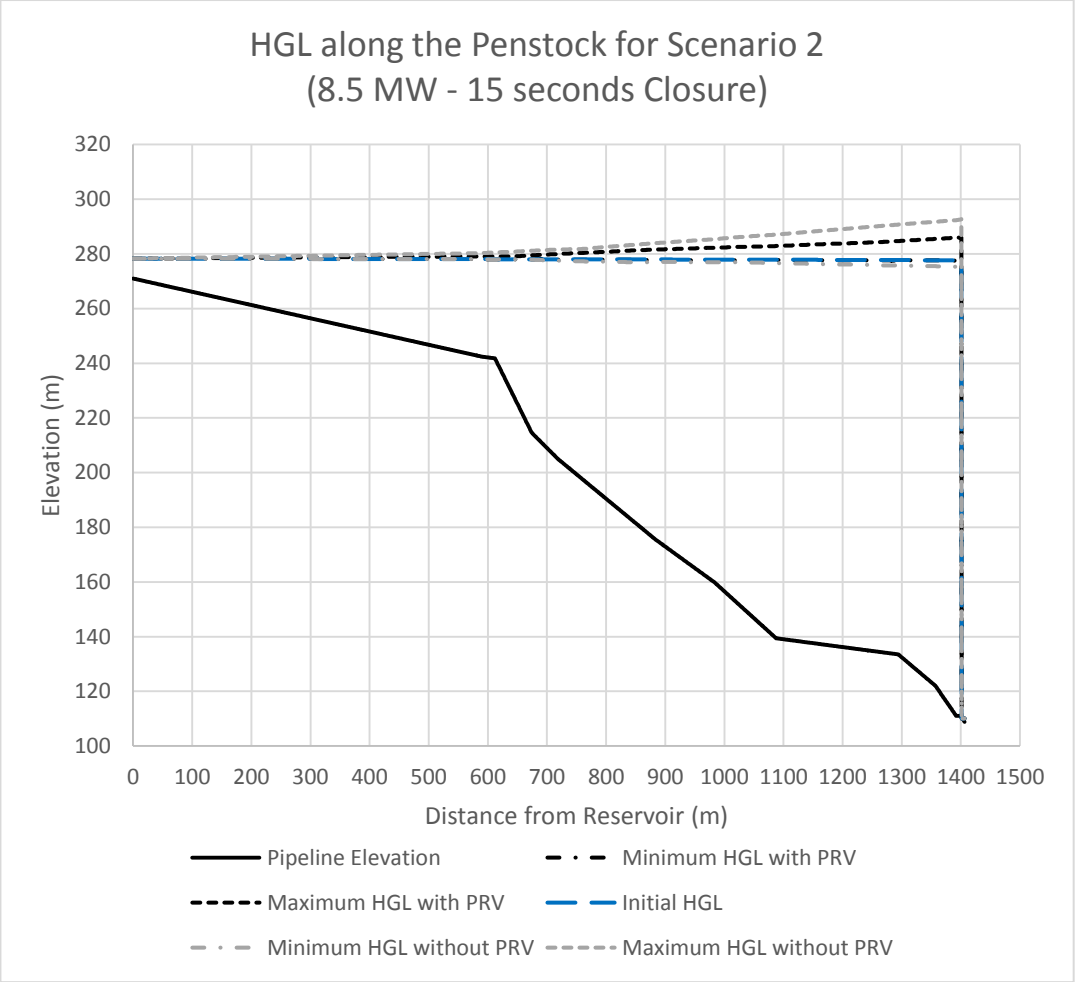

Figure 5.31 HGLs along the Penstock for 8.5 MW Test in Scenario 2 with and without PRV

The most significant variation is obtained at the turbine inlet. Therefore, investigations focus on that point. Initial piezometric head is 276.7, maximum piezometric head is 286.02 with %3.37 increase, and minimum piezometric head is 276.57 with 0.04% decrease just before the turbine for protected system. Unprotected case maximum and minimum pizometric heads are 292.74 m with 5.79% rise and 275.29 m 0.51% reduction respectively. Pressure rise is decreased from 5.79% to 3.37% with PRV. This reduction is calculated as 41.8%.

Regarding the 9.35 MW test, simulations start with initial conditions that are 6.41 m^3/s flow rate and 166.6 m net head at turbine. Therefore, pressure starts from 1617 kPa for this case. The same methodology is followed, and Figure 5.32 is constructed to determine the critical closure time for load rejection case with provided steady-state conditions.

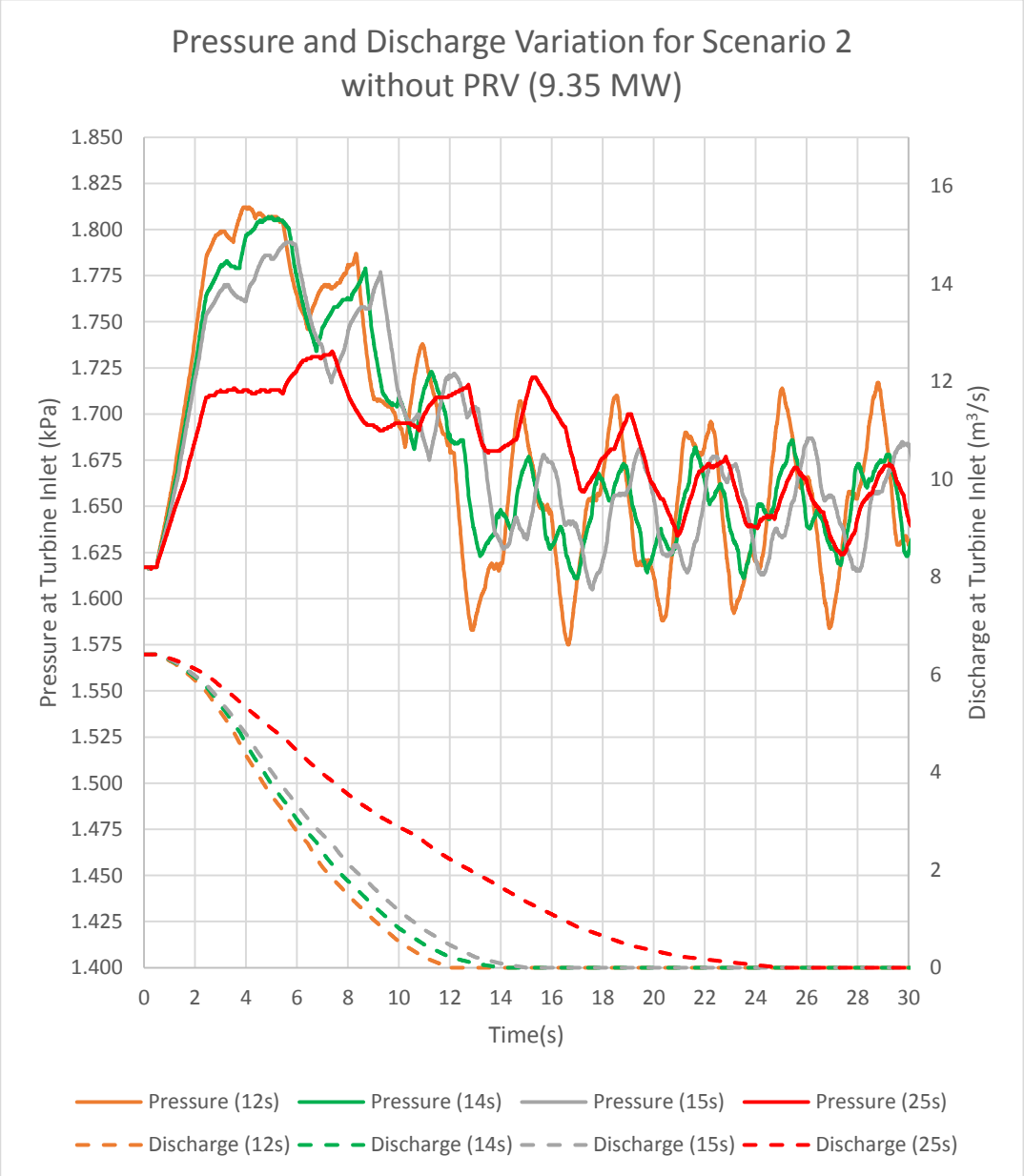

Figure 5.32 Pressure and Discharge Variations for different wicket gate closure times in Load Rejection Scenario for 9.35 MW

Since the wicket gate closure becomes slower, pressure variations are decreased, as seen in wicket gate closure in 25 seconds case from Figure 5.32. Discharge rates are proportional to wicket gate opening percentage because flow is controlled by the only turbine in the system.

As in the 8.5 MW test, the most critical closure time is 15 seconds in this case. Therefore, conditions are analyzed in detail with and without PRV for this wicket gate closure time. Figure 5.33 indicates the simulation results for protected and unprotected cases.

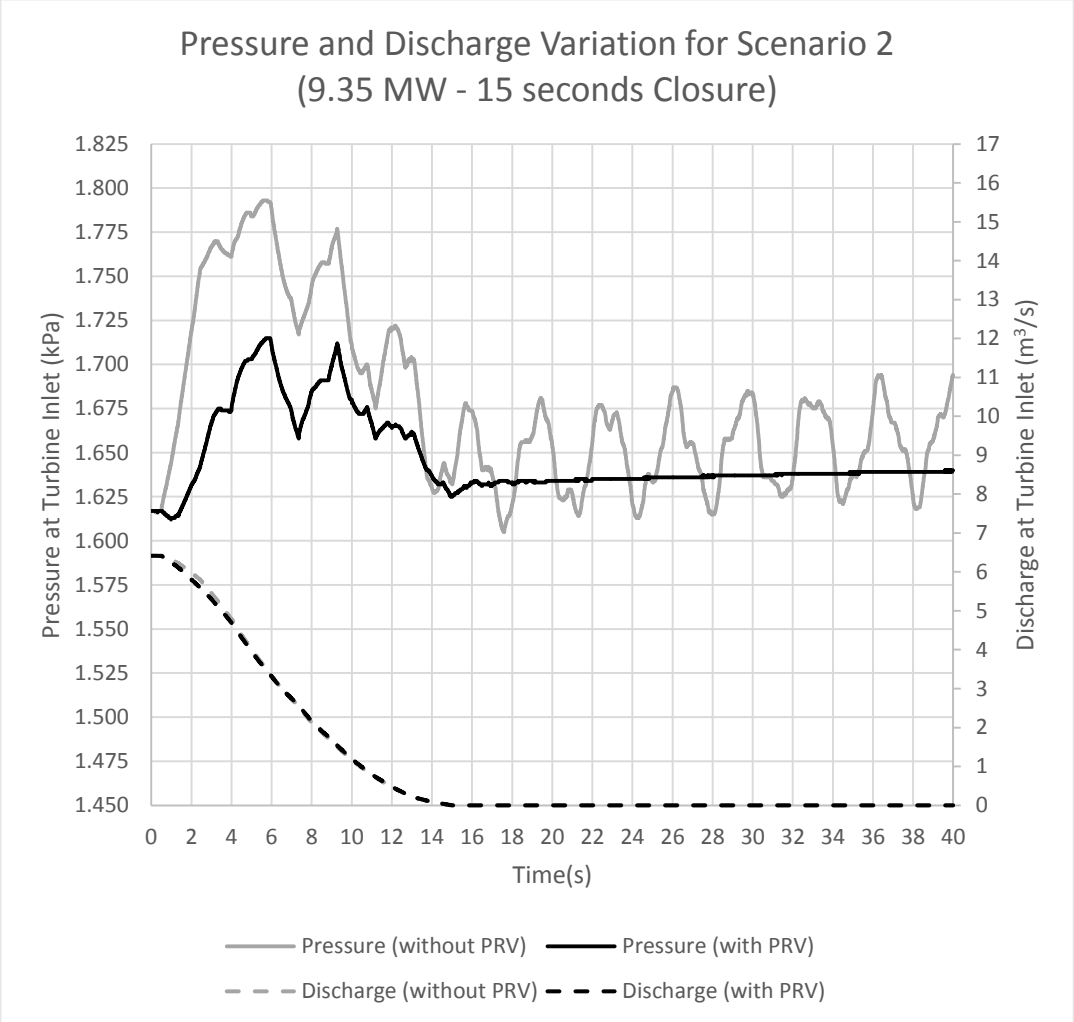

Figure 5.33 Pressure and Discharge Variation for Scenario 2 with and without PRV in 9.35 MW Test

After collecting related data from the results for investigating the PRV effect, maximum pressures are obtained as 1715 kPa with 6.06% increase for protected case and 1793 kPa with 10.88% increase for unprotected case. As a consequence, PRV effect is a %44.34 decrease in the maximum pressure rise quantity. In figure 5.34, piezometric heads are analyzed for the system whose wicket gate is closed in 15 seconds with 9.35 MW initial turbine power. PRV decreases the piezometric head ascending by 44.38%.

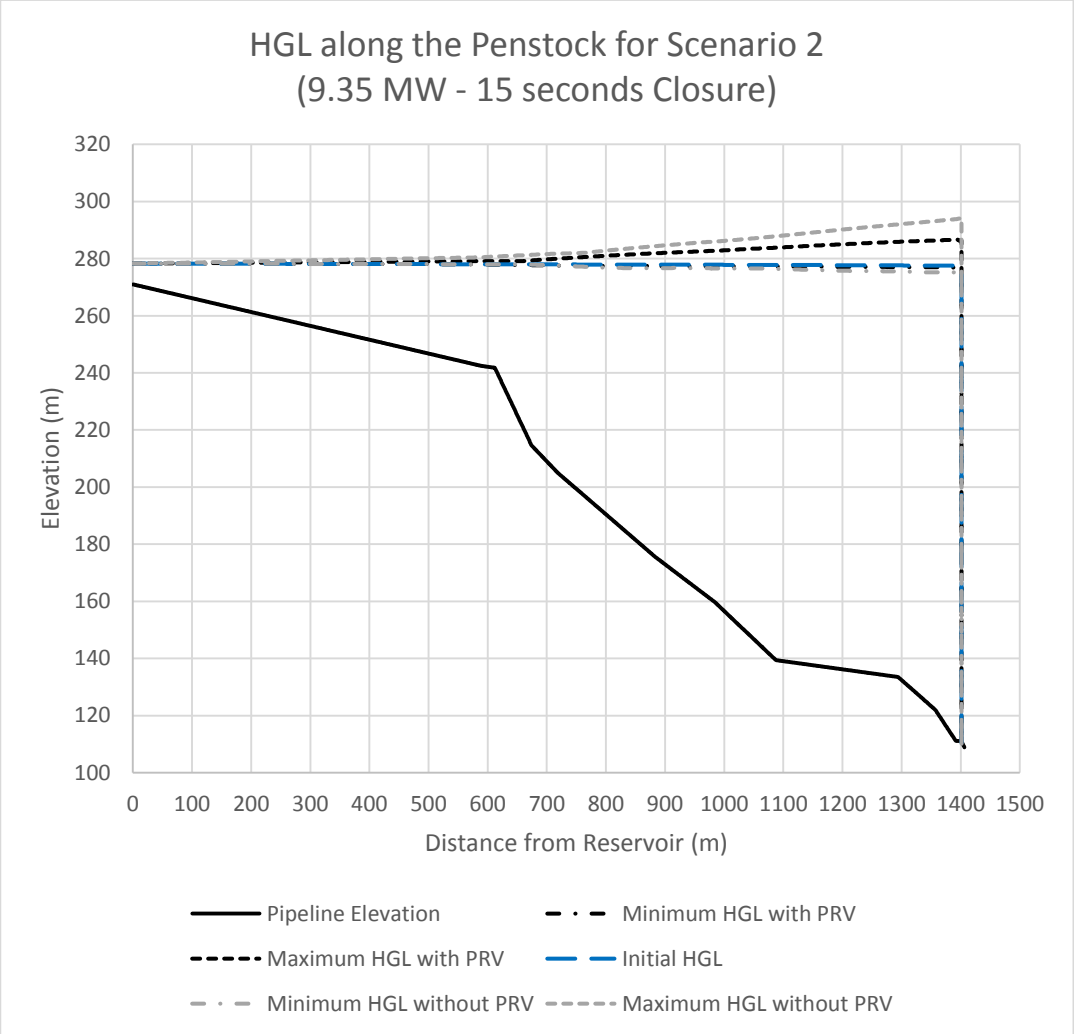

Figure 5.34 HGLs along the Penstock for 9.35 MW Test in Scenario 2 with and without PRV

5.3.3 Scenario 3: Load Acceptance

In this scenario, the turbine is closed in initial status and starts to work with opening the wicket gate by governor. Then, it turns with small amount of discharge until the frequency of the turbine reaches the grid frequency. After the equality of frequency is satisfied between grid, turbine, and generator, electrical grid starts to take the electrical energy from the generator with the help of a breaker in the connection. Finally, governor begins to open wicket gate from about 5%-7% percent to the required opening percentage according to electrical load in the grid.

In HAMMER, turbine is assumed to be operating at no-load speed, which is just before satisfying the equality of frequency between grid and turbine. Therefore, the turbine does not generate electrical power**,** and HAMMER assumes that the grid is linked to the generator's output when the simulation starts. (Bentley, 2010)

Load acceptance case is less severe than load rejection cases. However, since there is a chance of forming negative pressures in the system, critical points should be checked to be on the safe side. If the pressure drops below the penstock elevation, cavitation and column separation can occur in the pipes, and components may take damage from these phenomena. As a result, six simulations are performed for different wicket gate opening times to see the behavior of the system in load acceptance case. Since there is no effect of the PRV in load acceptance case, system with PRV is not simulated.

Regarding the 8.5 MW test, after simulations and analysis are completed for 5.82 m^3/s flow rate and 166.66 m net head, the most critical wicket gate opening time is determined as 5 seconds. Figure 5.35 shows the pressure and discharge variations of different cases. Since the pressure reduction is more significant in 5 seconds opening case, this case should be checked whether the piezometric head is below the pipeline elevation or not.

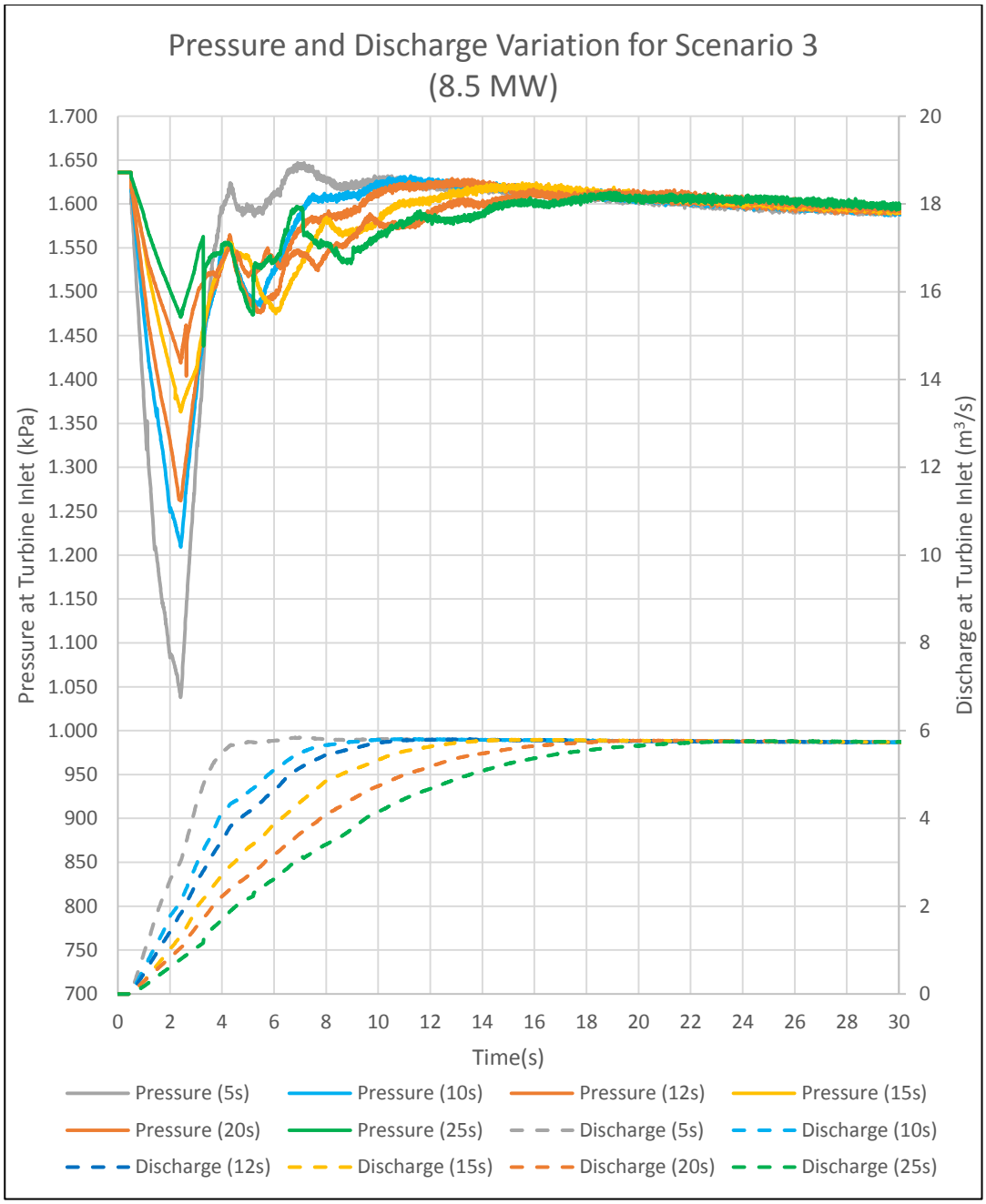

Figure 5.35 Pressure and Discharge Variations for different wicket gate opening times in Scenario 3, 8.5 MW Test

If the wicket gate opening rule is rapid, pressure value decreases more slightly. Discharge is determined by wicket gate pattern. Minimum pressure is 1471 kPa with 10.08% decrease for 25 seconds closure. As a result, load acceptance should be performed for a long time if there is no emergency situation.

Figure 5.36 indicates the wicket gate operating rule with 2nd order smooth curve equation for 5 seconds in Scenario 3. Since the HAMMER accepts that wicket gate opening is 100% at the end of load acceptance case, 5.82 m^3/s discharge and 166.66 m net head is arranged for 100% wicket gate opening condition by taking ratio from field measured tests.

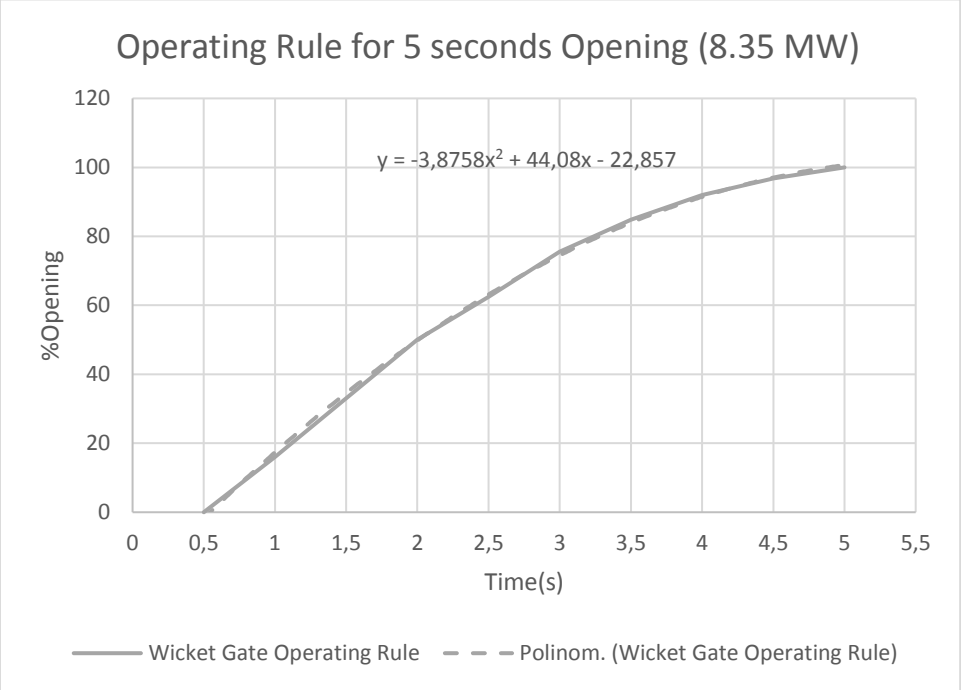

Figure 5.36 Wicket Gate Opening in 5 seconds for Scenario 3 (8.5 MW)

Since data are not recorded for the load acceptance case, the wicket gate pattern is arranged using validation stage information. Measured data are taken from location sensors on the servomotors, which regulate the operation of the wicket gate in the field. On the other hand, simulation data are taken from the circular gate in HAMMER model. Therefore, wicket gate opening pattern cannot be linear. While modeling the wicket gate operating rule in load acceptance case, the same methodology is applied with validation stage calibrations by considering the difference of field and model.

Pressure and discharge variation of the worst case is indicated in Figure 5.37. Since the initial pressure decreases from 1636 kPa to 1038 kPa with 36.55% reduction

Turbine does not work in initial conditions, and minor losses in the turbine are not calculated by computer program. Therefore, initial pressure amount is larger than in other cases.

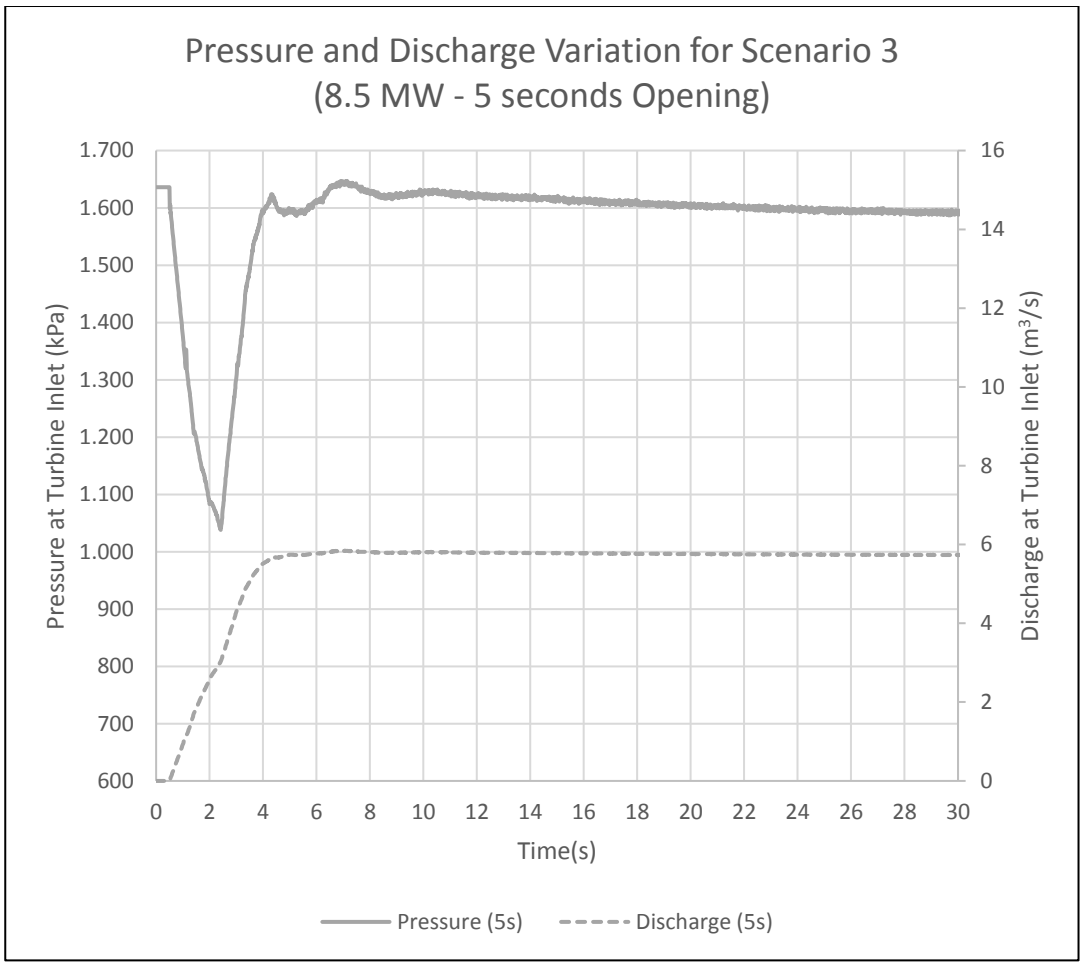

Figure 5.37 Pressure and Discharge Variation of 5 seconds Wicket Gate Opening Case for Scenario 3 (8.5 MW)

Although %36.55 decrease in pressure is a more significant variation according to other scenarios, this change is not severe for the system. Because the system has a surge tank with a volume of 1,466,540 m^3, it prevents negative pressures in the penstocks.

In order to check the piezometric heads, hydraulic grade lines are analyzed in Figure 5.38. Minimum piezometric head decreases from 278.3 m to 217.03 m with 22.06% reduction. It can be concluded from the below figure that the minimum hydraulic

grade line does not drop below the penstock elevation anywhere. The system is safe against negative pressures. Surge tank does not allow a significant decrease of pressure by supplying water to the system. Therefore, surge tank is enough to prevent the drop of pressure head to negative values in the load acceptance scenario. Maximum hydraulic grade line is 279.58 m at turbine inlet. It is 1.28 m larger than initial status. The maximum pressure is observed as 1647 kPa, which is 11 kPa larger than the initial pressure value in Figure 5.37. As a result, load acceptance case causes a slight increase in the pressure according to steady-state conditions.

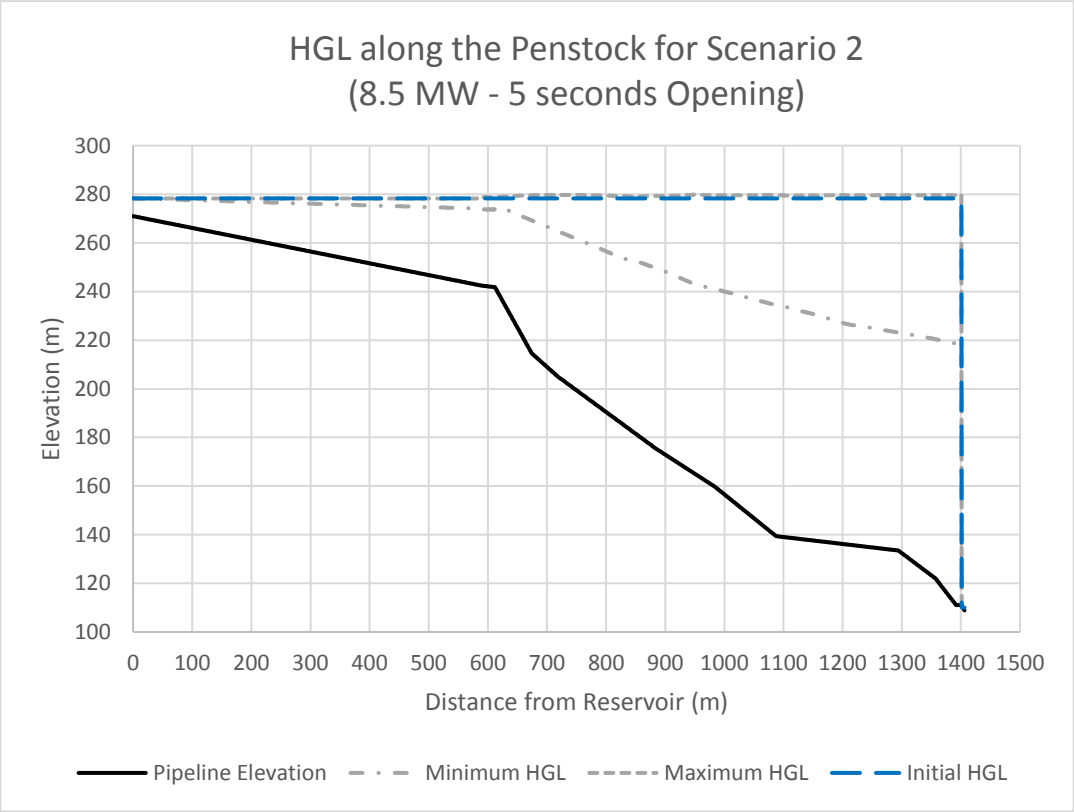

Figure 5.38 HGLs along the Penstock for 5 seconds Wicket Gate Opening Case in Scenario 3 (8.35 MW)

Regarding the 9.35 MW test, the methodology is the same as the previous steps. Firstly, all the simulations' results for pressure and discharge are exported into one graph in Figure 5.39, and the most critical case is determined by analyzing the minimum pressure points. Then, the worst case is investigated to check the negative

pressures in the system. Simulations are held for 6.41 m^3/s flow rate and 166.3 m net head at turbine.

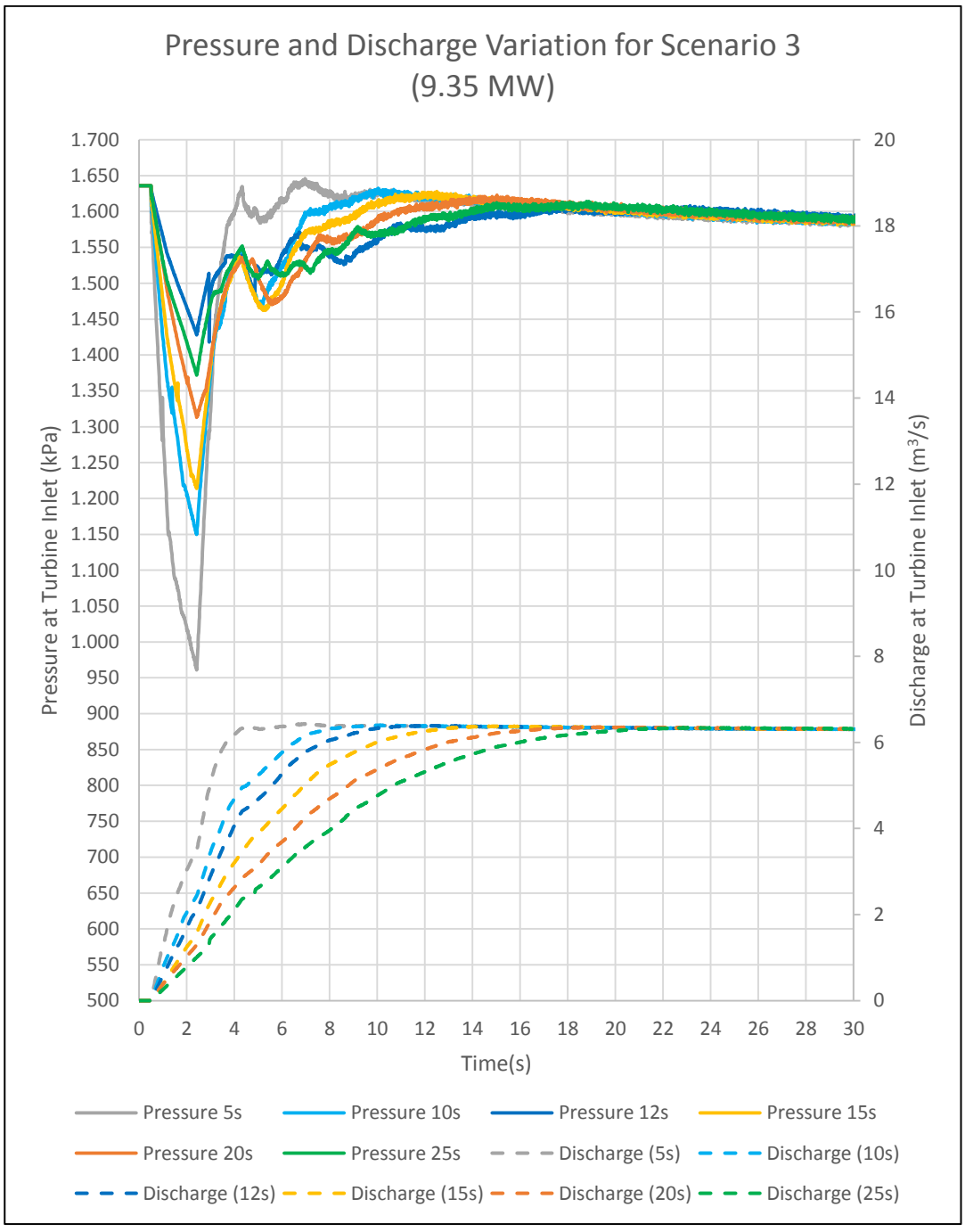

Figure 5.39 Pressure and Discharge Variations for different wicket gate opening times in Scenario 3 (9.35 MW)

As in the 8.5 MW test, the most critical opening time is determined as 5 seconds. Operating discharge is 6.41 m^3/s for 9.35 MW turbine power, and opening times are taken the same as in 8.5 MW. Therefore, wicket gate opening and discharge slopes are steeper. As a result, the minimum pressure values are smaller than the previous test, so pressure variations are more significant.

From Figure 5.39, it is observed that the worst case is 5 seconds wicket gate operating for the 9.35 MW turbine power load acceptance scenario. Therefore, a detailed check will be performed for this operating rule in the following figures. Wicket gate pattern is illustrated for 9.35 MW with 5 seconds opening in Figure 5.40.

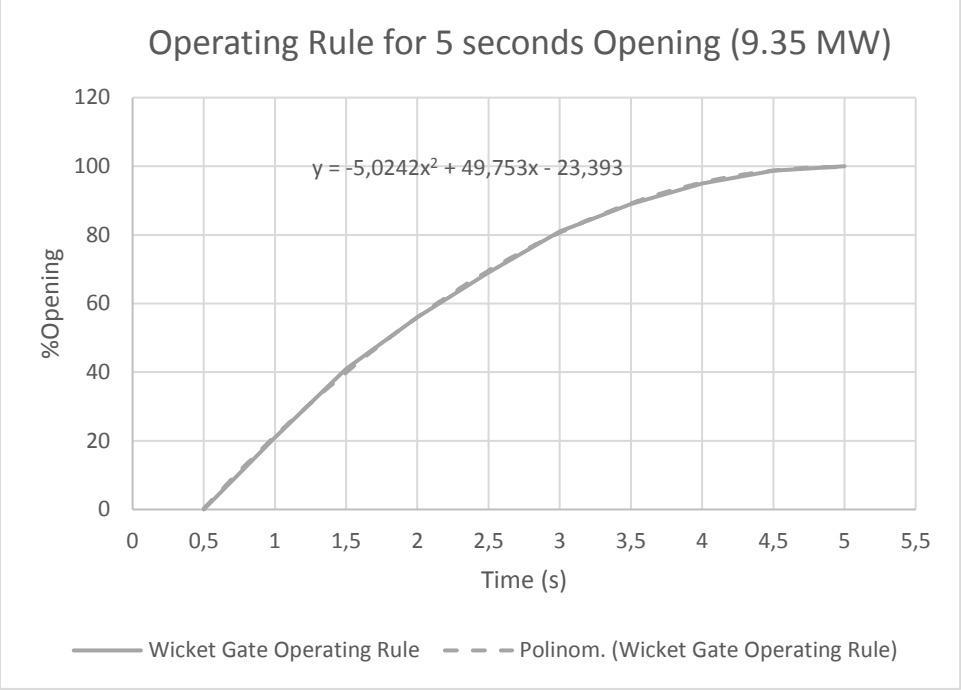

Figure 5.40 Wicket Gate Opening in 5 seconds for Scenario 3 (9.35 MW)

After wicket gate opening rule is defined to the computer program, simulations are held for the case. Discharge and pressure variations versus time graphs are indicated in Figure 5.41. Since the target discharge is larger and opening times are the same as the 8.5 MW turbine power test, minimum pressure amount is decreased to 961 kPa. Initial pressure is 1636 kPa, and reduction of pressure is calculated as 41.26%. The difference between pressure reduction of the 8.35 MW and 9.35 MW tests is 4.71%.

This result proves that while accepting the load for turbine, if the operating discharge is greater, the slope of discharge versus time graph increases. Therefore, the pressure change is more significant.

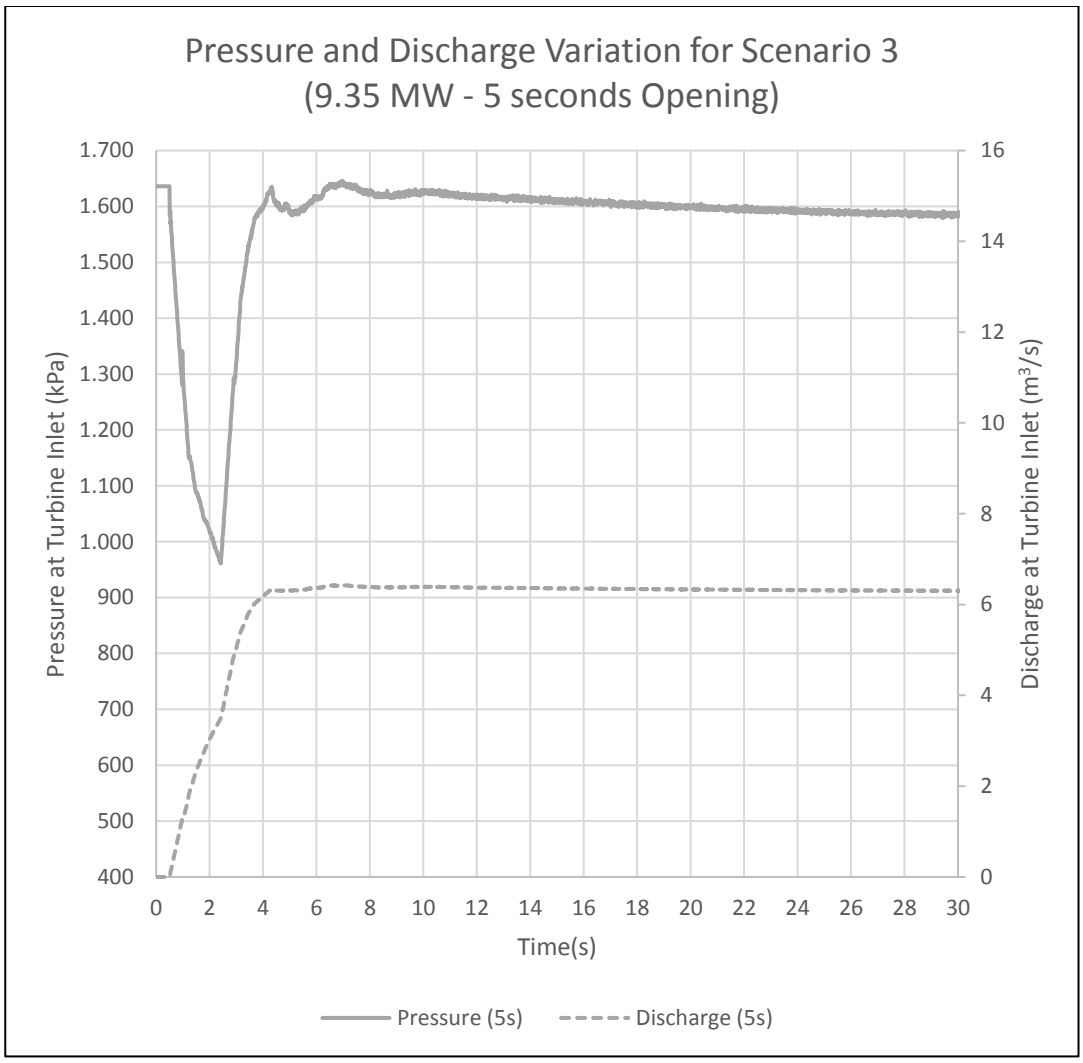

Figure 5.41 Pressure and Discharge Variation of 5 seconds Wicket Gate Opening Case for Scenario 3 (9.35 MW)

Hydraulic grade lines are checked to determine the safety of the system against negative pressures. Figure 5.42 shows the piezometric head change along the penstock from reservoir to tailwater. Since the piezometric head or HGL never drops below the pipe center line, there is no chance for cavitation or column separation formation in the load acceptance case. Piezometric heads at any point are above the

penstock elevation. The major head variation occurs at the turbine inlet. The initial piezometric head decreases from 278.3 m to 209.22 m just upstream of the turbine. This means reduction is 24.82% for hydraulic grade line level. Maximum piezometric head is slightly larger than initial values because load acceptance case does not increase the pressure in the system.

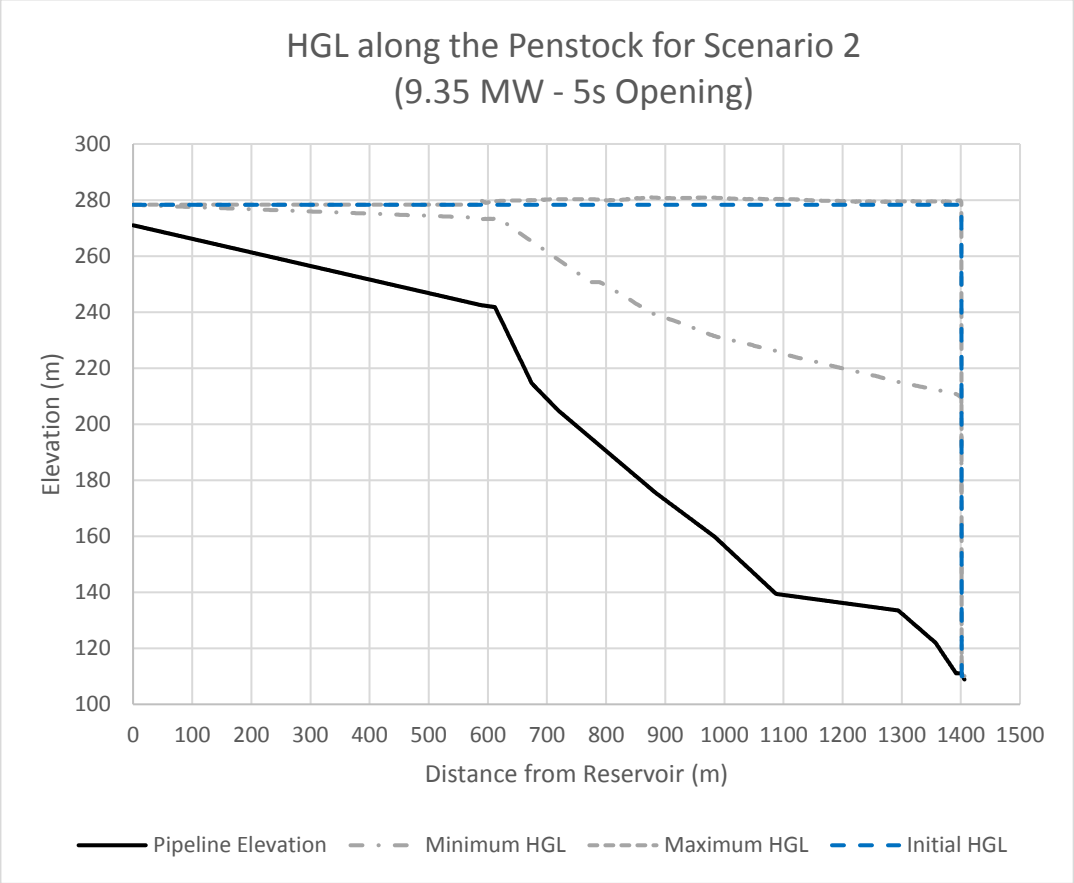

Figure 5.42 HGLs along the Penstock for 5 seconds Wicket Gate Opening Case in Scenario 3 (9.35 MW)

5.3.4 Scenario 4: Load Variation

During the generation of energy from the turbine, electrical load can change in the grid because of alterations in daily electricity demands. According to electrical load amount, governor regulates the wicket gate opening to maintain equality in frequency between generator and electrical grid. Governor adjusts the flow rate that

determines the generated energy in the turbine units. This phenomenon results in flow acceleration and deceleration in the penstocks, so pressure starts to fluctuate in the system. HAMMER assumes that governor matches the electrical loads between generator and electrical grid without any mistake or phase differences. Therefore, turbine always operates at synchronous speed.

Although excessive pressures are not observed in load variation case, sudden increase and decrease in discharge may cause negative pressures and critical pressure rises in the system. Therefore, six load reduction simulations are performed for different generated energy intervals at various times to find the worst case. Then, the most critical case is analyzed individually. As the critical wicket gate opening time is known from the load acceptance scenario in Section 5.3.3, a wicket gate operating rule is determined to analyze the results for investigating negative and maximum pressures together. Because excessive maximum pressures are not expected in load variation case, PRV is not opened in the simulations.

Since the wicket gate opening should be started from 100% in computer program. The initial flow rate is arranged per turbine power, and wicket gate rule is regulated by taking a ratio of initial status. Discharges are calculated by using Equation 3.1 for related generated energy. Table 5.9 indicates the turbine power for single unit and discharge values.

Table 5.6 Discharge values corresponding to Turbine Power

Turbine Power (MW)	Discharge (m^3/s)
2	1.36
3	2.04
4.5	3.06
5	3.40
5.5	3.75
6.5	4.43
7.5	5.12
8.5	5.82
9.35	6.41

Pressure and discharge changes for six different load reduction simulations are analyzed in Figure 5.43 to determine the worst case that results in maximum pressure magnitude which is close to the allowable pressure magnitude of the system.

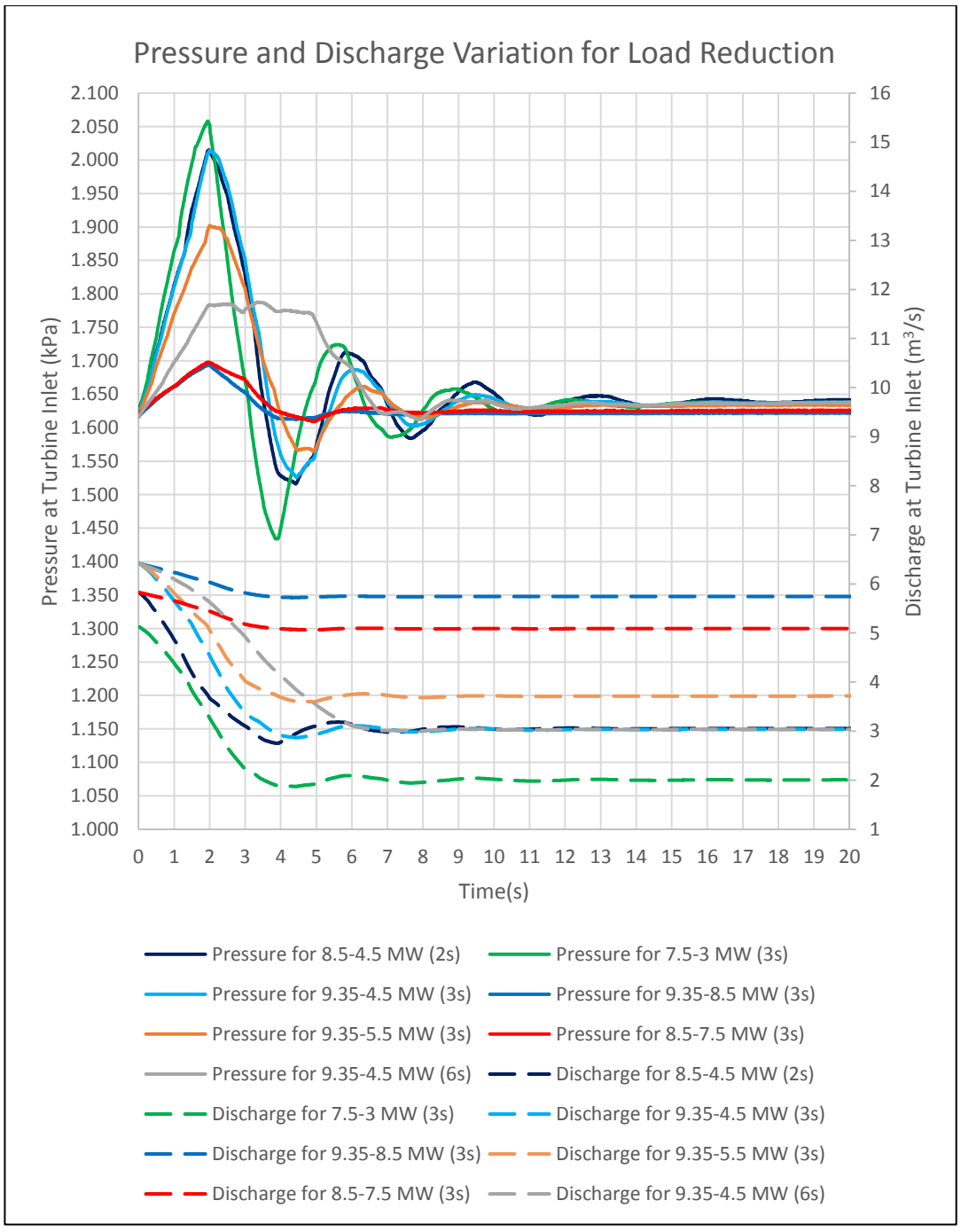

Figure 5.43 Pressure and Discharge Variations for Different Load Reduction Cases without PRV

The worst case is determined as decreasing turbine power from 9.35 MW to 4.5 MW in 6 seconds because the maximum pressure values are close to allowable pressure values for the system. In some cases, maximum pressure values exceed the limits, but these operating rules do not reflect reality, so they are not taken as critical. This study aims to find and analyze an expectable scenario in real life that is close to the pressure limits of the HPP. Then, the most critical load reduction and load acceptance cases are combined in load variation scenario to determine the closing or opening time limits between turbine power ranges. Wicket gate closure rule is determined based on load rejection scenario patterns by changing the opening percentage at the end of operation and time, as seen from Figure 5.44.

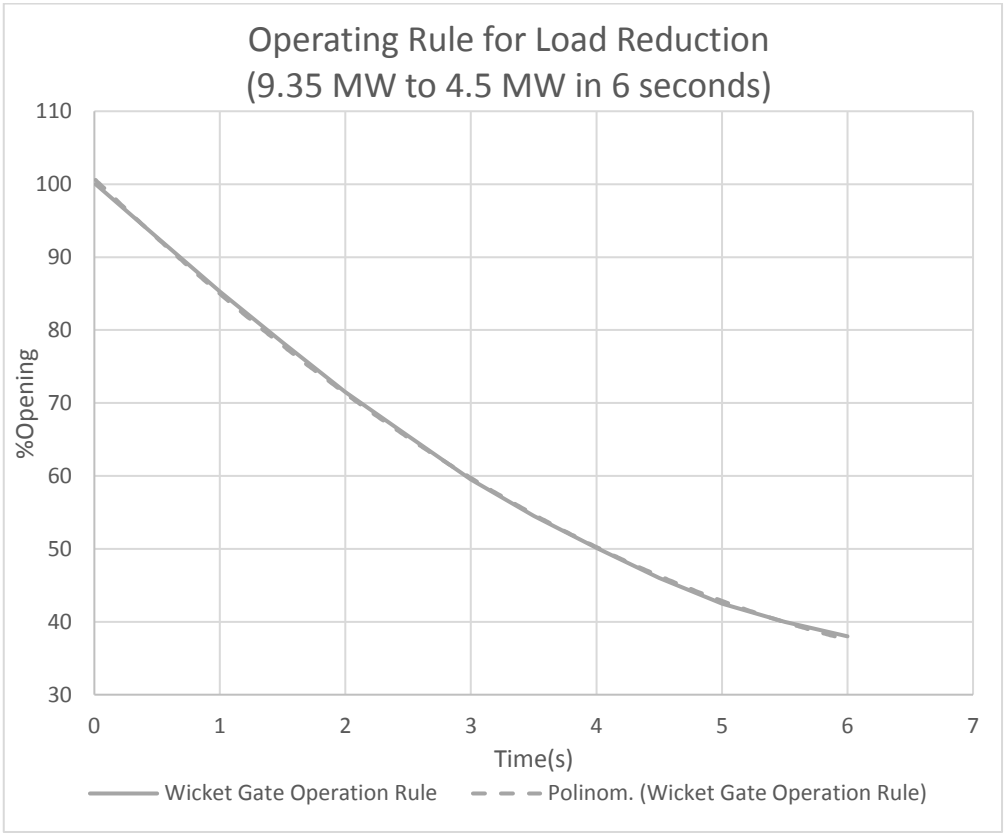

Figure 5.44 Wicket Gate Operating Rule for Load Reduction from 9.35 MW to 4.5 MW Turbine Power in 6 seconds

In this case, discharge is decreased from 6.41 m^3/s to 3.05 m^3/s, and turbine power is decreased from 9.35 MW to 4.5 MW by reducing the wicket gate opening. This

phenomenon represents the change in electricity demand for HPP. The case is analyzed to understand the effect of reduction by investigating the results of pressure and discharge values from Figure 5.45 and hydraulic grade line levels from Figure 5.46. Pressure increases from the initial value, which is 1617 kPa, to 1785 kPa as maximum value with 10.39% in 2.37 seconds. While reflected waves from surge tank start to decrease pressure at turbine inlet, new wave pressures occur just before the turbine because of wicket gate closure. There is an equilibrium after 2 seconds between these two waves for 2 seconds. Therefore, the pressure line seems constant between 2 and 4 seconds in Figure 5.45.

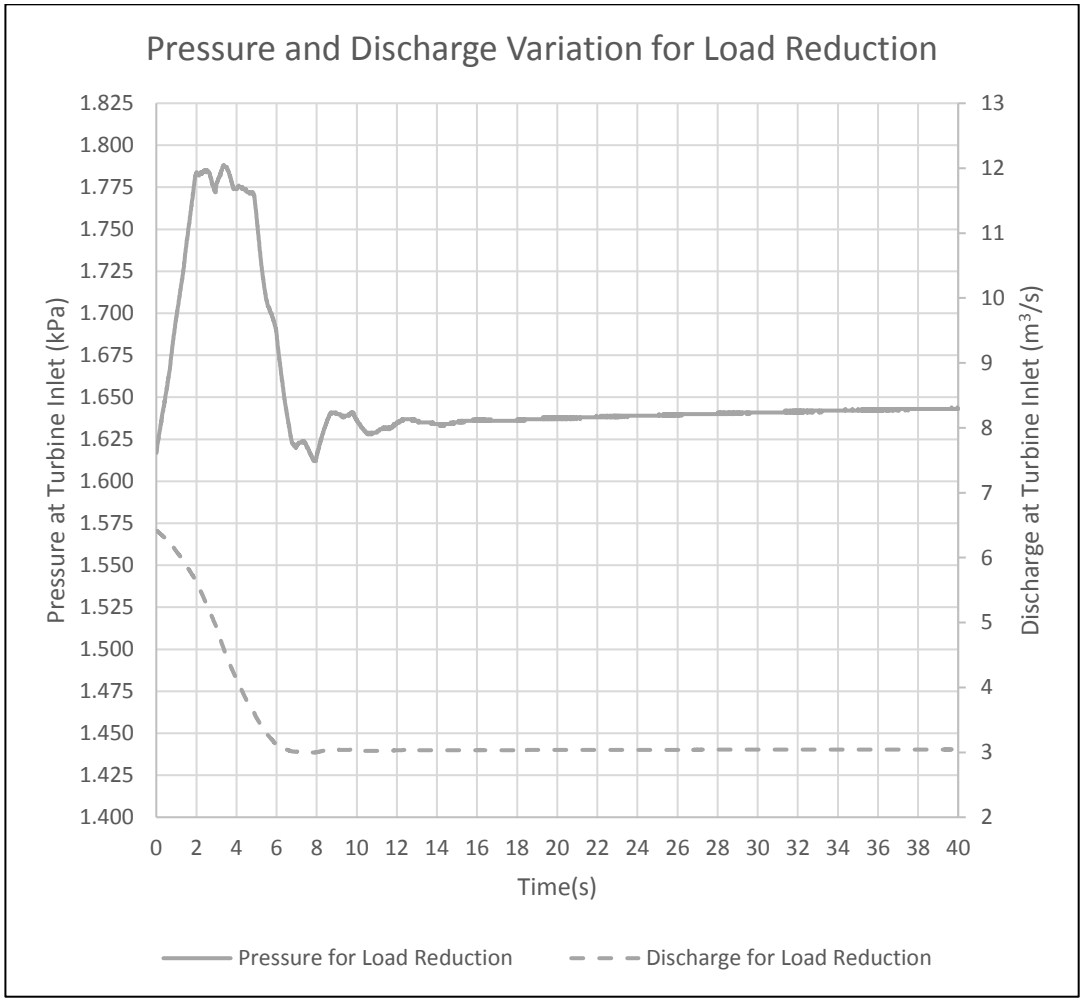

Figure 5.45 Pressure and Discharge Variation of Load Reduction from 9.35 MW to 4.5 MW in 6 seconds

Piezometric heads are checked in order to obtain increases and decreases in the system. Figure 5.46 indicates the hydraulic grade line levels for the critical case of load reduction simulations. Minimum hydraulic grade level does not change significantly, and the system is not affected by low pressures for this scenario. Maximum hydraulic level increases from 276.36 m to 293.79 m with 6.31% rise, which is not severe for the system.

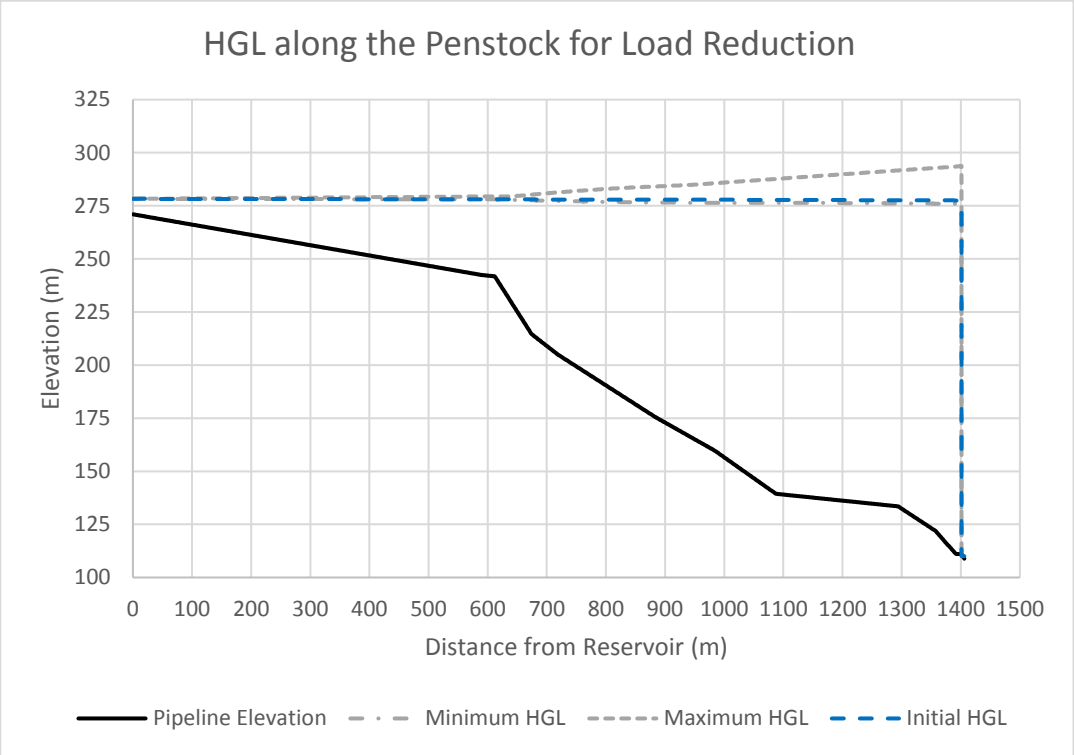

Figure 5.46 HGL's along the Penstock for Load Reduction from 9.35 MW to 4.5 MW in 6 seconds

After the most critical case is analyzed for the system, a wicket gate pattern is defined for load variation scenario. It is known that the worst cases are reducing the turbine power from 9.35 MW to 4.5 MW in 6 seconds and accepting the load for 9.35 MW in 5 seconds. Therefore, wicket gate operating rule is arranged according to this information. First, turbine power will be decreased from 9.35 MW to 4.5 MW in 6 seconds, and then, it will be increased to 9.35 MW in 5 seconds. Figure 5.47 shows the graphical representation of wicket gate operating rule.

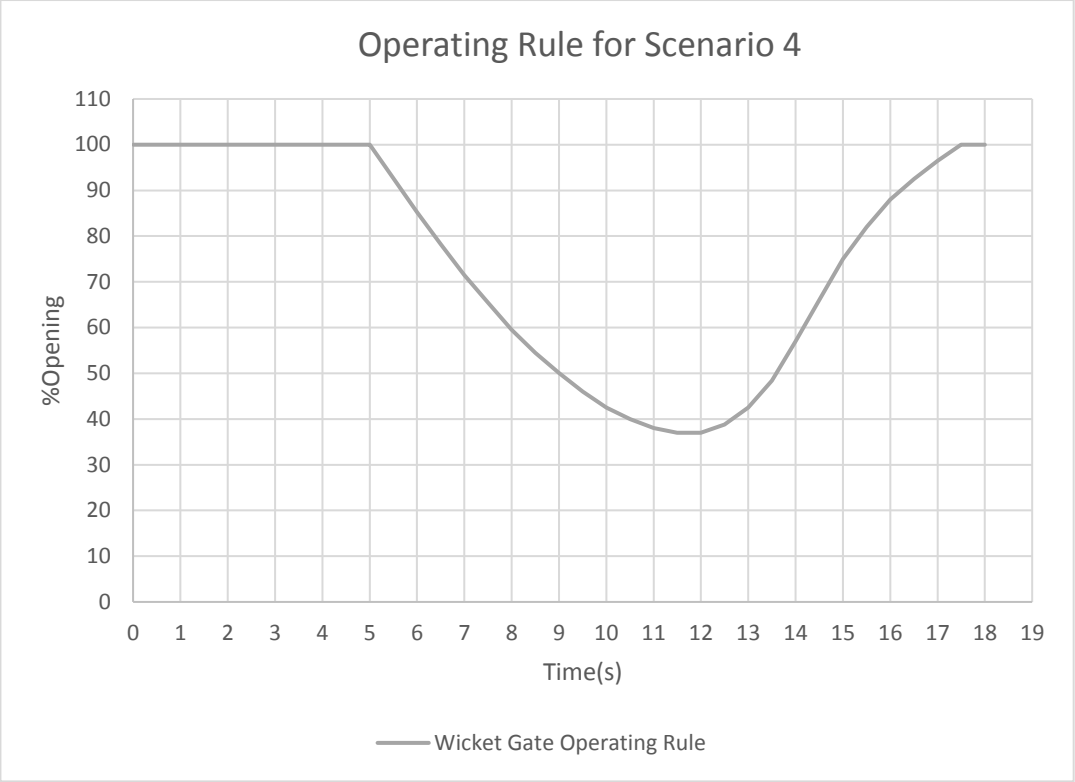

Figure 5.47 Wicket Gate Operating Rule for Scenario 4

The beginning part of the wicket gate pattern is directly taken from the critical load reduction case, and the remaining part is taken from the critical load acceptance case. Simulating the load variation for high slopes of closure or opening patterns instead of slight changes in the wicket gate gives more significant pressure values. Since the aim is to investigate the limits of operation methods without harming the HPP, this way is preferred for simulations.

Figure 5.48 indicates the pressure and discharge variation for Scenario 4. As observed from the figure, pressure change between the minimum and maximum pressure points is 411 kPa which is 25.42% of the initial pressure. Total pressure change percentage is lower than load acceptance because system is exposed to pressure rise before decrease. While wicket gate is closed, new water hammer waves occur and increase the pressure of the system. The maximum pressure is 1784 kPa with a 10.33% increase, and the minimum pressure is 1373 kPa with a 15.09% decrease according to the initial pressure of 1617 kPa.

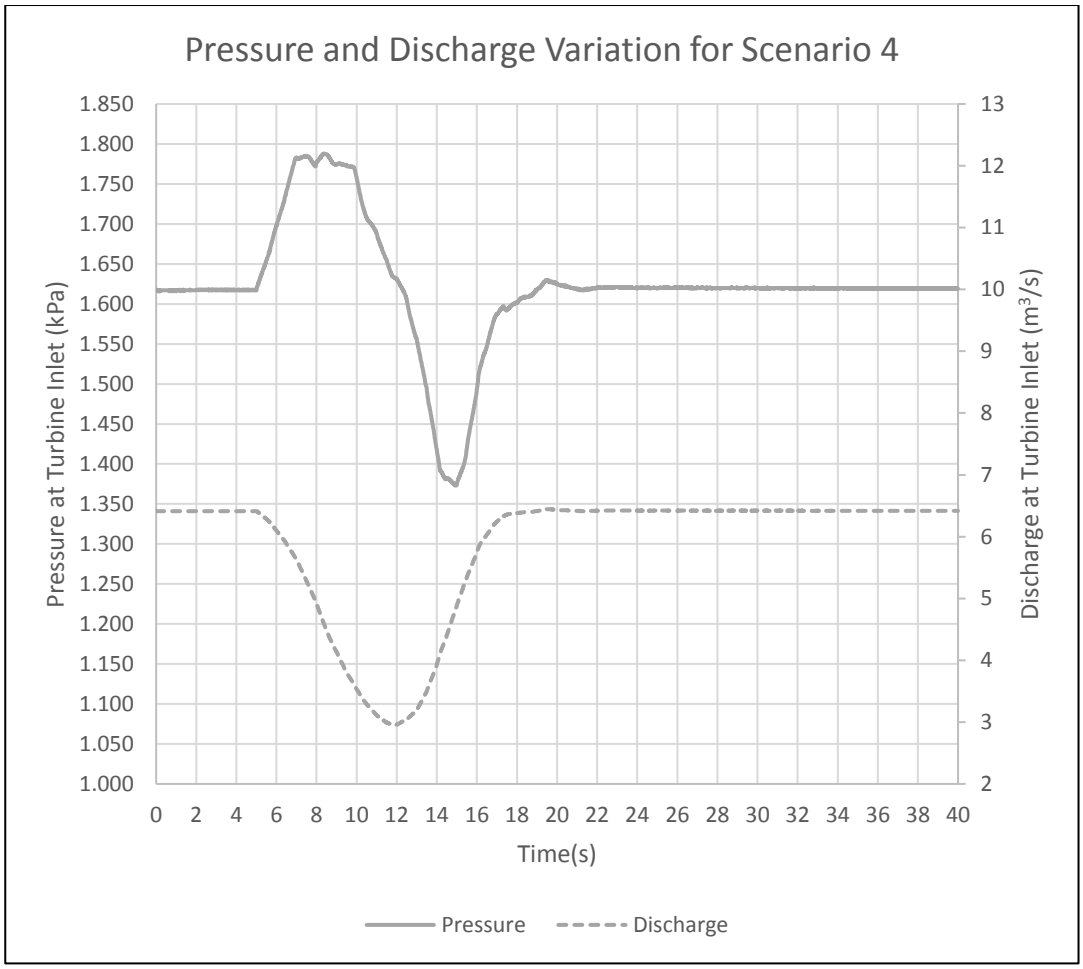

Figure 5.48 Pressure and Discharge Variation for Scenario 4

Discharge follows the wicket pattern if the wicket gate operating rule does not have sudden changes. Sudden changes in the slope cause fluctuations in the flow rate and pressure.

Hydraulic grade line levels are checked for the system in Figure 5.49. Since the critical point is seen as point just before turbine, HGL values are taken for that part of the pipeline system. Initial hydraulic grade line at turbine inlet is 276.36 m. According to initial status, the maximum and minimum piezometric heads are 293.83 m with 6.32% rise and 251.3 m with 9.07% reduction. As a result, system is safe for load variation scenario. The system can manage this type of electricity demand change without operating PRV. If PRV is used, higher load reduction cases are not

severe for the system. Since there is a surge tank in HPP, an increase in turbine power in load variation scenario will not cause any excessive change in the system

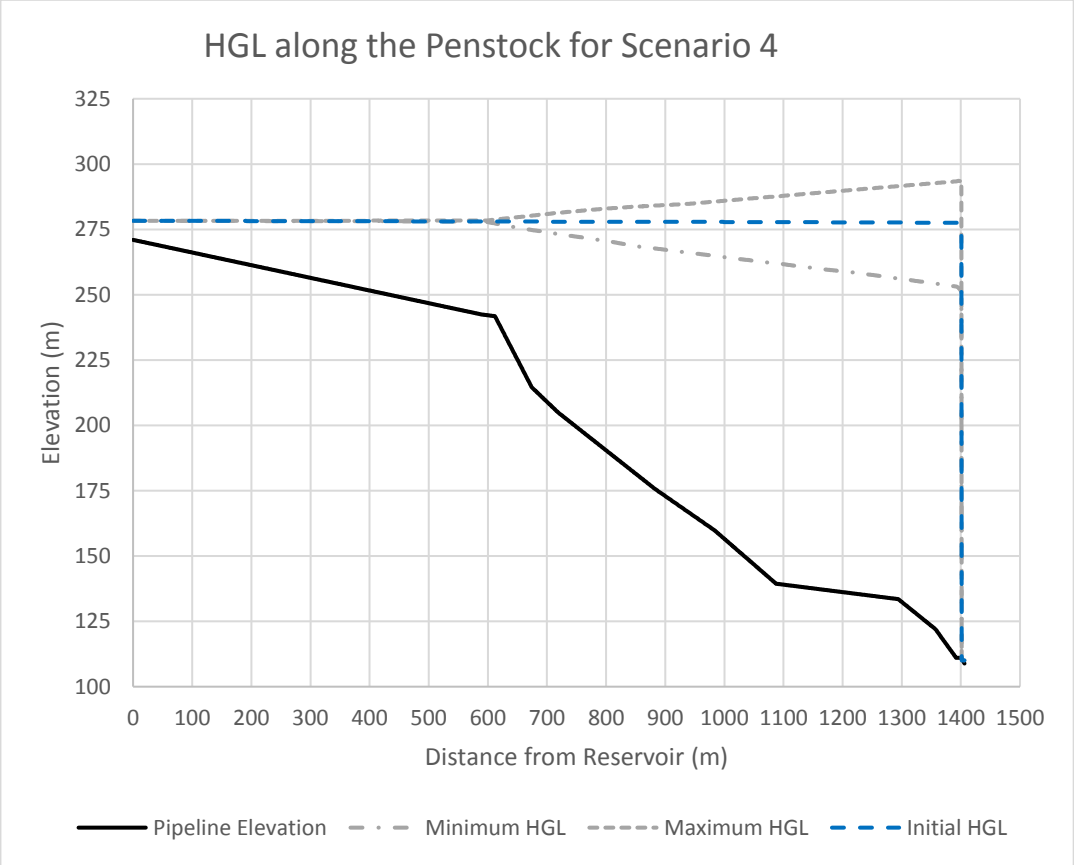

Figure 5.49 HGLs along the Penstock for Load Variation Scenario

5.4 Discussion of the Results

In the present study, after validation of the model is completed, simulations are performed for different scenarios, and results are compared with the help of computer software. Pressure and discharge variations, hydraulic grade lines along the pipeline system, wicket gate, and PRV operating rules are analyzed and numerically. The most critical cases are obtained and the operating conditions for these cases are presented. The effects of the PRV on the system is understood with

the comparisons. Wicket gate closure times are checked for critical time, and it is observed that all the closure operations are performed gradually.

In the validation part, three different models are developed to simplify the system and obtain the reference discharge variation. Simulation results are compared with measured data collected from the field tests. In the first step, a simple case is developed with GPV for 8.5 MW and 9.35 MW tests, and results fit measured data with minor errors. It is deduced that the model is capable of reflecting field conditions. Therefore, reference discharge variation is obtained and the second step is started. Next, PRV is added to the system, and its opening patterns are arranged with obtained reference discharge variation for pipes after branch. In the last step, turbine is modeled instead of GPV, and wicket gate operating rule is determined according to provided information. Measured data are satisfied with a maximum 4.33% error in pressure peak occurrence time and 1.14% error in the magnitude of the pressure peak points for the 8.5 MW test. In the 9.35 MW test, the maximum error is 1.61% in pressure peak occurrence time and %2.53 error in the magnitude of the pressure peak points. As a result, it is proved that the model represents the field conditions accurately, and validation is completed successfully.

In the instant load rejection scenario, simulations are performed for cases with and without PRV. Since the 8.5 MW and 9.35 MW tests are analyzed, wicket gate and PRV operating rules are taken from validation stage. First, unprotected systems are investigated individually, and it is observed that excessive pressure values occur without PRV. Then, comparison of protected and unprotected systems is analyzed in the same graphics for pressure and discharge. PRV decreases the pressure rise by approximately 50% for the system. After wicket gate is closed, wave pressures continue to fluctuate in the system without PRV because surge tank, friction and minor losses can not dissipate the energy of the flow. Since flow rate is slight, losses can not decrease the energy of the pressure waves, and surge tank orifice is not enough to dissipate the energy, pressure waves are absorbed in a long time, such as 5 minutes. This phenomenon is valid for load rejection scenario.

In the load rejection scenario, 8.5 MW and 9.35 MW tests are investigated for a linear decrease of electrical load in the system with and without PRV. First, in order to determine the worst cases, simulations are held for different closure times. Then, critical cases are analyzed for pressure, discharge, and piezometric head. It is resulted that wicket gate should not be closed lower than 15 seconds without PRV. For emergency conditions, the closing time decreases to approximately 8-9 seconds with PRV. PRV effect is the same as instant load rejection case. However, since the governor operates two components and spends more energy if the PRV is opened, it is not suitable for everyday conditions.

In the load acceptance scenario, simulations are run for different opening times to determine the most critical cases for 8.5 MW and 9.35 MW tests. In this case, load is accepted in 5 seconds for both turbine powers. However, even if the wicket gate is opened in 1 second, although it is impossible, negative pressures do not occur in the system because of the supplied water from the surge tank. Therefore, it is obvious that load acceptance is not severe for HPP.

In the load variation scenario, results are analyzed for load reduction cases for different closure times. The most critical case is determined as reduction from 9.35 MW and 4.5 MW turbine power in 6 seconds. Reduction slope should not be lower than 0,8 MW/s to prevent any damage to components. Then, using the information from load acceptance scenario and load reduction simulations, a wicket gate pattern is formed by combining the worst cases for these conditions. The difference between the maximum and minimum pressure is 412 kPa, but it does not affect the operation of the system.

CHAPTER 6

CONCLUSIONS

In the present study, determination of the effect of the PRV on the transients near a turbine in a power plant is the main concern. The power plant used as a case study is the KEPEZ – I Hydropower Plant in which one of the turbines is rehabilitated. During the commissioning of the rehabilitated powerplant, various tests are performed and valuable data is collected in different power production cases. A PRV mounted near the turbine is used as a protective measure against possible water hammer events. It is important to understand how this PRV affects the transients generated by different turbine operations. It should be kept in mind that although there is also a surge tank in the system closer to the upstream reservoir than the turbines, the protective response of the PRV has more rapid and direct effect on mitigating the transients since it is is mounted to the turbine spiral case with a by-pass pipe. PRV used in KEPEZ – I HPP site does not work with a set pressure limit in the system. That is why PRV is simulated by TCV in all of the simulations. It is opened according to an algorithm related to wicket gate operation. PRV opening starts with wicket gate closure. According to the results, transient pressure increase can be prevented before it reaches extreme values by opening PRV at the beginning of the water hammer event. This dual mechanism of closure and opening increases PRV efficiency.

According to the field observations and the numerical simulations performed in the study, the following observations and conclusions may be drawn;

- Using a powerful computer software like HAMMER for numerical analyses enables designers to save time and increase accuracy in the calculations. Complex systems can be simulated, and critical pressure (high or low) points

can be detected. Computer software helps the designer to model protective measures and provide results for different scenarios.

- Since the discharge variation is the main cause of the transient events, and it helps one to understand the system response, obtaining reliable data for discharge variation is essential for the accurate simulations of the wicket gates of the turbine and PRV maneuvers while one is closing, the other one is opening. Therefore, three cases were used in the validation stage, in order to obtain the reference discharge variation in both components (i.e. turbine and PRV). In the simplest case, Case-1, which includes a general purpose valve (GPV) simulating the turbine behavior only, the simulation results of pressure variation near the turbine, are compared with the corresponding measured pressure variations in the field. In this case, the discharge variation through the turbine is to be obtained while taking into consideration the amount of discharge being released from the system by the PRV. Measured pressure values are matched by achieving and defining the most suitable operating rule for the GPV simulating the turbine. Next, the obtained discharge variation data producing the same pressure variation as in the field are used as the reference data in the following validation steps to develop a model that represents the hydropower plant more precisely. Finally, at the end of the validation stages, in Case-3, a model is constructed with actual turbine features and a TCV simulating the PRV, and simulation results fit the measured field test data. Now that we have a calibrated model, a number of simulations were performed with important scenarios.
- In the operation stage, transient analysis helps to determine the operation limits of the facility and gives an idea about the effectiveness of the operating method against water hammer. A sudden change in the wicket gates pattern causes a significant rise or reduction of pressure in the system. Therefore, required operation times and allowable pressure limits should be calculated for emergency scenarios with transient analysis. Specifically, in Kepez – I HPP, allowable pressure is calculated as 1900 kPa, and the critical time for

wicket gate operation is determined as 3.14 seconds. Measured data indicate that minimum turbine closure time is not lower than the critical time, and pressure does not exceed 1800 kPa in the field tests for instant load rejection case. Because the wicket gates closed gradually in the tests, adverse or damaging conditions are not observed in the power plant. Therefore, operators should know the critical time for closure in emergency situations not to cause harmful effects while protecting the system from transients.

- Because the surge tank is approximately 800 m away from the turbine and PRV is mounted into turbine spiral case with a by-pass pipe, compared to surge tank PRV's positive effect is much faster and more reliable on controlling pressure increases due to transients. As a result, in order to benefit from a surge tank or PRV efficiently, they should be placed as close to the critical point in the system, such as the turbine inlet, as possible. However, surge tank prevents the negative pressures in the system by supplying water immediately during load acceptance. On the other hand, PRV does not have any significant effect on pressure decrease.
- Since the surge tank volume is large, it behaves like a reservoir and reflects the pressure waves arriving there from the turbine. In the measured data, it is observed that pressure decrease starts at 2.5 seconds. Although the duration for a wave to return to the turbine after being formed by wicket gate is 3.14 seconds, reflected waves affect the system after 2 seconds. If a wave is formed because of wicket gate operation and returns to the wicket gate after being reflected from the surge tank, this phenomenon takes 2 seconds.
- Unprotected and protected cases are analyzed, and PRV effect is investigated for the system. PRV decreases the pressure rise by approximately 50% in every case. Therefore, mounting a PRV is an efficient way to protect the system from pressure increase with proper operation.
- Various simulations are performed for different opening times in load acceptance scenario. It is concluded that the system is safe for load acceptance because of surge tank effect. Because the surge tank has enough

volume to supply water for rapid wicket gate openings, according to simulation results, even if the wicket gate is opened in 1 second, which is an impossible case, a surge tank can prevent negative pressures. In addition, as mentioned before, the surge tank behaves like a reservoir in the system and decreases the critical closure time to 2.2 seconds. As a result, the surge tank may be deemed to be overdesigned in the system. In order to design a surge tank more efficiently and economically, the transient analysis should be performed before the actual construction.

Recommendations can be made for future research based on the experience gained in this study. Applying the validation method to different HPPs which do not have enough measured data, comparing the results of the study with different HPPs, investigation of PRV operations for different HPPs, comparing the results for executing PRV with a set pressure limit and method which is applied in this thesis may be the aspects of future studies.

REFERENCES

Allievi, L. (1902). General theory of the variable motion of water in pressure conduits. Annali della Societa degli Ingegneri ed Architetti Italiani 17(5): 285-325 (in Italian). (French translation by Allievi, in Revue Me' canique, Paris, 1904) (Discussed by Bergant et al., 2006).

Azoury, P. H., Baasiri, M., & Najm, H. (1986). Effect of Valve-Closure Schedule on Water Hammer. Journal of Hydraulic Engineering, 112(10), 890-903.

Bentley HAMMER V8i Edition User′s Guide. (2010).

Bozkuş Z. (2008). Water Hammer Analyses of Çamlıdere-İvedik Water Treatment Plant (IWTP) Pipeline. Teknik Dergi/Technical Journal of Turkish Chamber of Civil Engineers, April, 4409-4422.

Chaudhry, M. H. (1987). Applied Hydraulic Transients. New York: Van Nostrand Reinhold Company Limited.

Chaudhry, M. H. (2014). Applied Hydraulic Transients Third Edition. In Applied Hydraulic Transients.

Calamak, M., & Bozkuş, Z. (2012). Protective measures against waterhammer in run-of-river hydropower plants. Teknik Dergi/Technical Journal of Turkish Chamber of Civil Engineers, 23(DECEMBER), 1623–1636.

Calamak, M. (2010). Investigation of Water Hammer Problems in the Penstocks of Small Hydropower Plants. Master's Thesis, Middle East Technical University, Ankara, Turkey.

Celebioğlu, K. (2019). Roughness Coefficient of a Highly Calcinated Penstock. Teknik Dergi, 9309–9326. https://doi.org/10.18400/tekderg.447265

DSI. (2020). Faaliyet Raporu. Retrieved from General Directorate of State Hydraulics: https://cdniys.tarimorman.gov.tr/api/File/GetFile/425/KonuIcerik/759/1107/DosyaGaleri/DS%C4%B0%202020-yili-faaliyet-raporu.pdf

Dincer, E. (2013). Investigation of Water Hammer Problems in the Penstocks of Pumped-Storage Power Plants. Master's Thesis, Middle East Technical University, Ankara, Turkey.

Dincer, A. E., & Bozkus, Z. (2016). Investigation of Waterhammer Problems in Wind-Hydro Hybrid Power Plants. Arabian Journal for Science and Engineering, 41(12), 4787–4798. https://doi.org/10.1007/s13369-016-2142-2

Dursun, S. (2013). Numerical Investigation of Protection Measures Against Water Hammer in the Yesilvadi Hydropower Plant. Master's Thesis, Middle East Technical University, Ankara, Turkey

Dursun, S., Bozkus, Z., & Dincer, A. E. (2015). Effect of pressure relief valves on the fluid transients in the penstocks of a small run-of-river plant. Retrieved From: https://www.researchgate.net/publication/284512453

EMRA (2021). Electricity Market Sector Report 2020. Retrieved from: https://www.epdk.gov.tr/Detay/Icerik/1-1271/electricityreports

ESHA. (2004). Guide on How to Develop a Small Hydropower Plant. European Small Hydropower Association, 296.

FENSU Engineering Construction Energy LTD. CO. (2015). TÜBİTAK-Kepez-1 HPP System Analyze Report

Joukowsky, N. (1898). "Über den hydraulischen Stoss in Wasserleitung-shrohren." [On the hydraulic hammer in water supply pipes.] Mémories de l'Académie Impériale des Sciences de St.-Pétersbourg (1900) Series 8, 9(5), 1-71 (in German).

Krivchenko, G. (1994). Hydraulic machines: Turbines and pumps. Lewis Publishers.

Munson, B. R., Young, D. F., Okiishi, T. H., & Huebsch, W. W. (2009). Elementary Fluid Dynamics - The Bernoulli Equation. Fundamental of Fluids Mechanics, 93–146.

Peicheng, H., Pusheng, Z., Elkouh, A. F. (1989). Relief Valve and Safety Membrane Arrangement in Lieu of Surge Tank. ASCE Journal of Energy Engineering, 78-83.

Penche, C. (2004). Guide on How to Develop a Small Hydropower Plant. Belgium: European Small Hydropower Association.

Rezaei, V., Calamak, M., & Bozkus, Z. (2017). Performance of a pumped discharge line with combined application of protection devices against water hammer. KSCE Journal of Civil Engineering, 21(4), 1493–1500. https://doi.org/10.1007/s12205-016-0747-3

Riasi, A., & Nourbakhsh, A. (2011). Influence of Surge Tank and Relief Valve on Transient Flow Behavior in Hydropower Stations. https://asmedigitalcollection.asme.org/FEDSM/proceedings-pdf/AJK2011/ 44403/1971/4584883/ 1971_1.pdf

Seleznev, V. S., Liseikin, A. V, Bryksin, A. A., & Gromyko, P. V. (2014). What Caused the Accident at the Sayano–Shushenskaya Hydroelectric Power Plant (SSHPP): A Seismologist's Point of View. Seismological Research Letters, 85(4), 817–824.

Sepetci et al. (2016). Conceptual Design of a Hydroelectric Power Plant for a Rehabilitation Project. 12th International Conference on Heat Transfer, Fluid Mechanics and Thermodynamics.

Sepetci, G. (2017). Hydraulic Analysis of KEPEZ Hydroelectric Power Plant Based on Site Measurements and Numerical Analysis. Master's Thesis, TOBB University of Economics and Technology, Ankara, Turkey

Tijsseling, A. S., & Anderson, A. (2007). Johannes von Kries and the history of water hammer. Journal of Hydraulic Engineering, 133(1), 1–8. https://doi.org/10.1061/(ASCE)0733-9429(2007)133:1(1)

Thorley, D. A. R. (2004). Fluid transients in pipeline systems, ASME Press, New York.

Vail, A. and Firoozabadi, B. (2009). Investigation of Valve-Closing Law on the Maximum Head Rise of a Hydropower Plant. Scientia Iranica Mechanical Engineering, 222-228.

Wylie, E. B., Streeter, V. L., Suo, L. (1993). Fluid Transients in Systems. New Jersey: Prentice-Hall.

Zhang, J., Ma, S., Xiaodong, J. H., Fulin, Y., Guangdong, C., & Water, Y. (2008). Application of Pressure Regulating Valve in the Hydraulic Transients of Hydropower Plants. http://asmedigitalcollection.asme.org/FEDSM/proceed ings-pdf /FEDSM2008/48418/341/2711048/341_1.pdf

Zhang K. Q., Karney, B. W., & McPherson, D. L. (2008) Pressure Relief Valve Selection and Transient Pressure Control. Journal – American Water Works Association, 100(8), 62-69, https://doi.org/10.1002/j.1551-8833.2008. tb09799.x